

AD-782 209

MANEUVER CRITERIA EVALUATION PROGRAM

T. L. Wood, et al

Bell Helicopter Company

Prepared for:

Army Air Mobility Research and Development
Laboratory

May 1974

DISTRIBUTED BY:

NTIS

National Technical Information Service
U. S. DEPARTMENT OF COMMERCE
5285 Port Royal Road, Springfield Va. 22151

Unclassified

SECURITY CLASSIFICATION OF THIS PAGE (When Data Entered)

REPORT DOCUMENTATION PAGE		READ INSTRUCTIONS BEFORE COMPLETING FORM
1. REPORT NUMBER USAAMRD-L-TR-74-32	2. GOVT ACCESSION NO.	3. RECIPIENT'S CATALOG NUMBER AD-792 209
4. TITLE (and Subtitle) MANEUVER CRITERIA EVALUATION PROGRAM		5. TYPE OF REPORT & PERIOD COVERED
		6. PERFORMING ORG. REPORT NUMBER
7. AUTHOR(s) T.L. Wood D.G. Ford G.H. Brigman		8. CONTRACT OR GRANT NUMBER(s) DAAJ02-73-C-0015
9. PERFORMING ORGANIZATION NAME AND ADDRESS Bell Helicopter Company P.O. Box 482 Fort Worth, Tex. 76101		10. PROGRAM ELEMENT, PROJECT, TASK AREA & WORK UNIT NUMBERS Task 1F262208AH9001
11. CONTROLLING OFFICE NAME AND ADDRESS Eustis Directorate U.S. Army Air Mobility R&D Laboratory Fort Eustis, Va. 23604		12. REPORT DATE May 1974
		13. NUMBER OF PAGES 144
14. MONITORING AGENCY NAME & ADDRESS (if different from Controlling Office)		15. SECURITY CLASS (of this report) Unclassified
		15a. DECLASSIFICATION/DOWNGRADING SCHEDULE
16. DISTRIBUTION STATEMENT (of this Report) Approved for public release; distribution unlimited.		
17. DISTRIBUTION STATEMENT (of the abstract entered in Block 20, if different from Report)		
18. SUPPLEMENTARY NOTES NATIONAL TECHNICAL INFORMATION SERVICE Springfield, VA 22161		
19. KEY WORDS (Continue on reverse side if necessary and identify by block number) Maneuverability Trajectories Flight Paths Computer Programming Mission Profiles Computerized Simulation Helicopters Flight		
20. ABSTRACT (Continue on reverse side if necessary and identify by block number) The Maneuver Criteria Evaluation Program (MCEP) is a digital computer program which solves the flight path equation of motion for a helicopter without auxiliary propulsion. The use of basic work, energy, and power relationships makes possible accurate representation of flight path trajectories. MCEP can be used to aid in the development of maneuver requirements		

Block 20

which provide the necessary maneuver capability to perform the desired mission. The desired mission is simulated in MCEP by using individual flight controllers to "fly" the helicopter through the mission profile. Key maneuver parameters are monitored throughout the flight profile to provide insight into the performance of the helicopter in achieving the desired flight trajectory.

This report presents a review of the program capabilities in addition to the background and development of the principal mathematical model in MCEP. A demonstration of MCEP is provided using a typical AH-1G helicopter gunship mission.

The appendix to the report, the User's Guide, contains the detailed information necessary for setting up an input data deck for MCEP.

PREFACE

This report and its accompanying computer program were developed under Contract DAAJ02-73-C-0015 (DA Task IF262208AH9001) awarded in November 1972 by the Eustis Directorate of the U. S. Army Air Mobility Research and Development Laboratory (USAAMRDL).

Technical program direction was provided by Mr. D. Merkley of USAAMRDL. Principal Bell Helicopter personnel associated with the contract were Messrs. G. H. Brigman, D. G. Ford, and T. L. Wood. The authors wish to acknowledge the helpful suggestions of Messrs. C. L. Livingston and J. R. Johnson.

TABLE OF CONTENTS

	<u>Page</u>
PREFACE	iii
LIST OF ILLUSTRATIONS	vii
LIST OF TABLES.	x
INTRODUCTION	1
DESCRIPTION OF MATHEMATICAL MODEL	2
Technical Approach	2
Helicopter Representation.	2
Representation of the Wing	5
Flight Dynamics	12
Command Generation	18
DESCRIPTION OF MCEP	25
Mission Specification	25
MCEP Maneuvers	25
Cruise.	25
Acceleration/Deceleration at Constant Attitude.	27
Turn at Constant Airspeed and Altitude	29
Climb/Descent at Constant Airspeed	32
Pullup/Pushover at Desired Load Factor	35
Auto Turn at Constant Airspeed and Altitude	35
Return to Target at Constant Altitude	40
Dive/Rolling Pullout	44
Climbing/Descending Turn at Constant Airspeed.	52
Sideward Acceleration/Deceleration	55
Sideward Acceleration/Pedal Turn Into Wind.	58
Orbit at Constant Airspeed	61
Pedal Turn at Hover	61
Collective Pop-Up at Constant Attitude and Low Airspeed.	65
Climbing Return to Target	67
Evaluation of Mission Profile	67
SIMULATION OF AH-1G HELICOPTER GUNSHIP MISSION USING MCEP	70
Definition of Mission Profile	70

TABLE OF CONTENTS - Continued

	<u>Page</u>
Results and Interpretation of Simulation of Mission Profile	70
LITERATURE CITED	108
APPENDIX-USER'S GUIDE.	109
LIST OF SYMBOLS	123

LIST OF ILLUSTRATIONS

<u>Figure</u>		<u>Page</u>
1	Wing Lift Coefficient Versus Wing Angle of Attack.	7
2	Wing Drag Coefficient Versus Wing Lift Coefficient	7
3	Comparison of Pushover Maneuver Between C81 and MCEP for a Winged Helicopter.	10
4	Comparison of Pullup Maneuver Between C81 and MCEP for a Winged Helicopter	11
5	MCEP Coordinate System	13
6	Time History of Command Generator Parameters	19
7	Application of Power in Acceleration or Deceleration Maneuver	27
8	Thrust Vectoring for Linear Acceleration	28
9	Time History of Acceleration Maneuver for AH-1G Helicopter at 9500 Pounds	30
10	Time History of Turn at Constant Airspeed and Altitude for AH-1G Helicopter at 90 Knots and 9500 Pounds.	33
11	Time History of Descent Maneuver for AH-1G Helicopter at 90 Knots and 9500 Pounds	36
12	Time History of Pullup Maneuver for AH-1G Helicopter at 90 Knots and 9500 Pounds	37
13	Orientation of Helicopter Relative to Aim Points	39
14	Prediction of Opportunity of Helicopter to Intersect Aim Points	39
15	Ground Track of Auto Turn Maneuver	41
16	Time History of Auto Turn Maneuver for AH-1G Helicopter at 90 Knots and 9500 Pounds.	42

LIST OF ILLUSTRATIONS - Continued

<u>Figure</u>		<u>Page</u>
17	Orientation of Helicopter Relative to Target.	43
18	Ground Track of Return to Target at Constant Altitude	45
19	Time History of Return to Target at Constant Altitude for AH-1G Helicopter at 90 Knots and 9500 Pounds	46
20	Ground Track of Return to Point at Constant Altitude	47
21	Time History of Return to Point at Constant Altitude for AH-1G Helicopter at 100 Knots and 9500 Pounds.	48
22	Prediction of Dive Point for Dive/Rolling Pullout Maneuver	50
23	Prediction of Pullup Point for Dive/Rolling Pullout Maneuver	50
24	Ground Track of Dive/Rolling Pullout Maneuver	53
25	Time History of Dive/Rolling Pullout Maneuver for AH-1G Helicopter	54
26	Time History of Climbing Turn at Constant Airspeed for AH-1G Helicopter at 90 Knots and 9500 Pounds	56
27	Time History of Sideward Acceleration From Hover and Deceleration to Hover for AH-1G Helicopter at 8500 Pounds	59
28	Time History of Sideward Acceleration From Hover and Turn Into the Wind for AH-1G Helicopter at 8500 Pounds	60
29	Ground Track of Orbit Maneuver.	62
30	Definition of Pedal Input for Pedal Turn Maneuver	63

LIST OF ILLUSTRATIONS - Continued

<u>Figure</u>		<u>Page</u>
31	Time History of Pedal Turn Maneuver for AH-1G Helicopter at Hover.	63
32	Definition of Recovery Load Factor for Collective Pop-Up Maneuver	66
33	Time History of Collective Pop-Up Maneuver for AH-1G Helicopter at Hover and 9000 Pounds .	66
34	Ground Track of Climbing Return to Target for AH-1G Helicopter at 90 Knots Entry Airspeed. .	68
35	Summary of Ground Track for Demonstration Maneuver in Landing Zone Area	102

LIST OF TABLES

<u>Table</u>		<u>Page</u>
I	MCEP Maneuver Identification	26
II	Definition of Mission Profile Using MCEP Maneuvers	71
III	AH-1G Helicopter Input Data	75
IV	Summary of Profile Step 1	77
V	Summary of Profile Step 2	78
VI	Summary of Profile Step 3	79
VII	Histograms for Clim'ing Turn Maneuver	80
VIII	Summary of Profile Step 4	82
IX	Summary of Profile Step 5	83
X	Summary of Profile Step 6	84
XI	Histograms for Climb Maneuver	85
XII	Summary of Profile Step 7	87
XIII	Summary of Profile Step 8	88
XIV	Summary of Profile Step 9	89
XV	Summary of Profile Step 10.	90
XVI	Summary of Profile Step 11.	91
XVII	Histograms for Dive/Rolling Pullout	92
XVIII	Summary of Profile Step 12.	94
XIX	Summary of Profile Step 13.	95
XX	Summary of Profile Step 14.	96
XXI	Summary of Profile Step 15.	97
XXII	Summary of Profile Step 16.	98
XXIII	Histograms for Turn at Constant Airspeed and Altitude Maneuver	99

LIST OF TABLES - Continued

<u>Table</u>		<u>Page</u>
XXIV	Summary of Profile Step 17	101
XXV	Summary of Profile Step 18	103
XXVI	Summary of Profile Step 19	104
XXVII	Summary of Profile Step 20	105
XXVIII	Summary of Profile Step 21	106
XXIX	Summary of Profile Step 22	107

INTRODUCTION

The execution of specific missions requires that a helicopter possess certain maneuver capability. This capability is assured by specifying maneuver requirements in design specifications. It is important that these requirements assure that the helicopter can perform the specified mission satisfactorily. Unnecessary maneuver requirements may result in penalties to the helicopter design and cost while making little or no improvement in the helicopter's ability to perform its mission.

The Maneuver Criteria Evaluation Program is a simplified method which allows the user to determine what maneuver capability is required to perform a given mission. MCEP is an acronym for Maneuver Criteria Evaluation Program and denotes the computer model. MCEP can be used to aid in the development of maneuver requirements which provide the necessary maneuver capability to perform the desired mission.

The desired mission is simulated in MCEP by using individual flight controllers to "fly" the helicopter through the mission profile. The flight trajectories of the helicopter are computed using the technique presented in Reference 1 which was developed under Air Force contract. Key maneuver parameters are monitored throughout the flight profile to provide insight into the performance of the helicopter in achieving the desired flight trajectory.

The individual flight controllers are designed to bound the maneuver in terms of maximum or minimum allowable values of various parameters such as load factor or airspeed to enable trade-off investigations to be made.

DESCRIPTION OF MATHEMATICAL MODEL

The methods used to represent and to control the helicopter in MCEP are reviewed in this section. The flight path of the helicopter is computed using well-known relationships of energy, work and power. The helicopter is controlled by specifying linear accelerations in the wind axes system.

TECHNICAL APPROACH

The computation of flight trajectories of a helicopter in MCEP is based on the energy method for predicting helicopter maneuverability as documented in References 1 and 2. This fundamental method uses the concepts of work and energy to predict the helicopter's ability to change its direction of flight. The helicopter is "flown" by controlling the linear accelerations in the wind axes. A technique is used which results in continuous specification of the control parameters to achieve the required flight trajectory. A wing simulation was developed which is dependent upon the fuselage angle of attack. Since the energy method does not provide fuselage angle of attack data, an empirical equation is provided for this purpose. However, this equation must be determined from another source for valid results in determining the influence of the wing on flight trajectories.

HELICOPTER REPRESENTATION

The helicopter is simulated by predicting its power required as a function of the flight condition, load factor, and certain physical parameters of the helicopter from a set of closed-form equations. The difference in the power supplied by the engine and the power required at the altitude-airspeed-flight condition may be used by the helicopter to increase altitude (potential energy), to increase airspeed (kinetic energy), to increase rotor speed (rotation energy), or to change the aircraft's direction of flight. These concepts of changing energy levels and controlling the direction of flight are explained in detail in Reference 2.

The power-required equations for the helicopter include the parasite power, rotor and wing induced powers, rotor blade profile power, and rotor compressibility and stall powers. The detailed derivation of the power equation is given in Reference 1. A summary of these equations is presented below.

$$\text{PARASITE POWER} = f\rho V^3/2$$

$$\text{ROTOR-INDUCED POWER} = Tv_i$$

$$\text{WING-INDUCED POWER} = \frac{2L_w^2}{\rho \pi e b^2 V}$$

ROTOR BLADE

$$\text{PROFILE POWER} = (\delta_0 + \delta_1 \alpha + \delta_2 \alpha^2) \frac{bcR}{8} (1 + 4.6 \mu^2) \rho (\Omega R)^3$$

$$\text{COMPRESSIBILITY POWER} = \rho A (\Omega R)^3 \lambda M^3 [0.0033 - \lambda M (0.022 - 0.11 \lambda M)]$$

$$\text{STALL POWER} = 550 [3410 (t_c - [t_c]_{Div})]^{3/2}$$

The parasite term includes the drag contributions of the fuselage, wing, elevator, fin, rotor hub, and external stores. The rotor thrust (T) is the vector sum of the propulsive force and the force along the fuselage Z axis. The wing lift (L_w) is a function of fuselage angle of attack, wing incidence, and rotor downwash. Compressibility power is a function of the amount by which the tip Mach number exceeds the drag rise Mach number (MCRO). The blade loading coefficient (t_c) is used in the computation of stall power. The symbol $[t_c]_{Div}$ represents the value of t_c at the first occurrence of power increase due to stall. This quantity can be expressed as follows:

$$[t_c]_{Div} = TC1 + TC2/\sqrt{1 + 50\mu^2} \quad (1)$$

where μ is the advance ratio, $V/\Omega R$.

The above equations were developed for the AH-1G helicopter. Predicted power-required data from the above equations and flight test data are correlated in Reference 1. Also, Reference 1 compares data predicted by the energy method and flight test data for level flight acceleration and deceleration, and 180-degree turning performance for the AH-1G helicopter.

The power equations were originally developed for predicting the total power required for the AH-1G helicopter. However, these equations have been evaluated for the prediction of the total power required for different single-main-rotor

helicopters. A procedure is outlined in Reference 1 showing how to determine a set of input coefficients for a helicopter based on the helicopter's speed-power data at different gross weights and from certain physical parameters of the helicopter. The sensitivity of the total power required to the input parameters is investigated to provide the user with insight into the impact of the various coefficients on the total power required. Several current operational helicopters were considered in the evaluation of the equations: the OH-6A, CH-3C, and CH-53A. Predicted data and flight test data for these various helicopters are compared in Reference 1. Based on flight test used, the equations yielded satisfactory results for use in simulating flight trajectories.

The power equations allow a rapid and simple representation of a helicopter to be made. However, it is not intended that the above equations be used to predict power-required data independently. Flight test data or data from another source should be compared with the predicted data to validate the input coefficients.

Since the above method does not consider fuselage force and moment data, an equation is needed to predict the fuselage angle of attack as a function of airspeed, load factor, gross weight, drag, and vertical velocity. A closed-form expression for the fuselage angle of attack was determined in Reference 1 for the AH-1G helicopter:

$$\begin{aligned} \alpha_F = & \text{KAF1} \left[\text{KAF2}(n-1)^2 + \text{KAF3}(n-1) \right] \frac{\sqrt{\rho} \text{GW}}{(\sigma'V)^{\text{KAF4}}} \\ & - \text{KAF5} V \sqrt{\frac{\rho}{\text{GW}}} - \tan^{-1} \left(\frac{-\text{KAF6} V_{ZE}}{V} \right) - \text{KAF7} \\ & - \sin^{-1} \left(\frac{ax_w}{ng \left[1 + \left(\frac{V}{\text{KAF8}} \right)^2 \right]} \right) \end{aligned} \quad (2)$$

where for the AH-1G helicopter

$$\text{KAF1} = 8.643$$

$$\text{KAF2} = 2.478$$

$$\text{KAF3} = 10.422$$

$$\text{KAF4} = 1.6$$

$$\text{KAF5} = 17.639$$

$$\text{KAF6} = 0.8$$

$$\text{KAF7} = 1.5$$

$$\text{KAF8} = 240.$$

The last term in Equation (2) represents the change in a_F for a pilot-induced acceleration or deceleration. It should be emphasized that this term is zero if the acceleration or deceleration is not pilot induced. It is recognized that the coefficients of Equation (2) are for a specified helicopter, but may be used for different helicopters since most helicopters have similar attitude variations with the parameters in the equation. If fuselage angle of attack data are available from flight test or another source for a specified helicopter, then the coefficients of Equation (2) can be modified to give a better fit while retaining the basic form of the fuselage angle of attack equation. This equation is important when a winged helicopter is being simulated.

The helicopter is limited in maneuvers by the maximum thrust which the rotor can produce. The user must determine this value from another source as suggested in References 1 and 2. The mathematical model limits the thrust which the rotor can produce in the following manner. If the desired rotor thrust is greater than the maximum thrust allowed ($t_{c_{\max}} = \text{TCM1} +$

$\text{TCM2} \mu$), then the rotor thrust is reset to the maximum value for the given flight condition. By observing this limit, the helicopter can not perform trajectories outside its performance capabilities.

REPRESENTATION OF THE WING

A method to represent a wing is provided to allow the influence of a wing on the flight path to be evaluated. However, since a force and moment representation is not used in the simulation, the fuselage angle of attack must be determined from another source. Then the coefficients of the existing fuselage angle expression (Equation (2)) can be modified to match the desired fuselage angle of attack data. The wing representation is defined for a wing angle of attack range of ± 90 degrees.

The following equations are used to represent the wing. The angle of attack of the wing is expressed as

$$\alpha_w = \alpha_F + i_w - \tan^{-1}\left(\frac{K_w v_i}{V}\right) \quad (3)$$

where

- α_F = fuselage angle of attack
- i_w = wing incidence
- K_w = wing-induced velocity factor
- v_i = main-rotor-induced velocity
- V = velocity

The wing incidence contribution to the wing angle of attack is given by

$$i_w = i_{w0} + \frac{\partial i_w}{\partial n}(n-1) \quad (4)$$

where

i_{w0} = wing incidence at $n=1$

$\frac{\partial i_w}{\partial n}$ = rate of change of wing incidence with load factor

n = load factor

The lift curve slope in the unstalled region is determined as follows:

$$C_{L_\alpha} = a_{2D} \frac{AR}{AR+3} \quad ; \quad \alpha'_{STALL} = \alpha_w = \alpha_{STALL} \quad (5)$$

A graphic representation of the wing lift coefficient as a function of wing angle of attack is presented in Figure 1. The stall angles are determined from

$$\alpha_{STALL} = \frac{C_{L_{MAXP}}}{C_{L_\alpha}} \quad (6)$$

and

$$\alpha'_{STALL} = \frac{C_{L_{MAXN}}}{C_{L_\alpha}} \quad (7)$$

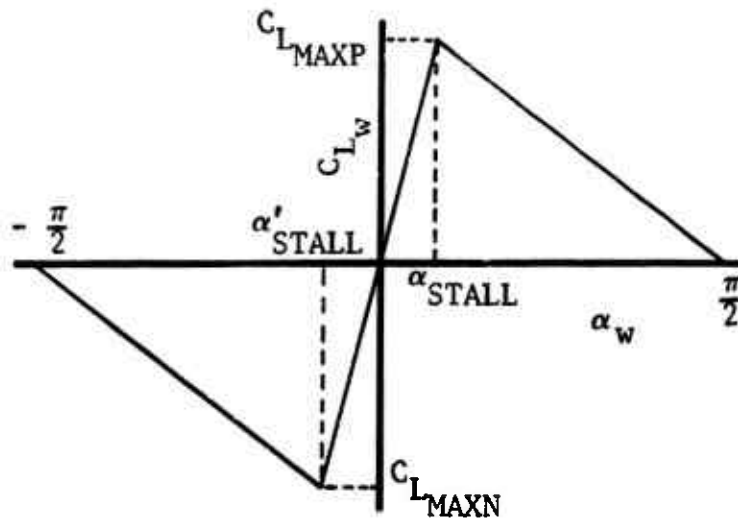


Figure 1. Wing Lift Coefficient Versus Wing Angle of Attack.

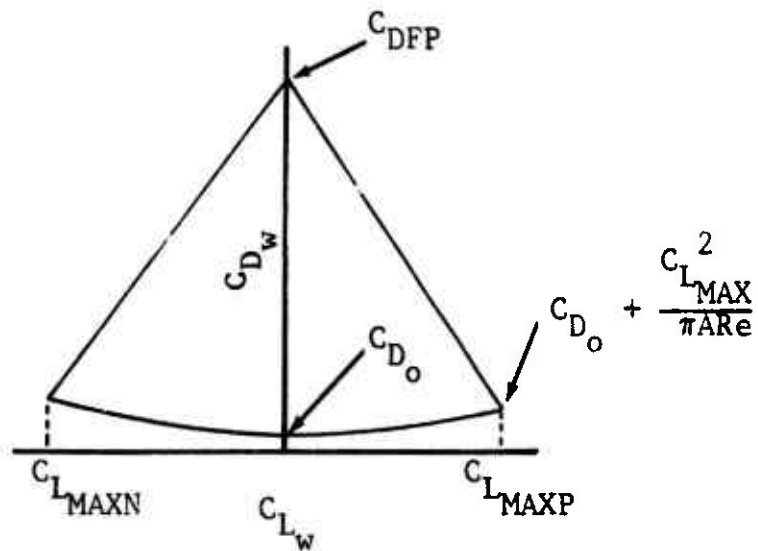


Figure 2. Wing Drag Coefficient Versus Wing Lift Coefficient.

where $C_{L_{MAXP}}$ = maximum positive lift coefficient
 $C_{L_{MAXN}}$ = maximum negative lift coefficient

The lift curve slopes in the stalled regions are calculated from the following expressions:

$$C_{L_a} = \frac{-C_{L_{MAXP}}}{\left(\frac{\pi}{2} - a_{STALL}\right)} \quad ; \quad a_{STALL} < a_w \leq \frac{\pi}{2} \quad (8)$$

$$C_{L_a} = \frac{C_{L_{MAXN}}}{\left(\frac{\pi}{2} + a'_{STALL}\right)} \quad ; \quad -\frac{\pi}{2} \leq a_w < a'_{STALL} \quad (9)$$

The wing lift coefficient can be written as shown below for the different regions of wing angle of attack using the lift curve slopes of Equations (5), (8), and (9).

$$C_{L_w} = C_{L_a} a_w \quad ; \quad a'_{STALL} \leq a_w \leq a_{STALL} \quad (10)$$

$$C_{L_w} = C_{L_a} (a_w - a_{STALL}) + C_{L_{MAXP}} \quad ; \quad a_{STALL} < a_w \leq \frac{\pi}{2} \quad (11)$$

$$C_{L_w} = C_{L_a} (a_w - a'_{STALL}) + C_{L_{MAXN}} \quad ; \quad -\frac{\pi}{2} \leq a_w < a'_{STALL} \quad (12)$$

The variation of wing drag coefficient with wing lift coefficient is shown in Figure 2. In the unstalled region, the wing drag coefficient can be determined as follows:

$$C_{D_w} = C_{D_o} + \frac{C_{L_w}^2}{\pi A R e} \quad ; \quad C_{L_{MAXN}} \leq C_{L_w} \leq C_{L_{MAXP}} \quad (13)$$

where C_{D_o} = drag coefficient at zero angle of attack
 e = wing efficiency factor

For the stalled region, the wing drag coefficient can be written as

$$C_{D_w} = \left[\frac{\left(C_{D_o} + \frac{C_{L_{MAX}}^2}{\pi A R e} \right) - C_{DFP}}{C_{L_{MAX}}} \right] C_{L_w} + C_{DFP} \quad (14)$$

where C_{DFP} = drag coefficient of flat plate

$$C_{L_{MAX}} = C_{L_{MAXP}} \quad \text{if } C_{L_w} > 0$$

$$C_{L_{MAX}} = C_{L_{MAXN}} \quad \text{if } C_{L_w} < 0$$

The wing lift is defined by

$$L_w = q_w S_w C_{L_w} \quad (15)$$

where $q_w = \frac{1}{2} \rho [V^2 + (K_w v_i)^2]$

S_w = wing area

The wing drag is calculated from

$$D_w = q_w S_w C_{D_w} \quad (16)$$

The above equations were evaluated using MCEP. The results of MCEP were compared to data generated by the maneuver section of C81 (Reference 3) as shown in Figures 3 and 4. The aircraft used for the evaluation was an AH-1G helicopter with a wing of 60 square feet and an aspect ratio of 6. The wing incidence was set at 14 degrees. The MCEP data were generated using the pullup/pushover controller. The C81 data were generated from a 1-inch pull and hold.

The comparison shows good agreement for both the pullup and pushover maneuvers. In the C81 maneuvers, no attempt is made to return the aircraft to level flight. In the MCEP maneuvers, the aircraft is returned to level flight.

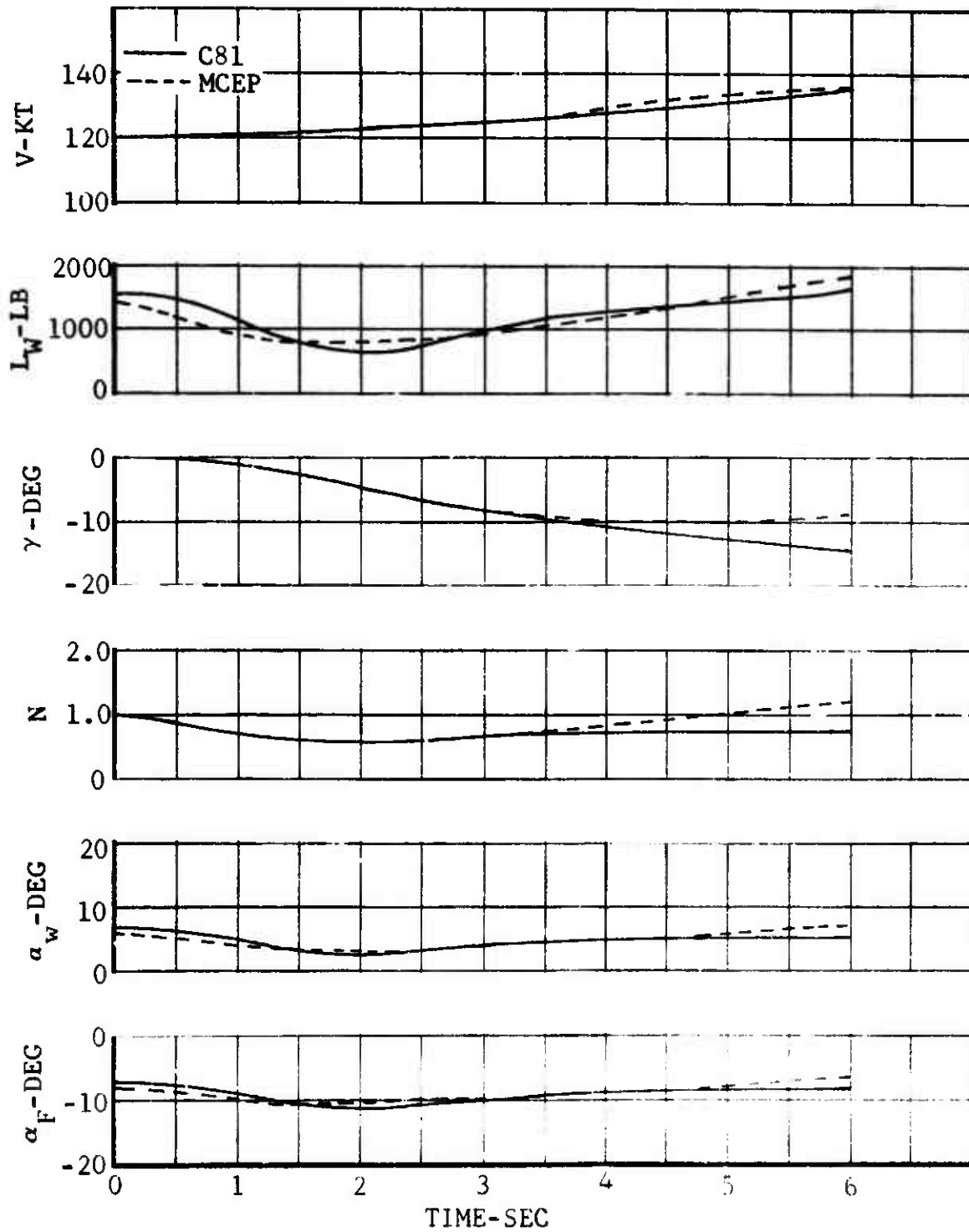


Figure 3. Comparison of Pushover Maneuver Between C81 and MCEP for a Winged Helicopter.

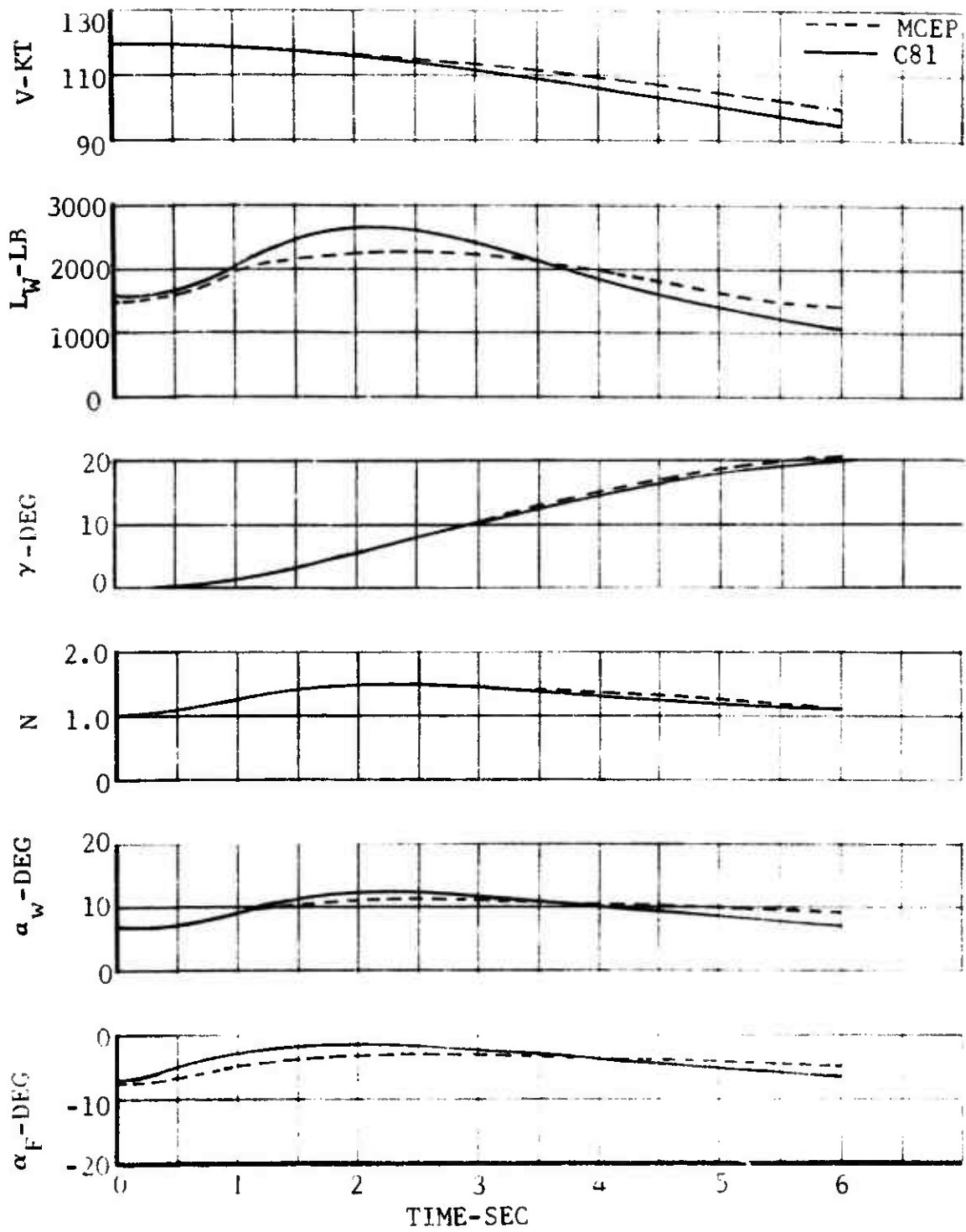


Figure 4. Comparison of Pullup Maneuver Between C81 and MCEP for a Winged Helicopter.

FLIGHT DYNAMICS

The flight controllers send commands to the flight dynamics subroutine where the response to these commands is generated. The helicopter is considered to be oriented in space as shown in Figure 5. This subroutine receives commands in the wind axes system in the form of linear accelerations. Then the accelerations are transformed into the inertial reference frame. Here the accelerations are integrated to determine velocity and position. The angular rates are determined from the accelerations and velocities in the inertial reference frame. The aircraft's constraints such as structural or aerodynamic are applied to prevent a commanded parameter from violating a constraint.

The coordinate system for flight dynamics shown in Figure 5 is the standard Euler axis system. In the ground reference system, X_E is positive due north, Y_E is positive to the east, and Z_E is positive downward. In the wind axes system, the X_W axis passes through the center of gravity of the aircraft and is directed along the velocity vector and is positive in the direction of the velocity vector. The Z_W axis is perpendicular to X_W axis, contained in the plane of symmetry, and positive downward. The Y_W axis is perpendicular to the $X_W Z_W$ plane and is directed in such a way that a right-handed trihedral is formed. The orientation of the wind axes with respect to the ground reference system is described in terms of three angles. The angles are chi (χ), gamma (γ), and phi (ϕ) as shown in Figure 5. These angles should not be confused with the standard body axes angles with respect to the ground reference system. The angle between the $X_E Z_E$ plane and the plane which contains the swinging of the velocity vector is ϕ . In this analysis, it is assumed that a plane passing through the longitudinal body axis and including the yaw axis, must also include the velocity vector (i.e., no sideslip).

The following transformation matrix [T] is used to resolve accelerations in the wind axes to accelerations in the ground reference system.

$$[T] = \begin{bmatrix} \cos\gamma\cos\chi & \sin\phi\sin\gamma\cos\chi & \cos\phi\sin\gamma\cos\chi \\ & -\cos\phi\sin\chi & +\sin\chi\sin\phi \\ \cos\gamma\sin\chi & \sin\phi\sin\gamma\sin\chi & \cos\phi\sin\gamma\sin\chi \\ & +\cos\phi\cos\chi & -\sin\phi\cos\chi \\ -\sin\gamma & \sin\phi\cos\gamma & \cos\phi\cos\gamma \end{bmatrix} \quad (17)$$

X'_E, Y'_E, Z'_E ARE THE
GROUND REFERENCE AXES
TRANSLATED TO THE
ROTORCRAFT CG

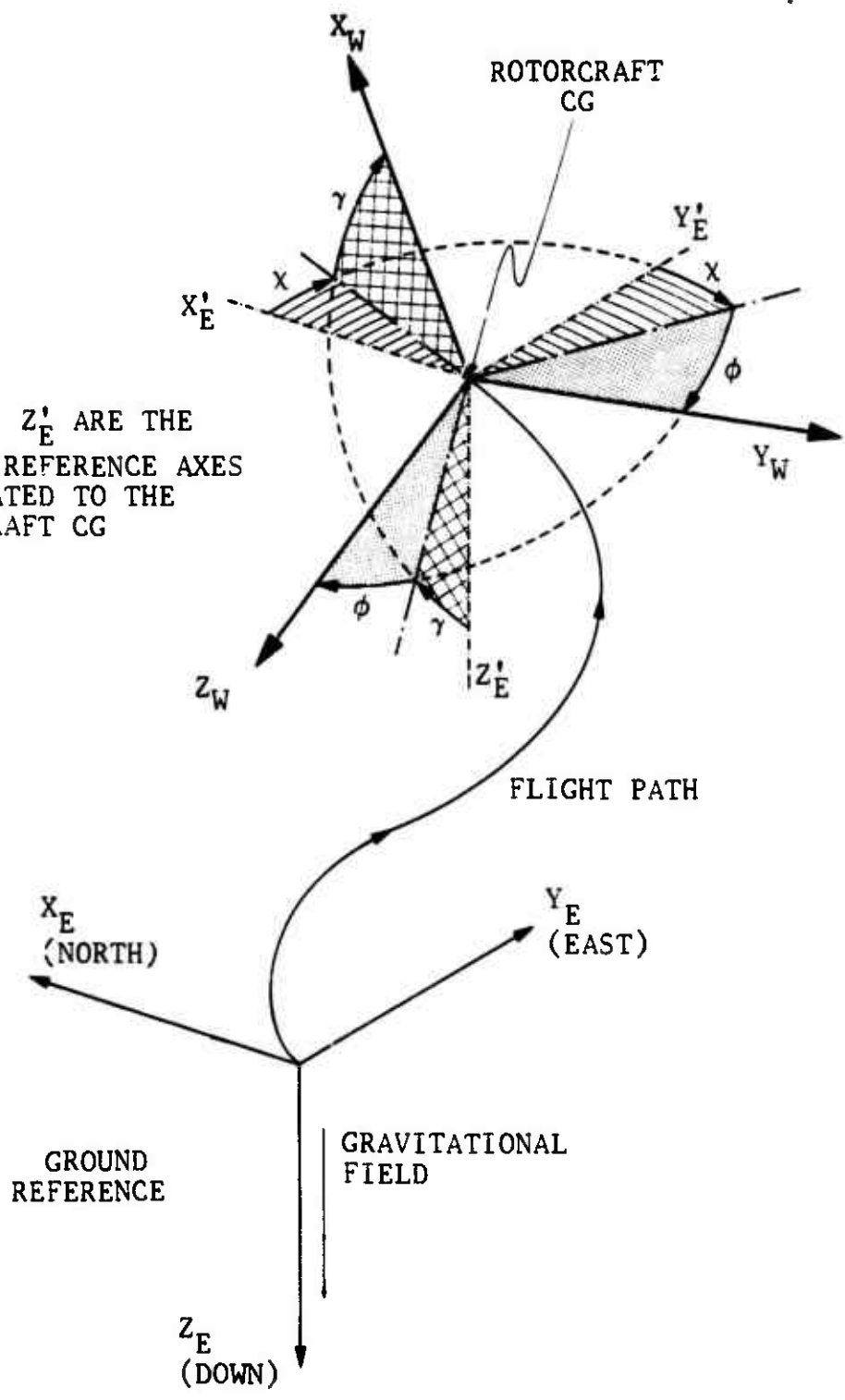


Figure 5. MCEP Coordinate System.

$$\begin{bmatrix} \bar{i}_E \\ \bar{j}_E \\ \bar{k}_E \end{bmatrix} = [T] \begin{bmatrix} \bar{i}_W \\ \bar{j}_W \\ \bar{k}_W \end{bmatrix} \quad (18)$$

The above matrix is orthogonal and thus has the property that $[T]^{-1} = [T]^T$.

The equation of motion for the aircraft relative to a flat, nonrotating earth becomes

$$\bar{F}_W = m \bar{a}_W = m \frac{d\bar{V}}{dt} \quad (19)$$

The rate of change of the velocity vector is

$$\frac{d\bar{V}}{dt} = \frac{d(\bar{i}_W V)}{dt} = \bar{i}_W \dot{V} + \frac{d\bar{i}_W}{dt} V \quad (20)$$

From Poisson's formulas, the time rate of change of the unit vector tangent to the flight path and the angular velocity are given by

$$\begin{aligned} \frac{d\bar{i}_W}{dt} &= \bar{\omega}_W \times \bar{i}_W = (\bar{i}_W p_W + \bar{j}_W q_W + \bar{k}_W r_W) \times \bar{i}_W \\ \frac{d\bar{i}_W}{dt} &= \bar{j}_W r_W - \bar{k}_W q_W \end{aligned} \quad (21)$$

Thus Equation (20) becomes

$$\frac{d\bar{V}}{dt} = \bar{i}_W \dot{V} + (\bar{j}_W r_W - \bar{k}_W q_W) V \quad (22)$$

Rewriting Equation (19) and using Equation (22), the scalar equations are

$$\Sigma F_{x_W} = m\dot{V} \quad (23)$$

$$\Sigma F_{y_W} = mVr_W \quad (24)$$

$$\Sigma F_{z_W} = -mVq_W \quad (25)$$

The wind axes rates are related to the fixed reference rates as follows:

$$\begin{bmatrix} p_W \\ q_W \\ r_W \end{bmatrix} = \begin{bmatrix} 1 & 0 & -\sin\gamma \\ 0 & \cos\phi & \sin\phi\cos\gamma \\ 0 & -\sin\phi & \cos\phi\cos\gamma \end{bmatrix} \begin{bmatrix} \dot{\phi} \\ \dot{\gamma} \\ \dot{\chi} \end{bmatrix} \quad (26)$$

From Equation (26) the wind pitch and yaw rates can be written as

$$q_W = \dot{\gamma}\cos\phi + \dot{\chi}\sin\phi\cos\gamma \quad (27)$$

$$r_W = -\dot{\gamma}\sin\phi + \dot{\chi}\cos\phi\cos\gamma \quad (28)$$

Putting Equations (27) and (28) into (23), (24), and (25) results in

$$\Sigma \frac{F_{x_W}}{m} = ax_W = \dot{v} \quad (29)$$

$$\Sigma \frac{F_{y_W}}{m} = ay_W = V(-\dot{\gamma}\sin\phi + \dot{\chi}\cos\phi\cos\gamma) \quad (30)$$

$$\Sigma \frac{F_{z_W}}{m} = az_W = -V(\dot{\gamma}\cos\phi + \dot{\chi}\sin\phi\cos\gamma) \quad (31)$$

The forces on the left side of Equations (29), (30), and (31) consist of the aerodynamic force and the weight vector. The weight vector in the wind axes becomes

$$\bar{W} = \bar{k}_E W = -\bar{i}_W W\sin\gamma + \bar{j}_W W\sin\phi\cos\gamma + \bar{k}_W W\cos\phi\cos\gamma \quad (32)$$

The aerodynamic force can be expressed as

$$\bar{F}_a = \bar{i}_W F_{ax} + \bar{j}_W F_{ay} + \bar{k}_W F_{az} \quad (33)$$

where the scalar components represent the resultant aerodynamic forces. Substituting Equations (32) and (33) into Equations (29), (30), and (31) results in

$$a_{x_W} = \frac{(F_{ax} - W\sin\gamma)}{m} = \dot{v} \quad (34)$$

$$a_{y_W} = \frac{(F_{ay} + W \sin \phi \cos \gamma)}{m} = V(-\dot{\gamma} \sin \phi + \dot{\chi} \cos \phi \cos \gamma) \quad (35)$$

$$a_{z_W} = \frac{(F_{az} + W \cos \phi \cos \gamma)}{m} = -V(\dot{\gamma} \cos \phi + \dot{\chi} \sin \phi \cos \gamma) \quad (36)$$

The energy method calculates the \dot{V} in Equation (34) instead of the resultant forces. The constraint of no sideslip results in the net aerodynamic force in the Y_W direction being zero ($F_{ay} = 0$). The net aerodynamic force in the Z_W direction is normalized by the weight. Therefore, the resulting wind axes linear acceleration components are

$$a_{x_W} = \dot{V} \quad (37)$$

$$a_{y_W} = g \sin \phi \cos \gamma \quad (38)$$

$$a_{z_W} = g \cos \phi \cos \gamma - ng \quad (39)$$

From Equations (37), (38), and (39), the control parameters available to the flight controllers are \dot{V} , γ , ϕ , and n .

The wind axes accelerations are resolved to the ground reference system using the transformation matrix given in Equation (17). The ground accelerations are assumed to vary linearly between time increments. The accelerations are integrated closed form to give velocity and position equations as follows:

$$a_i = a_{i-1} + m \tilde{t} \quad (40)$$

where $\tilde{t} = t - t_{i-1}$ and

$$m = (a_i - a_{i-1}) / (t_i - t_{i-1})$$

Integrating the acceleration from Equation (40) for the velocity results in the following expression:

$$V_i = V_{i-1} + a_{i-1} \tilde{t} + \frac{1}{2} m \tilde{t}^2 \quad (41)$$

Now integrating the velocity for position yields

$$X_i = X_{i-1} + V_{i-1} \tilde{t} + \frac{1}{2} a_{i-1} \tilde{t}^2 + \frac{1}{6} m \tilde{t}^3 \quad (42)$$

The evaluation of Equations (41) and (42) at $t=t_i$ gives

$$V_i = V_{i-1} + \frac{1}{2}(a_i + a_{i-1})dt \quad (43)$$

$$\text{and } X_i = X_{i-1} + V_{i-1} dt + \frac{1}{6}(a_i + 2a_{i-1})dt^2 \quad (44)$$

$$\text{where } dt = t_i - t_{i-1}$$

Velocity and position are then determined from Equations (43) and (44) at each time increment.

The angular rates are determined from the accelerations in the ground reference system (X_E, Y_E, Z_E). By using the inverse of the transformation matrix of Equation (17), Equations (30) and (31) can be expressed as a function of the ground acceleration as follows:

$$\begin{aligned} ax_E(\sin\phi\sin\gamma\cos\chi - \cos\phi\sin\chi) + ay_E(\sin\phi\sin\gamma\sin\chi + \cos\phi\cos\chi) \\ + az_E\sin\phi\cos\gamma = V(-\dot{\gamma}\sin\phi + \dot{\chi}\cos\phi\cos\gamma) \end{aligned} \quad (45)$$

$$\begin{aligned} ax_E(\cos\phi\sin\gamma\cos\chi + \sin\phi\sin\chi) + ay_E(\cos\phi\sin\gamma\sin\chi - \sin\phi\cos\chi) \\ + az_E\cos\phi\cos\gamma = -V(\dot{\gamma}\cos\phi + \dot{\chi}\sin\phi\cos\gamma) \end{aligned} \quad (46)$$

The results of the simultaneous solution of Equations (45) and (46) for the angular rates ($\dot{\gamma}$ and $\dot{\chi}$) are presented below.

$$\dot{\gamma} = (-ax_E \sin\gamma\cos\chi - ay_E \sin\gamma\sin\chi - az_E \cos\gamma)/V \quad (47)$$

$$\dot{\chi} = (-ax_E \sin\chi + ay_E \cos\chi)/V \cos\gamma \quad (48)$$

The denominator of Equation (48) is the velocity in the $X_E Y_E$ plane and may be calculated from the ground velocities by

$$V_{XYP} = \sqrt{V_{XE}^2 + V_{YE}^2} = V \cos\gamma \quad (49)$$

Roll rate is generated externally by the flight controller.

The angular rates are integrated using the trapezoidal rule as demonstrated below.

$$\gamma_i = \gamma_{i-1} + \frac{1}{2}(\dot{\gamma}_i + \dot{\gamma}_{i-1})dt \quad (50)$$

The flight controllers generate the necessary parameters for Equations (37), (38), and (39).

COMMAND GENERATION

The flight controllers command the helicopter through the linear accelerations in the wind axes. From Equations (37), (38), and (39), the control parameters are \dot{V} , γ , ϕ , and n . The control of \dot{V} is maintained through the rate and magnitude of power supplied from the engine.

The other control parameters are generated by estimating the load factor as a function of time to produce the desired flight trajectory. The relation between the load factor and γ and ϕ can be determined as follows. The solution of Equations (35) and (38) for $\dot{\lambda}$ yields the following expression.

$$\dot{\lambda} = \frac{g \sin\phi \cos\gamma}{V \cos\phi \cos\gamma} + \frac{\dot{V} \sin\phi}{V \cos\phi \cos\gamma} \quad (51)$$

The solution of Equations (36) and (39) for $\dot{\lambda}$ gives the expression below.

$$\dot{\lambda} = \frac{ng}{V \sin\phi \cos\gamma} - \frac{g \cos\phi \cos\gamma}{V \sin\phi \cos\gamma} - \frac{\dot{V} \cos\phi}{V \sin\phi \cos\gamma} \quad (52)$$

An expression for n can be determined from equating Equation (51) and (52). Then n becomes

$$n = \frac{V\dot{\gamma}}{g \cos\phi} + \frac{\cos\gamma}{\cos\phi} \quad (53)$$

To produce a continuous load factor trace, the flight controller selects the required value of γ or ϕ to achieve the desired flight trajectory. Then, the controller predicts the angular accelerations, rates, and displacements required to achieve the angles. From these predicted quantities, the command load factor is generated for flight dynamics according to Equation (53).

The required angular displacement to generate a command load factor is obtained as shown in Figure 6. The following assumptions are made to allow closed-form gains to be calculated. The angle is divided into four stages of equal time increments. The angular acceleration is zero at the end of the second stage.

$$\ddot{\phi}(t_2) = 0 \quad (54)$$

The angular acceleration and rate are zero at the end of the fourth stage and the angular displacement is the commanded angle (ϕ_c).

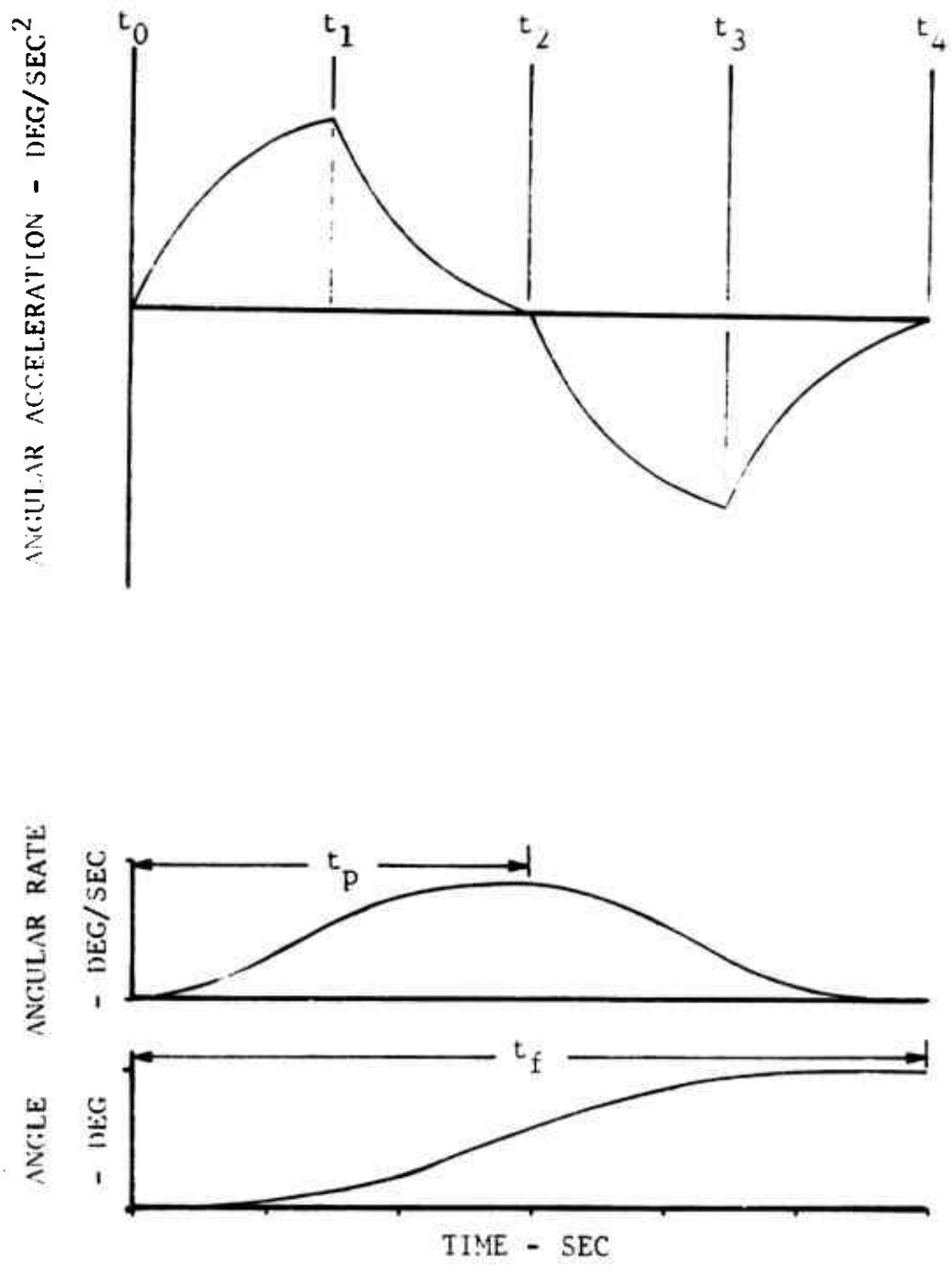


Figure 6. Time History of Command Generator Parameters.

$$\ddot{\phi}(t_4) = 0 \quad (55)$$

$$\dot{\phi}(t_4) = 0 \quad (56)$$

$$\phi(t_4) = \phi_c \quad (57)$$

The angular acceleration is assumed to be of the following form for any one of the four stages:

$$\ddot{\phi}(t) = GK_n \left(1 - e^{-\frac{(t-t_{n-1})}{\tau}} \right) + \ddot{\phi}(t_{n-1}) \quad (58)$$

where

GK_n = gain for the nth stage

$$t_{n-1} \leq t \leq t_n$$

After integrating Equation (58), the angular rate is

$$\begin{aligned} \dot{\phi}(t) = GK_n \left[(t-t_{n-1}) + \tau e^{-\frac{(t-t_{n-1})}{\tau}} - \tau \right] \\ + \ddot{\phi}(t_{n-1})(t-t_{n-1}) + \dot{\phi}(t_{n-1}) \end{aligned} \quad (59)$$

where

$$t_{n-1} \leq t \leq t_n$$

The angular displacement is determined from the integration of Equation (59) to be

$$\begin{aligned} \phi(t) = GK_n \left[0.5(t-t_{n-1})^2 - \tau^2 e^{-\frac{(t-t_{n-1})}{\tau}} - \tau(t-t_{n-1}) + \tau^2 \right] \\ + 0.5 \ddot{\phi}(t_{n-1})(t-t_{n-1})^2 + \dot{\phi}(t_{n-1})(t-t_{n-1}) + \phi(t_{n-1}) \end{aligned} \quad (60)$$

where

$$t_{n-1} \leq t \leq t_n$$

The angular acceleration at the end of the fourth stage ($t=t_4$) can be written as follows.

$$\ddot{\phi}(t_4) = GK_4 \left(1 - e^{-\frac{(t_4 - t_3)}{\tau}} \right) + \ddot{\phi}(t_3) \quad (61)$$

It is convenient to make the following definitions at this time.

$$C_1 = \left(1 - e^{-\frac{t_s}{\tau}} \right) \quad (62)$$

$$C_2 = \left(t_s + \tau e^{-\frac{t_s}{\tau}} - \tau \right) = t_s - \tau C_1 \quad (63)$$

$$C_3 = \left(0.5 t_s^2 - \tau^2 e^{-\frac{t_s}{\tau}} - \tau t_s + \tau^2 \right) = \frac{1}{2} t_s^2 - \tau C_2 \quad (64)$$

where

$$t_s = t_n - t_{n-1} \quad \text{for } n = 1, 2, 3, 4$$

With the use of Equation (62), Equation (61) can be written as

$$\ddot{\phi}(t_4) = GK_4 C_1 + \ddot{\phi}(t_3) \quad (65)$$

Equation (65) can be expanded through the use of Equation (61) and (62) to include the first stage in the following manner.

$$\begin{aligned} \ddot{\phi}(t_4) &= GK_4 C_1 + GK_3 C_1 + \ddot{\phi}(t_2) \\ \ddot{\phi}(t_4) &= GK_4 C_1 + GK_3 C_1 + GK_2 C_1 + \ddot{\phi}(t_1) \\ \ddot{\phi}(t_4) &= GK_4 C_1 + GK_3 C_1 + GK_2 C_1 + GK_1 C_1 + \ddot{\phi}(t_0) \end{aligned} \quad (66)$$

The initial conditions for the angular acceleration, rate, and displacement are defined as shown below.

$$\ddot{\phi}(t_0) = \ddot{\phi}_0 \quad (67)$$

$$\dot{\phi}(t_0) = \dot{\phi}_0 \quad (68)$$

$$\phi(t_0) = \phi_0 \quad (69)$$

Now, the angular acceleration at $t=t_4$ can be written in terms of its initial condition from Equation (66) and (67) as

$$\ddot{\phi}(t_4) = (GK_4 + GK_3 + GK_2 + GK_1)C_1 + \ddot{\phi}_0 \quad (70)$$

The angular rate at $t=t_4$ can be expressed as a function of its initial conditions using Equations (59), (63), and (68) using the method demonstrated above for angular acceleration. This expression becomes

$$\begin{aligned} \dot{\phi}(t_4) = & [4\dot{\phi}_0 + (3GK_1 + 2GK_2 + GK_3)C_1]t_s \\ & + (GK_1 + GK_2 + GK_3 + GK_4)C_2 + \dot{\phi}_0 \end{aligned} \quad (71)$$

A similar expression for the angular displacement at $t=t_4$ can be developed using Equations (60), (63), and (69). The angular displacement is

$$\begin{aligned} \phi(t_4) = & 0.5[16\ddot{\phi}_0 + (9GK_1 + 4GK_2 + GK_3)C_1]t_s^2 \\ & + [4\dot{\phi}_0 + (3GK_1 + 2GK_2 + GK_3)C_2]t_s \\ & + (GK_1 + GK_2 + GK_3 + GK_4)C_3 + \phi_0 \end{aligned} \quad (72)$$

Closed-form expressions for the individual gains can be determined by applying the constraints of Equations (54), (55), (56), and (57) to Equations (59), (60), (61), (70), (71), and (72). The results of the above application are presented below as expressions for the four gains.

$$\begin{aligned} GK_1 = \frac{1}{4C_1} \left\{ \frac{2}{t_s^2} \left[\phi_c - \phi_0 + \frac{\ddot{\phi}_0 C_3}{C_1} - \left(4\dot{\phi}_0 - \frac{2\ddot{\phi}_0 C_2}{C_1} + \frac{\ddot{\phi}_0 C_2^2}{C_1^2 t_s} \right. \right. \right. \\ \left. \left. - \frac{\dot{\phi}_0 C_2}{C_1 t_s} - \frac{2\ddot{\phi}_0 C_2}{C_1} \right) t_s \right] - 10\ddot{\phi}_c - \frac{\ddot{\phi}_0 C_2}{C_1 t_s} + \frac{\dot{\phi}_0}{t_s} \right\} \end{aligned} \quad (73)$$

$$GK_2 = -\frac{\ddot{\phi}_0}{C_1} - GK_1 \quad (74)$$

$$GK_3 = - GK_4 \quad (75)$$

$$GK_4 = \frac{2\ddot{\phi}_o}{C_1} - \frac{\ddot{\phi}_o C_2}{t_s C_1^2} + \frac{\dot{\phi}_o}{t_s C_1} + GK_1 \quad (76)$$

By collecting terms in Equations (73), (74), (75), and (76), and using the definitions of Equations (62), (63), and (64), the gain equations can be reduced to the following form.

$$GK_1 = \frac{1}{(2C_1 t_s^2)} \left\{ \phi_c - \phi_o - \dot{\phi}_o \left[\tau + t_s (7/2 - 1/C_1) \right] - \ddot{\phi}_o t_s \left[t_s (5 - 4/C_1 + 1/C_1^2) + (7/2 - 1/C_1) \right] \right\} \quad (77)$$

$$GK_2 = - \frac{\ddot{\phi}_o}{C_1} - GK_1 \quad (78)$$

$$GK_3 = - GK_4 \quad (79)$$

$$GK_4 = \frac{1}{C_1 t_s} \left[\dot{\phi}_o + \ddot{\phi}_o \left(2t_s - \frac{C_2}{C_1} \right) + GK_1 C_1 t_s \right] \quad (80)$$

In MCEP, a command generator subroutine computes the gains required to achieve a commanded angle based on the initial conditions using Equations (77) through (80).

If the predicted peak rate is greater than the maximum angular rate, then the command generator subroutine increases the stage time until the peak rate is less than the maximum angular rate. The command generator subroutine creates table values for C_1 , C_2 , C_3 , and the exponential function for increments of .05 second. The current values of angular acceleration and rate are computed from Equations (58) and (59) using the table values. If the predicted angle is different from the actual angle by 0.001 radian at the end of the second stage, then the gains are recomputed for the third and fourth stages to match the constraints of Equations (55), (56), and (57).

The value of angular rate from the pitch command generator subroutine is used to predict $\dot{\gamma}$ in Equation (53). The value of angular rate from the roll command generator subroutine is used for roll rate which is integrated in flight dynamics to produce a roll angle.

The stage times for the roll, pitch, and yaw command generator subroutines are initialized using the maneuver urgency factor, MUF, unless otherwise specified. MUF controls the time required for the aircraft to achieve the desired angles. For maneuvers involving roll angle changes, MUF influences the roll-in and roll-out times for the turn. For maneuvers involving flight path changes, MUF influences the times for pulling-up and pushing-over. A MUF of 1 means that the aircraft will achieve the commanded angle in the shortest time possible. MUF is related to the time for achieving the desired angle change through the time to reach peak angular rate. The time to reach peak roll rate is determined from

$$t_{pr} = \frac{|\phi_c - \phi_o|}{MUF \dot{\phi}_{MAX}} \quad (81)$$

where $\dot{\phi}_{MAX}$ = maximum allowable roll rate

The peak roll rate required in achieving the desired angle is influenced by MUF. For example, the time to peak roll rate is .1 second for an angle change of 60 degrees, a MUF of 1, and a $\dot{\phi}_{MAX}$ of 60 degrees per second. The peak roll rate would be 60 degrees per second. For the same conditions with a MUF of 0.5, the time to peak roll rate would be 2 seconds and the peak roll rate would be 30 degrees per second. The above method for determining time to peak roll rate is also used for determining pitch and yaw times. Therefore, a decrease in MUF results in lower angular rate and increased time to achieve the desired angle. The time to peak angular rate may be increased to keep the peak load factor within the prescribed bounds. This modification occurs in maneuvers involving flight path angle changes. By increasing the time to peak angular rate, $\dot{\gamma}$ is reduced and the value of the load factor varies according to Equation (53).

DESCRIPTION OF MCEP

The Maneuver Criteria Evaluation Program was designed to simulate mission profiles by specifying the appropriate MCEP maneuvers in the desired order. The capability and function of the MCEP maneuvers are reviewed as they relate to the mission simulation. The evaluation of the mission profile is considered in terms of the quantitative information provided from the program.

MISSION SPECIFICATION

The simulation of mission profiles using MCEP required defining the profile as a series of individual maneuvers. The maneuvers available for simulating mission profiles in MCEP are listed in Table I. The mission profile can consist of any number of the MCEP maneuvers. To set up the profile, the required maneuvers are placed in order of their occurrence in the profile. Then each maneuver is performed prior to calling and reading the data for the next maneuver. The maneuver identification number determines which maneuver is called in MCEP. If a specific maneuver is required for a profile and it is not a MCEP maneuver, then it may be possible to use several MCEP maneuvers to achieve a similar result. It is inconvenient to estimate the ground distances traveled in performing the individual maneuvers as the profile is being formulated. Since the locations of targets are specified in terms of ground positions, it is difficult to determine, before the maneuvers are executed, exactly where the target should be placed to correspond to the desired location after the completion of the maneuvers. Several MCEP maneuvers can be used to locate the aircraft and then fly the aircraft to the desired ground location. The aircraft can be in free flight while approaching the target area. Then the aircraft is returned to captive flight by re-establishing a desired ground track.

MCEP MANEUVERS

Each of the MCEP maneuvers is described to define its capabilities. The assumptions made in the formulation of the maneuvers are reviewed and the input requirements are listed.

Cruise

The cruise maneuver flies the helicopter to a specified aim point or a specified slant range from the air point at constant airspeed, altitude, and heading. This maneuver can be used to arrive within a specified target area or to regroup at a given point to initiate another sequence of maneuvers which require a certain ground location.

TABLE I. MCEP MANEUVER IDENTIFICATION

Identification Number	Title
M01	Cruise
M02	Acceleration/Deceleration at Constant Altitude
M03	Turn at Constant Airspeed and Altitude
M04	Climb/Descent at Constant Airspeed
M05	Pullup/Pushover at Desired Load Factor
M06	Auto Turn at Constant Airspeed and Altitude
M07	Return to Target at Constant Altitude
M08	Dive/Rolling Pullout
M09	Climbing/Descending Turn at Constant Airspeed
M10	Sideward Acceleration/Deceleration
M11	Sideward Acceleration/Pedal Turn Into Wind
M12	Orbit at Constant Airspeed
M13	Pedal Turn at Hover
M14	Collective Pop-Up at Constant Attitude and Low Airspeed
M15	Climbing Return to Target

The cruise maneuver is controlled in the horizontal plane (X_{EY_E}) by calculating the slant range and comparing it to the desired slant range. The time increment is controlled by the projected slant range which is the estimated slant range at the next time point. A time increment of 0.5 second is used until the projected slant range is within one time increment of the desired slant range. At this point the time increment is switched to 0.05 second. The maneuver is completed when the slant range is less than the desired slant range. If the slant range is not decreasing, then the maneuver is terminated.

The input data required by the cruise maneuver are the aim points (XAP, YAP) and the minimum slant range to the aim point (CSLANT).

Acceleration/Deceleration at Constant Altitude

The acceleration/deceleration controller flies the aircraft to a velocity which is within the specified error band of the commanded velocity. This maneuver can be used in mission simulation to increase or decrease the velocity of the aircraft while maintaining constant altitude.

This maneuver is controlled by the magnitude and rate of application of power. The maneuver is initiated by the application of power as shown in Figure 7. A maneuver urgency factor, MUF, of 1 results in the fastest application of power. The energy method computes ax_W as

$$ax_W = \dot{V} = \frac{(HPA-HP)550\eta g}{(GW V)} \quad (82)$$

where $\eta = 1$ if $HPA > HP$

$\eta = 0.8$ if $HPA < HP$

HP = power required at the flight condition

HPA = power supplied from the engine

Equation (82) causes \dot{V} to approach infinity as velocity approaches zero. A method of calculating \dot{V} was developed for the low speed regime in Reference 1. Horizontal accelerations are performed most effectively at low speed by tilting the rotor thrust vector so that the horizontal component acts to accelerate the helicopter, as illustrated in Figure 8. The

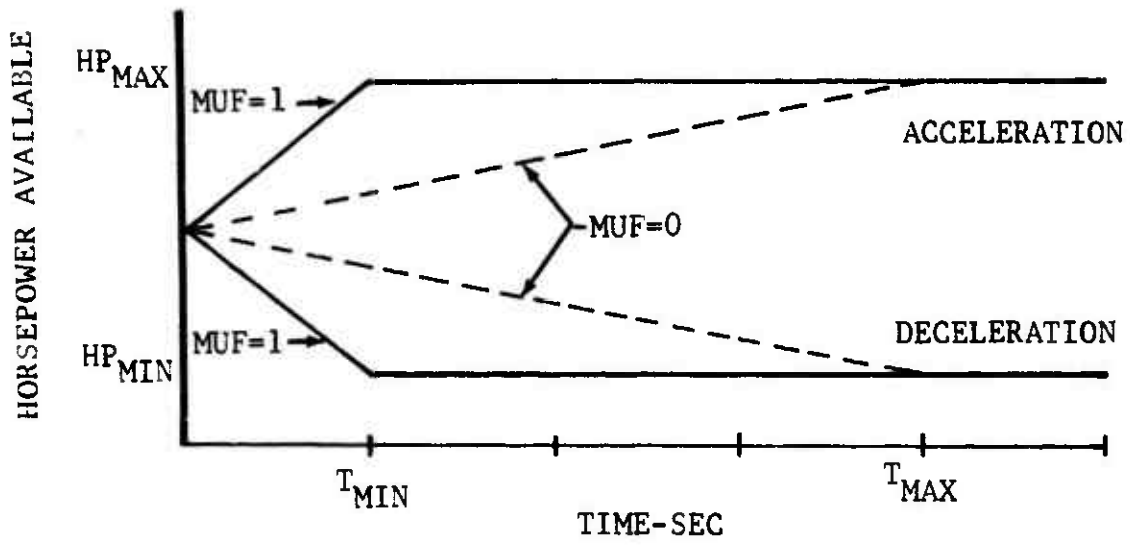


Figure 7. Application of Power in Acceleration or Deceleration Maneuver.

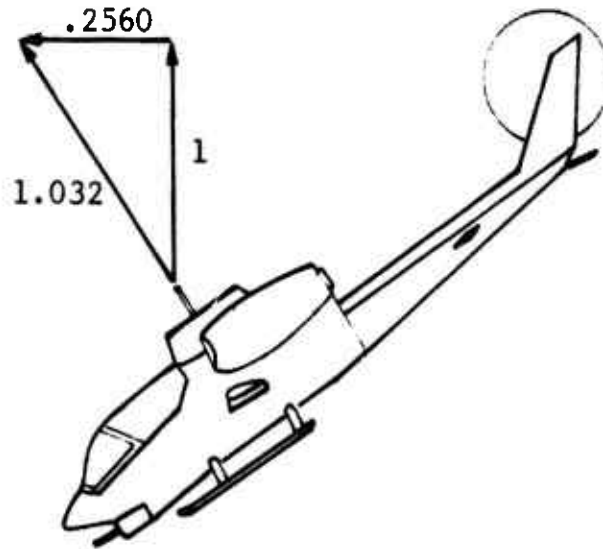


Figure 8. Thrust Vectoring for Linear Acceleration.

method requires that the horizontal component be increased until the power required matches the power supplied by the engine. This method requires an iterative process to match the power and vector summation constraints. A special flight dynamic subroutine was created to handle the iteration procedure for this maneuver. Equation (82) yields excellent results for airspeeds above 30 knots.

The controller restricts the maximum deceleration to a negative 0.5 g in the low speed regime. The power supplied by the engine is increased automatically to maintain this value. The flight controller increases or decreases the power supplied by the engine according to the value of the weighting factor (WF). The weighting factor is computed from

$$WF = \left[\frac{(V - V_c)}{V_{ERR}} \right]^2 \quad (83)$$

where

WF = 1 if WF > 1

V_c = command velocity

V = velocity

V_{ERR} = error band on velocity

Once the velocity is within the error band, the power difference between power supplied by the engine and the power required for the flight condition is multiplied by the weighting factor. As the velocity approaches the command velocity, the weighting factor approaches zero, which results in no change in power available, and the velocity is stabilized. The controller stabilizes the velocity by setting the power available equal to the power required when the acceleration is less than 0.05 ft/sec². This terminates the maneuver in a reasonable amount of time.

An example of this maneuver is shown in Figure 9. The input requirements are the command velocity, velocity error band, maneuver urgency factor, and the minimum power setting.

Turn at Constant Airspeed and Altitude

The level turn maneuver flies the aircraft through a given heading change at constant airspeed and constant altitude. This maneuver is accomplished by rolling into a turn and

MCEP INPUT

VC=60

VERR=2

MUF=1

PSL=0.5

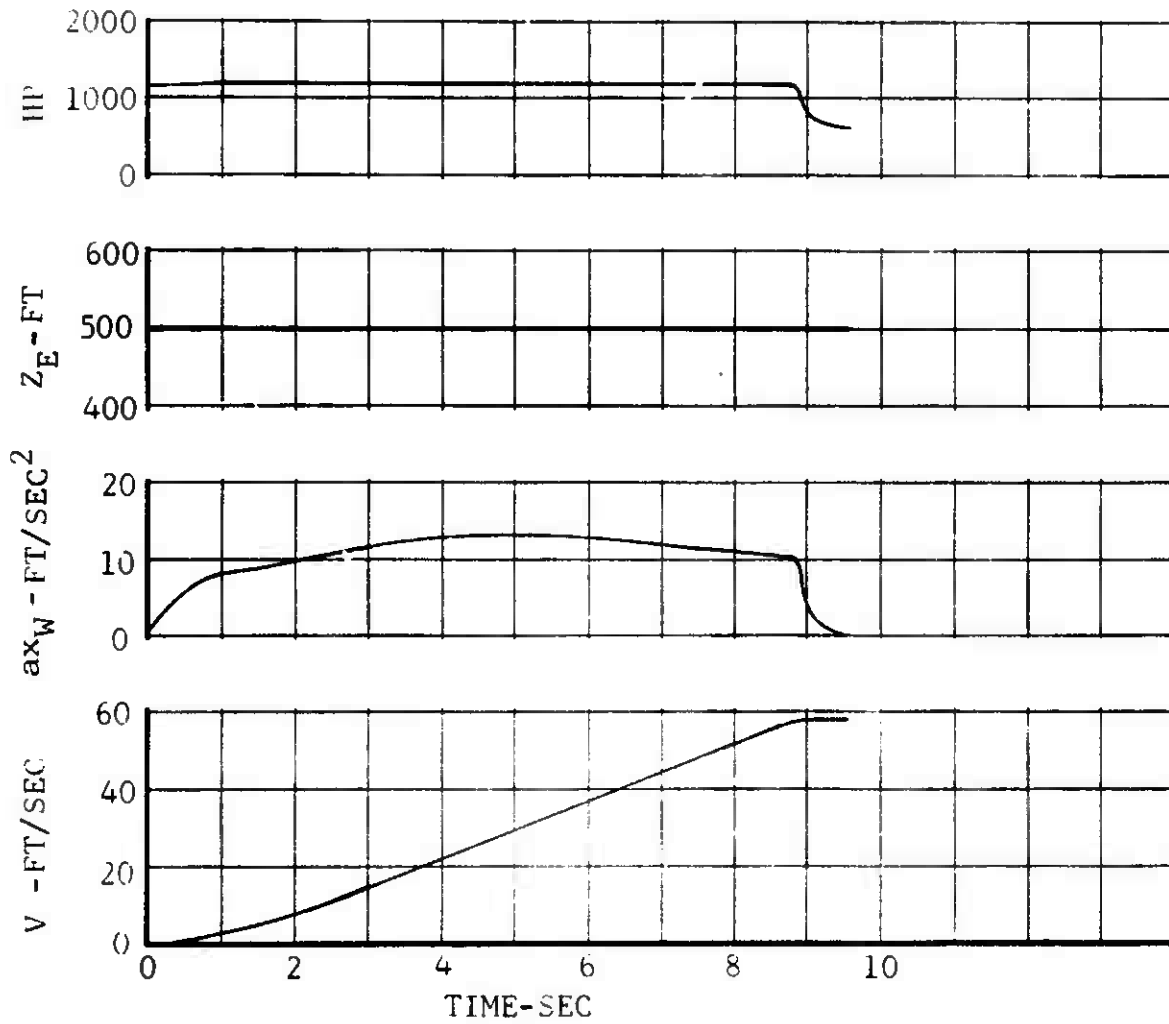


Figure 9. Time History of Acceleration Maneuver for AH-1G Helicopter at 9500 Pounds.

holding the resulting turn rate until the proper time to roll-out on the desired heading. This maneuver can be used in mission simulation to obtain heading changes when either the absolute heading is known or the delta heading is known. If the direction of the turn is not specified, the controller will execute the maneuver in the direction of minimum heading change.

The turn controller was designed to match the constraints of constant airspeed and constant altitude. The constraint of constant altitude results in a curvature of the flight path in the horizontal plane ($X_E Y_E$). For this curvature to occur, the acceleration (az_E) and the velocity (V_{ZE}) in the vertical plane ($X_E Z_E$) must be zero. From equation (17), az_E can be written as a function of the wind axes accelerations as follows:

$$az_E = -ax_W \sin \gamma + ay_W \sin \phi \cos \gamma + az_W \cos \phi \cos \gamma \quad (84)$$

The constraint of constant airspeed results in ax_W being zero while the constraint of V_{ZE} being zero forces γ and az_E to be zero. Equation (84) may now be written in the following form.

$$az_W = -ay_W \sin \phi / \cos \phi \quad (85)$$

Rewriting Equation (85) using Equations (38) and (39), the following expression results.

$$\begin{aligned} g \cos \phi - ng &= -g \sin^2 \phi / \cos \phi \\ n &= 1 / \cos \phi \end{aligned} \quad (86)$$

Therefore, for the turn to be executed at constant airspeed and constant altitude, the turn controller must insure that the load factor meets the requirements of Equation (86) and that ax_W is zero. The airspeed is controlled by not allowing the aircraft to roll to a bank angle greater than the bank angle which requires maximum power at that airspeed.

The initiation of the roll-out occurs at the time when the sum of the estimated heading change from the roll-out and the current heading is equal to or greater than the desired heading. The estimation of heading change resulting from a change in roll angle is computed as follows. First, eight values of roll angle are predicted for returning the roll angle to zero from the current values of roll acceleration, rate, and displacement in the specified time. Then eight values of turn rate are computed using the expression

$$\dot{\chi}_i = \frac{g \tan(\phi_i)}{V} \quad (87)$$

where ϕ_i represents the predicted value of ϕ at $t = t_i$.

The values of turn rate are then integrated to produce the estimated heading change.

An example of this maneuver is presented in Figure 10. The input requirements are the desired load factor, command heading, maneuver urgency factor, delta heading, and the direction of turn.

Climb/Descent at Constant Airspeed

The climb/descent controller flies the aircraft to a specified altitude at constant airspeed. This maneuver is performed by establishing the desired flight path angle within the specified load factor limits. The flight path angle is maintained until the time to return the flight path angle to zero to arrive at the desired altitude within the specified load factor limits.

The constraint of constant airspeed is satisfied by the controller through the proper choice of the flight path angle. The controller predicts the maximum or minimum flight path angle based on the power available. If the commanded flight path angle is within the limit of the angle based on power available, then the commanded angle is executed. However, if the commanded angle is outside the power limited angle, then the power limited angle is executed. The above procedure insures that sufficient horsepower is available to maintain zero acceleration in the wind axes ($ax_w = 0$).

This maneuver results in curvature of the flight path in the vertical plane to establish the flight path angle. The constraint of motion in the vertical plane establishes that ϕ is zero. If $\phi=0$, then Equation (38) becomes

$$ay_w = 0 \quad (88)$$

The constraint of constant airspeed yields

$$ax_w = 0 \quad (89)$$

From Equation (47), the rate of change of gamma is a function of the ground accelerations. The ground accelerations can be

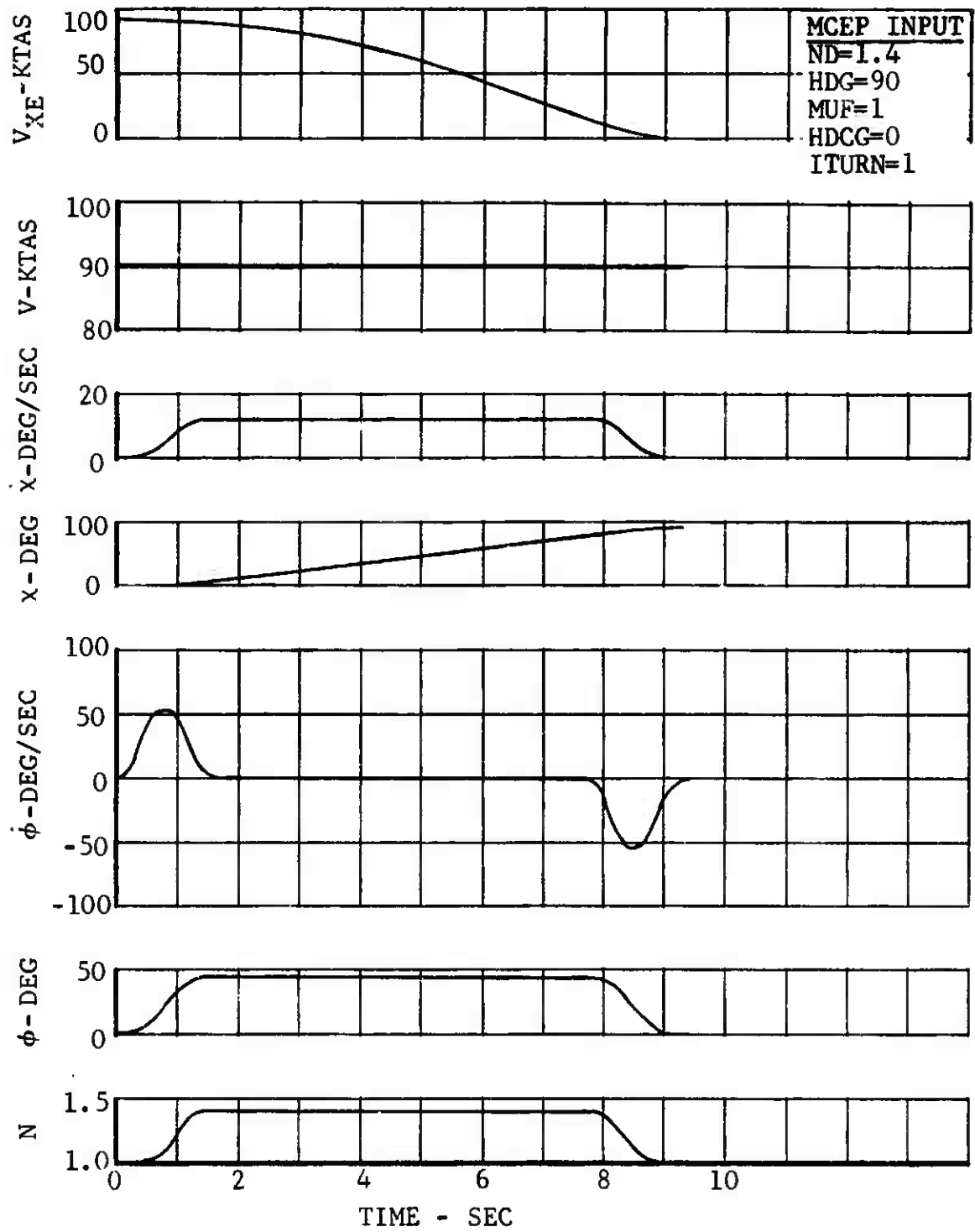


Figure 10. Time History of Turn at Constant Airspeed and Altitude for AH-1G Helicopter at 90 Knots and 9500 Pounds.

expressed as follows after applying Equations (88) and (89).

$$\begin{aligned}ax_E &= az_W \sin \gamma \cos \chi \\ay_E &= az_W \sin \gamma \sin \chi \\az_E &= az_W \cos \gamma\end{aligned}\tag{90}$$

From Equation (47) and Equation (90), the expression for the time rate of change of gamma is

$$\dot{\gamma} = - \frac{az_W}{V}\tag{91}$$

The expression for load factor can be determined from Equations (91) and (39) which yield

$$n = \frac{\dot{\gamma}V}{g} + \cos \gamma\tag{92}$$

The climb/descent controller insures that the load factor meets the requirements of Equation (92). The load factors required to achieve the flight path angle are bounded by input values of load factor limits. The peak load factor in achieving the flight path angle is compared against the appropriate limit. If it is outside the limit, then the time to achieve the angle is increased, which reduces γ and $\dot{\gamma}$ in Equation (92). This time change results in a new value of peak load factor to be compared against the limit. This procedure is continued until a value of time is found which passes the load factor test. Some variation in airspeed will occur if the value of peak load factor and flight path angle result in the power required being greater than the power available.

The recovery portion of the maneuver is initiated when the sum of the estimated altitude change in returning the flight path angle to zero and the current altitude is equal to the desired altitude. The estimation of altitude change in reducing gamma to zero is computed as follows. Eight values (two per stage of angular command generation) of gamma are predicted for returning gamma to zero from the current values of gamma acceleration, rate, and displacement in the specified time. The peak load factor is estimated and compared to the appropriate load factor limit. If the peak load factor fails the test, the time is extended and the values of gamma are predicted using the new time. From the values of gamma, the vertical velocity is computed from

$$V_{Z_i} = V \sin(\gamma_i)\tag{93}$$

where γ_i represents the predicted value of γ at $t = t_i$.

The altitude change is calculated from the integration of the vertical velocities.

An example of this maneuver is shown in Figure 11. The input requirements for this maneuver are the command altitude, maneuver urgency factor, minimum power setting, command gamma, maximum load factor, and minimum load factor.

Pullup/Pushover at Desired Load Factor

The pullup/pushover controller flies the aircraft to a desired load factor within a specified time. The desired load factor is maintained for the required time if the input airspeed limits are not violated. This maneuver can be used in mission simulation to evaluate the impact of specification maneuvers on the flight path.

This maneuver results in a curvature of the flight path in the vertical plane ($X_F Z_E$). This requires that the acceleration in the Y_W direction (a_{Y_W}) be zero, which means that $\delta = 0$. The expression for load factor is the same as for the level turn, given in Equation (92). The pullup/pushover controller selects the value of gamma which will produce the desired value of load factor in the specified amount of time. The desired load factor is maintained by the controller for the required time unless the airspeed limits are violated. At the conclusion of the holding time, the flight path angle is returned to zero while staying within the appropriate load factor limit.

An example of this maneuver is presented in Figure 12. The input requirements for this maneuver are command load factor, maximum load factor, minimum load factor, minimum power setting, time to achieve command load factor, time to hold command load factor, and minimum velocity.

Auto Turn at Constant Airspeed and Altitude

The auto turn maneuver flies the aircraft to the necessary heading to intersect the input aim points while maintaining constant airspeed and altitude. The auto turn controller determines the direction and required heading change to acquire the heading which intersects the aim points. This maneuver can be used in mission simulation to align the nose of the aircraft with a target or to locate the aircraft's position with respect to a known ground position.

The auto turn maneuver is controlled by the required heading change to achieve a heading which intersects the aim points. The auto turn controller meets the same constraints as the turn controller discussed in the above section. The primary difference is the determination of the direction and magnitude of the

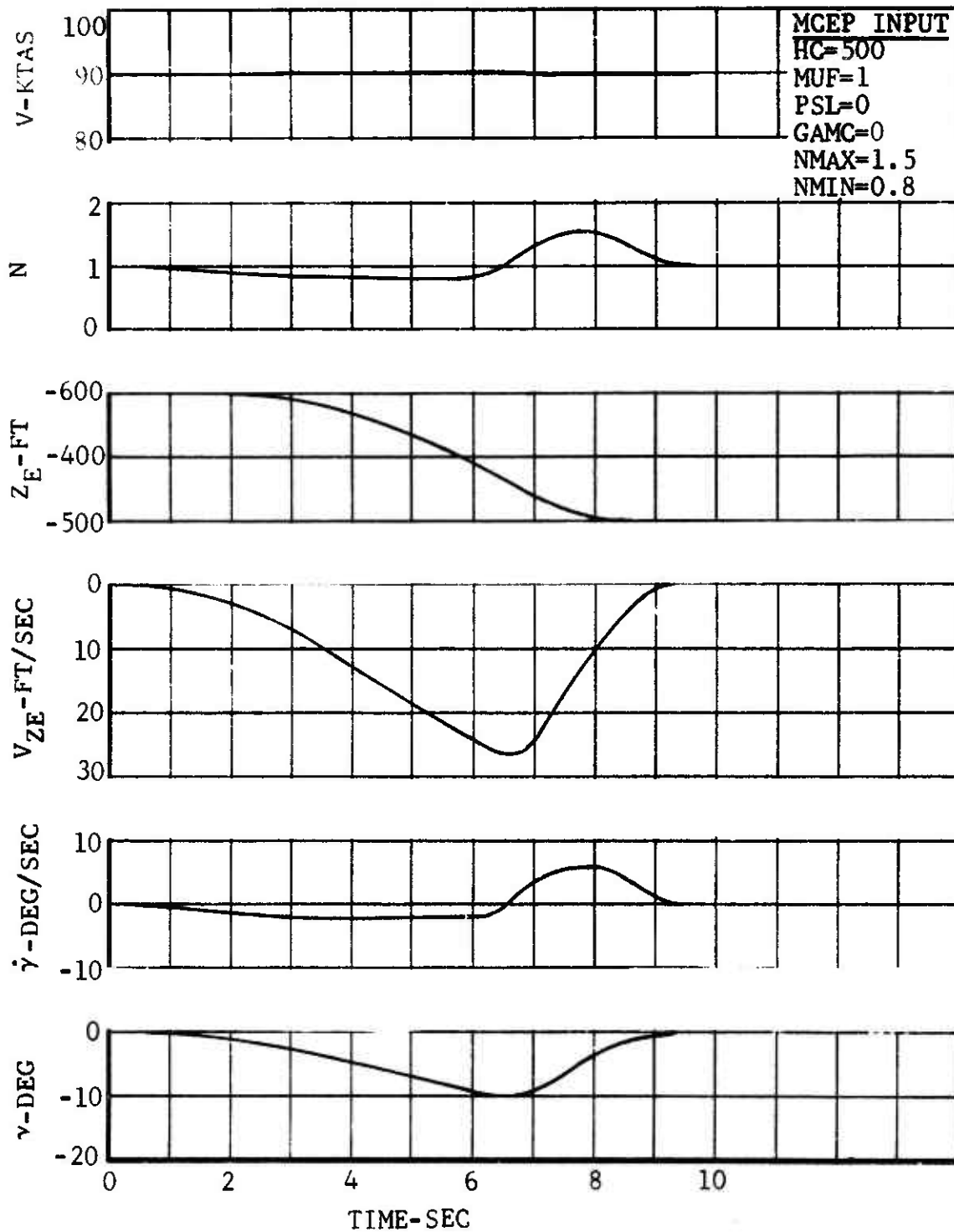


Figure 11. Time History of Descent for AH-1G Helicopter at 90 Knots and 9500 Pounds.

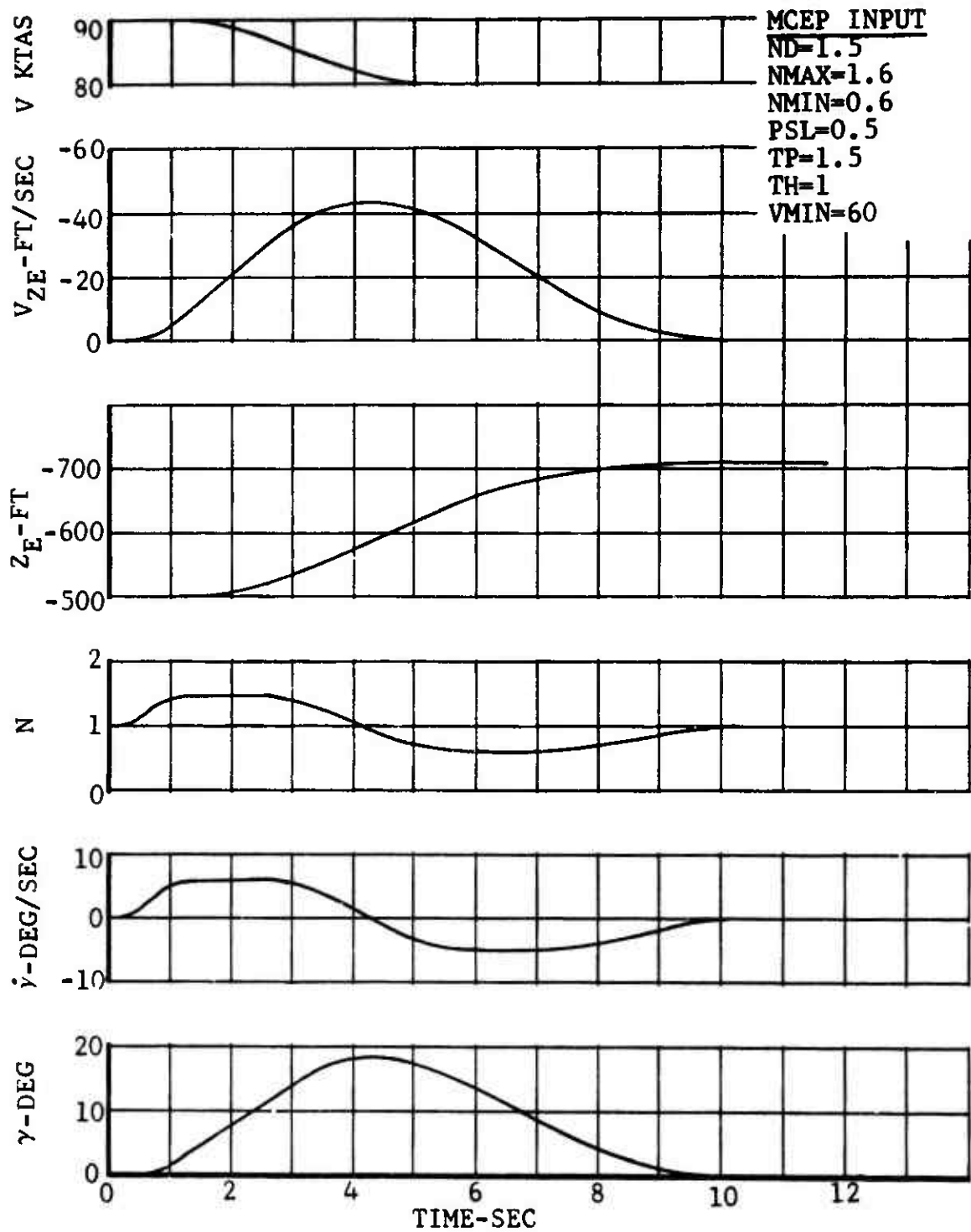


Figure 12. Time History of Pullup Maneuver for AH-1G Helicopter at 90 Knots and 9500 Pounds.

required heading change. The auto turn controller makes the choice using the following method. A typical orientation of the aircraft and the aim point is presented in Figure 13. First, the magnitude of the initial heading change is calculated from the dot product of the velocity vector and the radius vector from the aircraft to the aim point. The expression for this magnitude is

$$\epsilon = \cos^{-1} \left(\frac{\mathbf{V} \cdot \mathbf{R}}{|\mathbf{V}| |\mathbf{R}|} \right) \quad (94)$$

where

$$\mathbf{V} = \bar{\mathbf{i}}_E V_{XE} + \bar{\mathbf{j}}_E V_{YE} \quad (95)$$

and

$$\mathbf{R} = \bar{\mathbf{i}}_E (XAP-X) + \bar{\mathbf{j}}_E (YAP-Y) \quad (96)$$

Equation (94) may be written as follows using Equations (95) and (96):

$$\epsilon = \cos^{-1} \left[\frac{V_{XE}(XAP-X) + V_{YE}(YAP-Y)}{V_{XYP} \sqrt{(XAP-X)^2 + (YAP-Y)^2}} \right] \quad (97)$$

The direction of turn is determined from the direction of the vector, $\bar{\mathbf{C}}$, which results from crossing the velocity vector into the radius vector. This operation results in the following definition.

$$\begin{aligned} \bar{\mathbf{C}} &= \mathbf{V} \times \mathbf{R} \\ \bar{\mathbf{C}} &= [\bar{\mathbf{i}}_E V_{XE} + \bar{\mathbf{j}}_E V_{YE}] \times [\bar{\mathbf{i}}_E (XAP-X) + \bar{\mathbf{j}}_E (YAP-Y)] \\ \bar{\mathbf{C}} &= \bar{\mathbf{k}}_E [V_{XE}(YAP-Y) - V_{YE}(XAP-X)] \end{aligned} \quad (98)$$

If the expression in brackets of Equation (98) is positive, then the auto turn controller will use a right turn. If the converse is true, then the auto turn controller will use a left turn. For the cases when the expression vanishes, the auto turn controller makes the decision on whether to turn or not based on the magnitude of ϵ calculated from Equation (97). If $\epsilon = 0$, no turn is executed; if $\epsilon = \pm\pi$, the auto turn controller will execute a right turn.

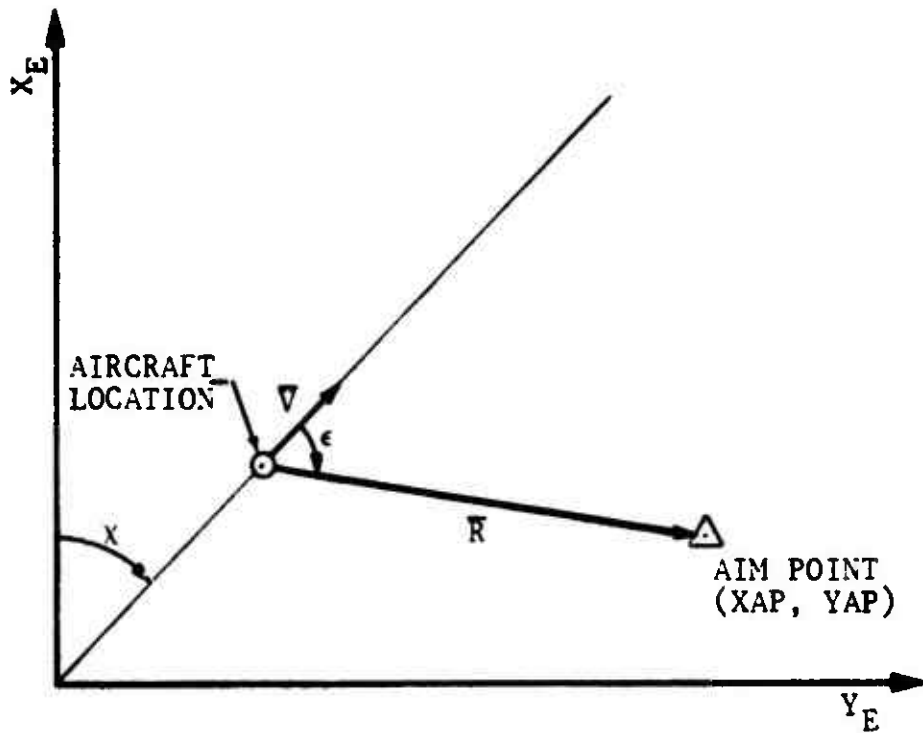


Figure 13. Orientation of Helicopter Relative to Aim Points.

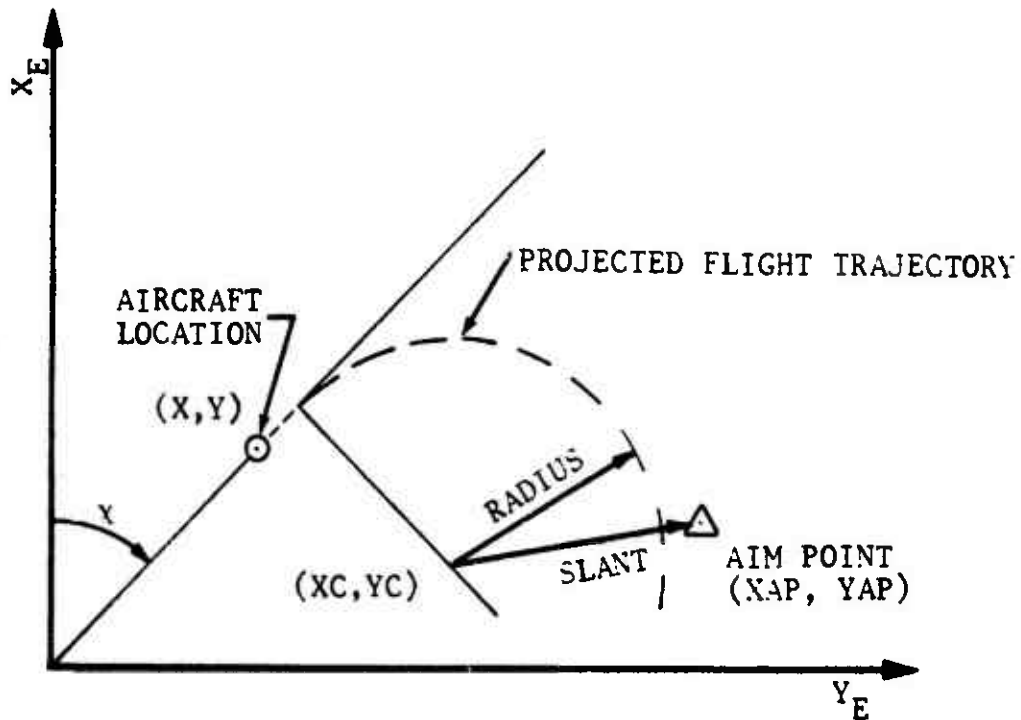


Figure 14. Prediction of Opportunity of Helicopter to Intersect Aim Points.

It may be possible for a situation to exist where the aircraft will not have an opportunity to achieve a heading which intersects the aim point. The controller estimates the possibility of this situation existing in the following manner. A projection of the flight trajectory is made as shown in Figure 14.

The turn radius is calculated using

$$\text{RADIUS} = v^2 / g \tan \phi_c \quad (99)$$

where ϕ is based on the input value of load factor. The center of rotation is then estimated by the following equations.

$$XC = X - \text{RADIUS} \sin x + 2 V_{XE} t_{pr} \quad (100)$$

$$YC = Y + \text{RADIUS} \cos x + 2 V_{YE} t_{pr} \quad (101)$$

The slant range from the estimated center of rotation and the aim point may be written as

$$\text{SLANT} = \sqrt{(XAP - XC)^2 + (YAP - YC)^2} \quad (102)$$

If $\text{RADIUS} > \text{SLANT}$, the controller concludes that the aircraft will not be able to find an intersection heading and, therefore, the controller elects to terminate the maneuver.

The initiation of the roll-out occurs when the estimated heading change equals the heading change calculated from Equation (97). The estimated heading change is computed in the same manner as is the turn controller.

Examples of this maneuver are shown in Figures 15 and 16. The input requirements for this maneuver are the desired load factor, maneuver urgency factor, and the aim points (XAP, YAP).

Return to Target at Constant Altitude

This controller flies the aircraft to a specified target. The maneuver is performed by executing a decelerating turn until the aircraft rolls out on the heading which intersects the target. Then full power is applied to accelerate the aircraft to the target. This maneuver can be used in the mission simulation to fly across a designated target or to arrive at a check point.

This maneuver is controlled by the heading change required for the aircraft to achieve intersection with the target. The required heading change as shown in Figure 17 is calculated

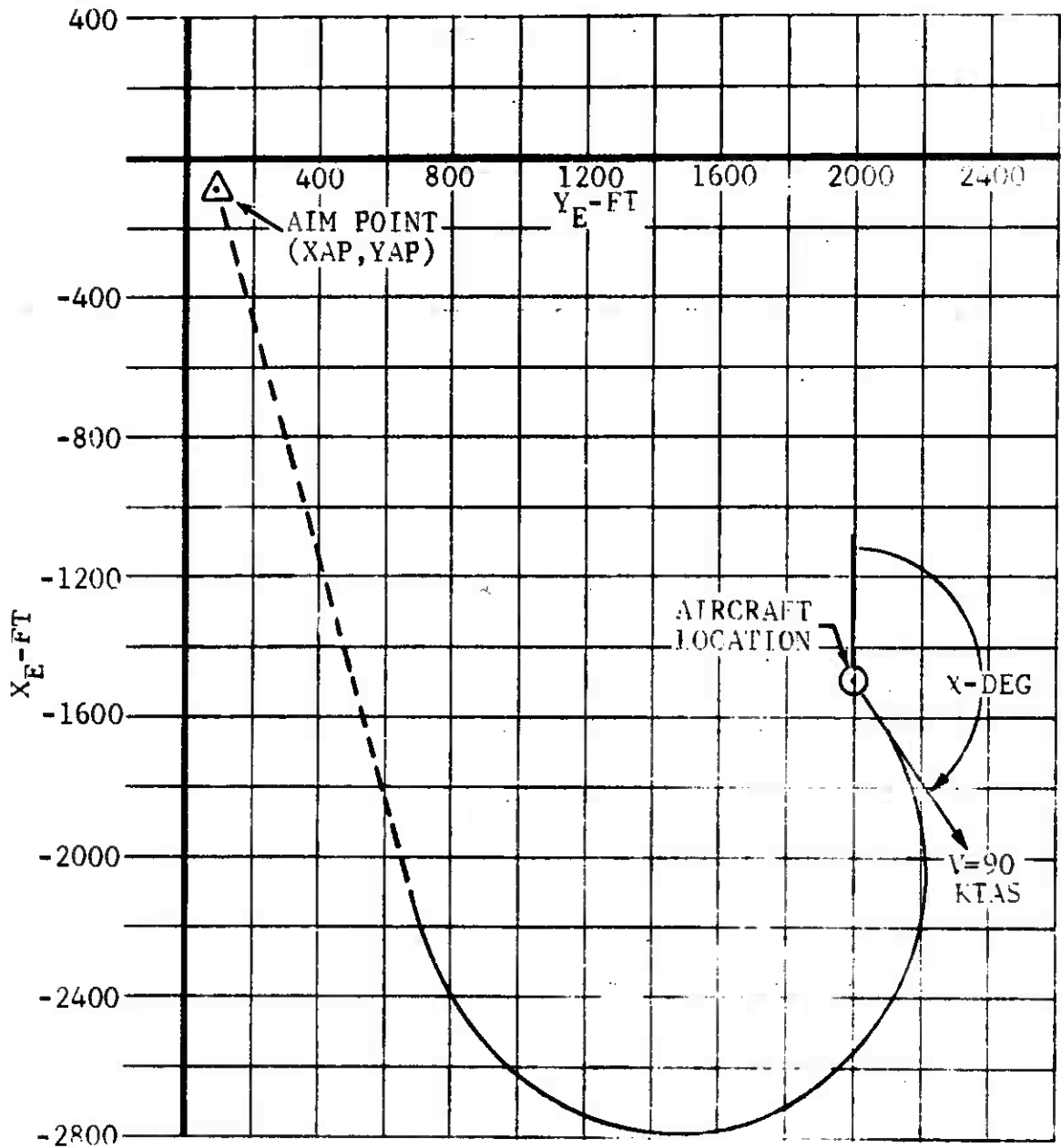


Figure 15. Ground Track of Auto Turn Maneuver.

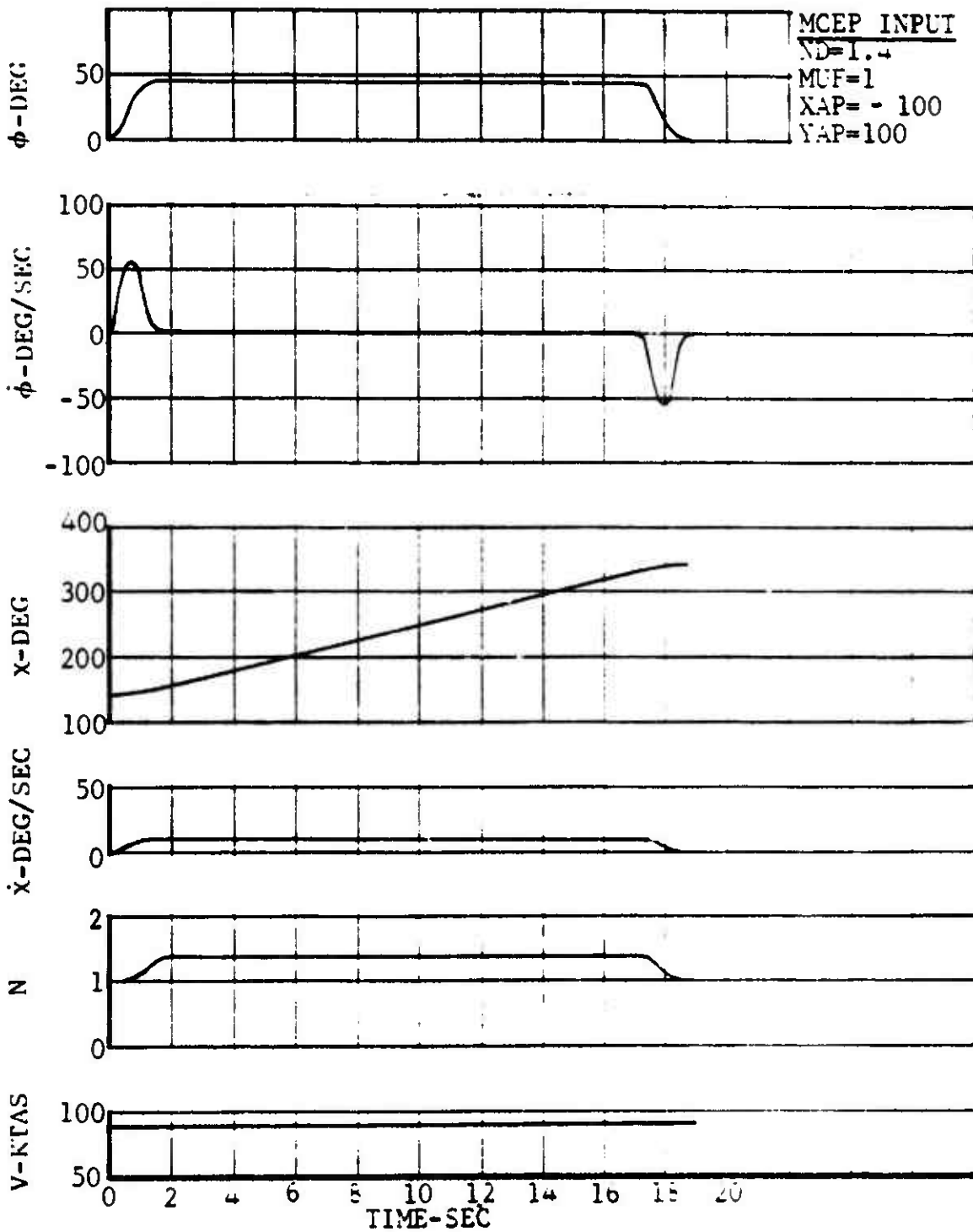


Figure 16. Time History of Auto Turn Maneuver for AH-1G Helicopter at 90 Knots and 9500 Pounds.

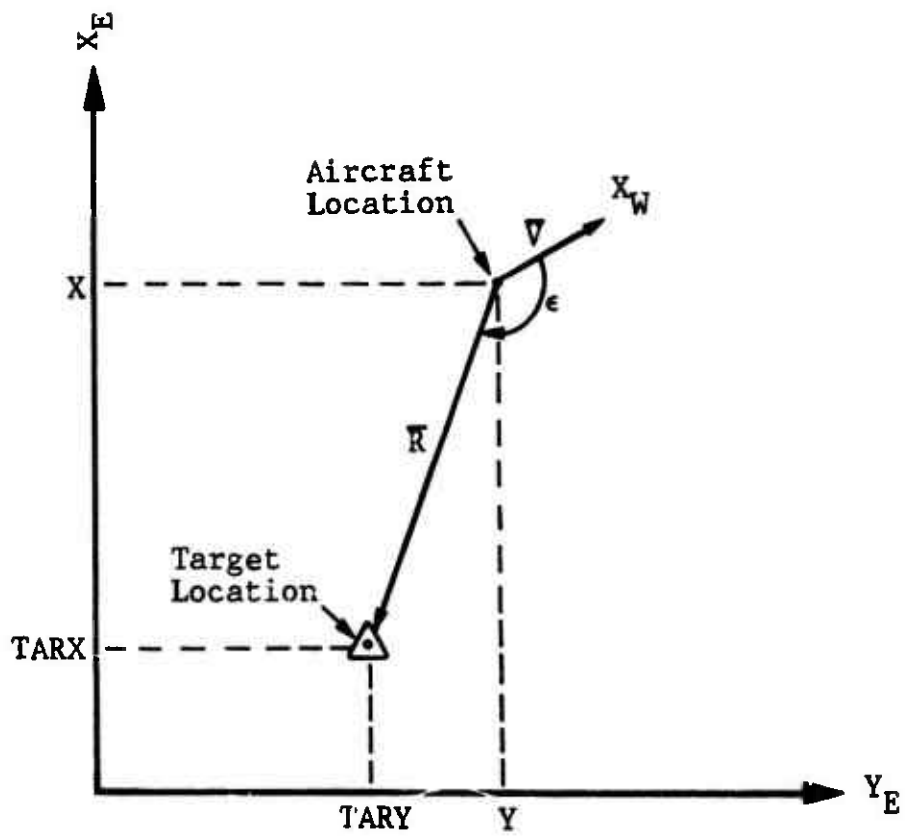


Figure 17. Orientation of Helicopter Relative to Target.

from the dot product of the velocity vector and the radius vector from the aircraft location to the target location divided by the product of the magnitudes of the two vectors. The expression for the heading change can be written in the following form.

$$\epsilon = \cos^{-1} \left(\frac{\mathbf{V} \cdot \mathbf{R}}{|\mathbf{V}| |\mathbf{R}|} \right)$$

$$\epsilon = \cos^{-1} \left[\frac{(TARX-X)V_{XE} + (TARY-Y)V_{YE}}{V_{XYP} \sqrt{(TARX-X)^2 + (TARY-Y)^2}} \right] \quad (103)$$

The heading change is varying throughout the maneuver.

A roll-out is initiated when the estimated heading change produced from returning the roll angle to zero from the current values of roll acceleration, rate, and displacement is equal to the heading change calculated from Equation (103). The heading change from roll-out is predicted in the same manner as discussed in turn at constant airspeed and altitude.

The time to roll-in can be an important factor in the ability of the aircraft to achieve a heading which intersects the target. The aircraft must turn inside the target to have an opportunity to roll-out on a heading which intersects the target. The controller reduces the roll angle to maintain a constant radius turn if the airspeed falls below the input minimum velocity. If the direction of the turn is not specified, then controller uses the logic presented in the discussion of auto turn to select the direction of turn for minimum heading change.

Examples of this maneuver are presented in Figures 18 through 21. In Figures 18 and 19, the aircraft flies over the target and then returns to it. In Figures 20 and 21, the aircraft flies from the current position to the target. The input requirements for this maneuver are desired load factor, time to peak roll rate, maneuver urgency factor, target position (TARX, TARY, TARZ), minimum velocity, and direction of turn.

Dive/Rolling Pullout

The dive/rolling pullout controller flies the aircraft through the setup of the engagement, the engagements, and the break-off of the engagement. The controller flies the aircraft to the correct position to establish the dive angle required for a line-of-sight on the target. Then the aircraft is flown down this angle until it is time to initiate recovery to stay above a minimum altitude or outside a minimum slant range

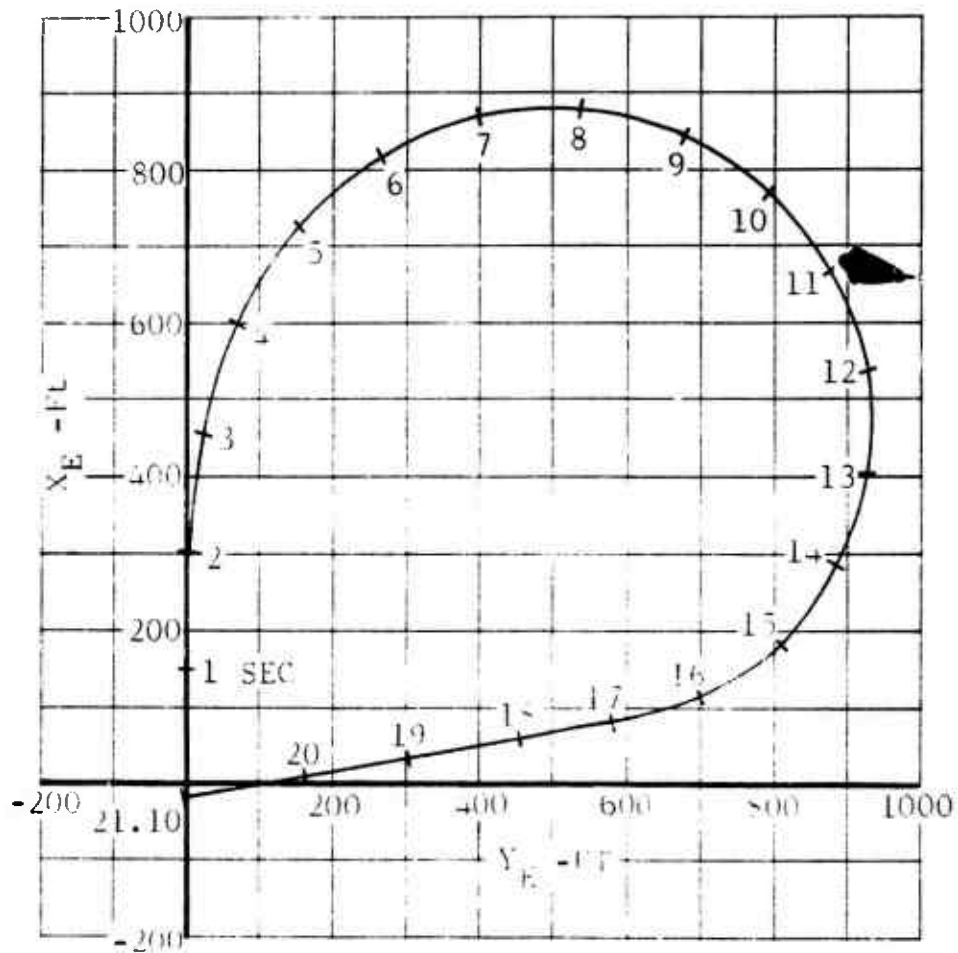


Figure 18. Ground Track of Return to Target at Constant Altitude.

MCEP INPUT
 ND=1.7
 TP=2.5
 MUF=1
 TARX=0
 TARY=0
 VMIN=60
 TURN=1

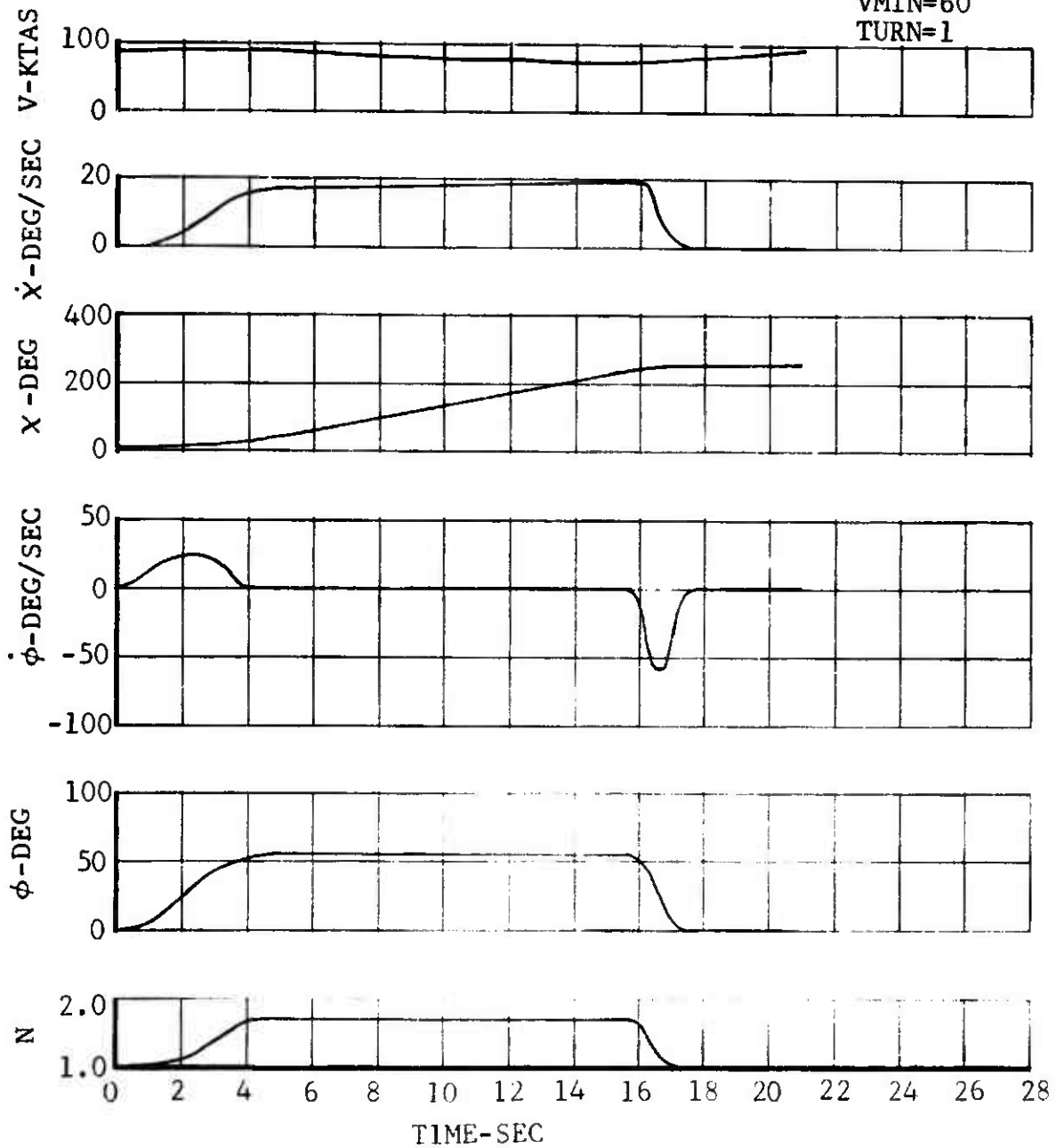


Figure 19. Time History of Return to Target at Constant Altitude for AH-1G Helicopter at 90 knots and 9500 Pounds.

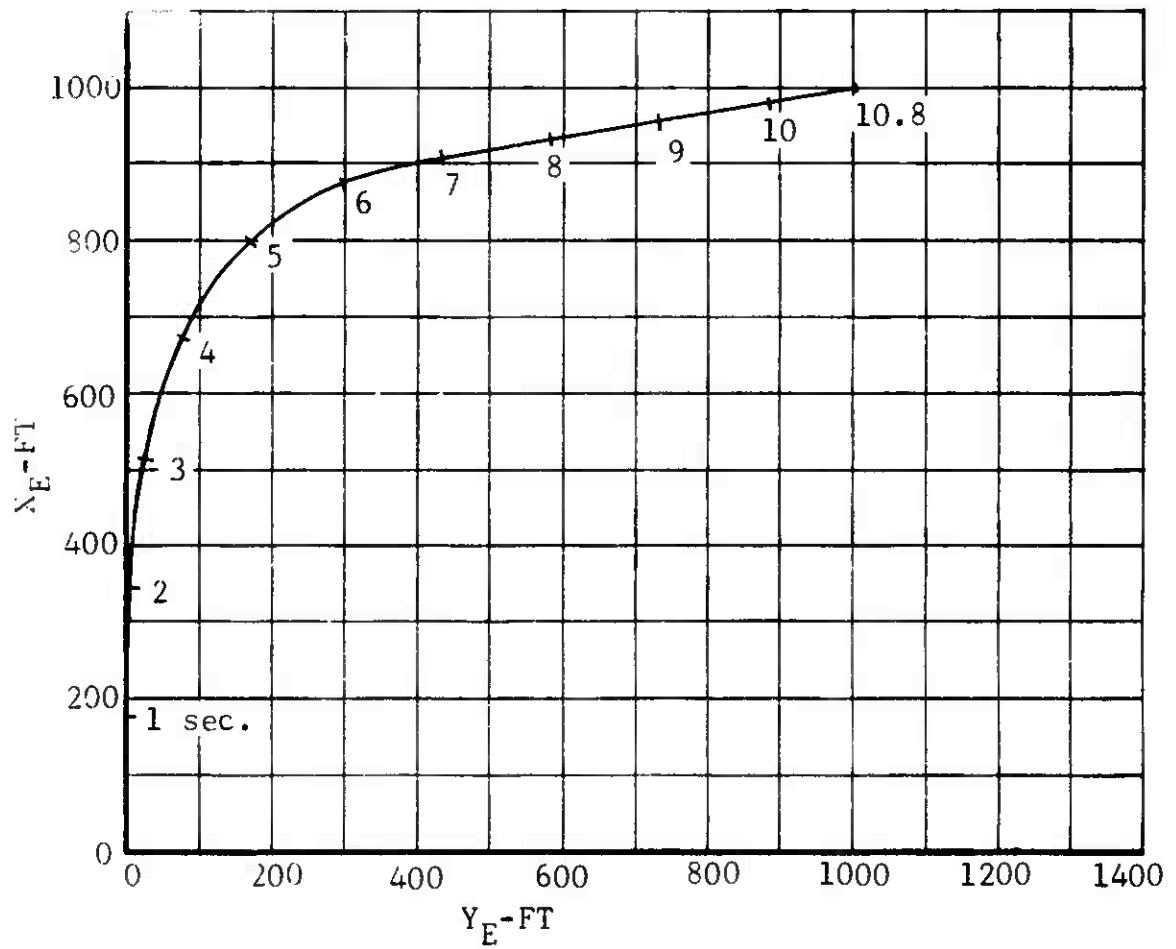


Figure 20. Ground Track of Return to Point at Constant Altitude.

MCEP INPUT

ND=2

TP=2.5

MUF=1

TARX=1000

TARY=1000

VMIN=60

TURN=1

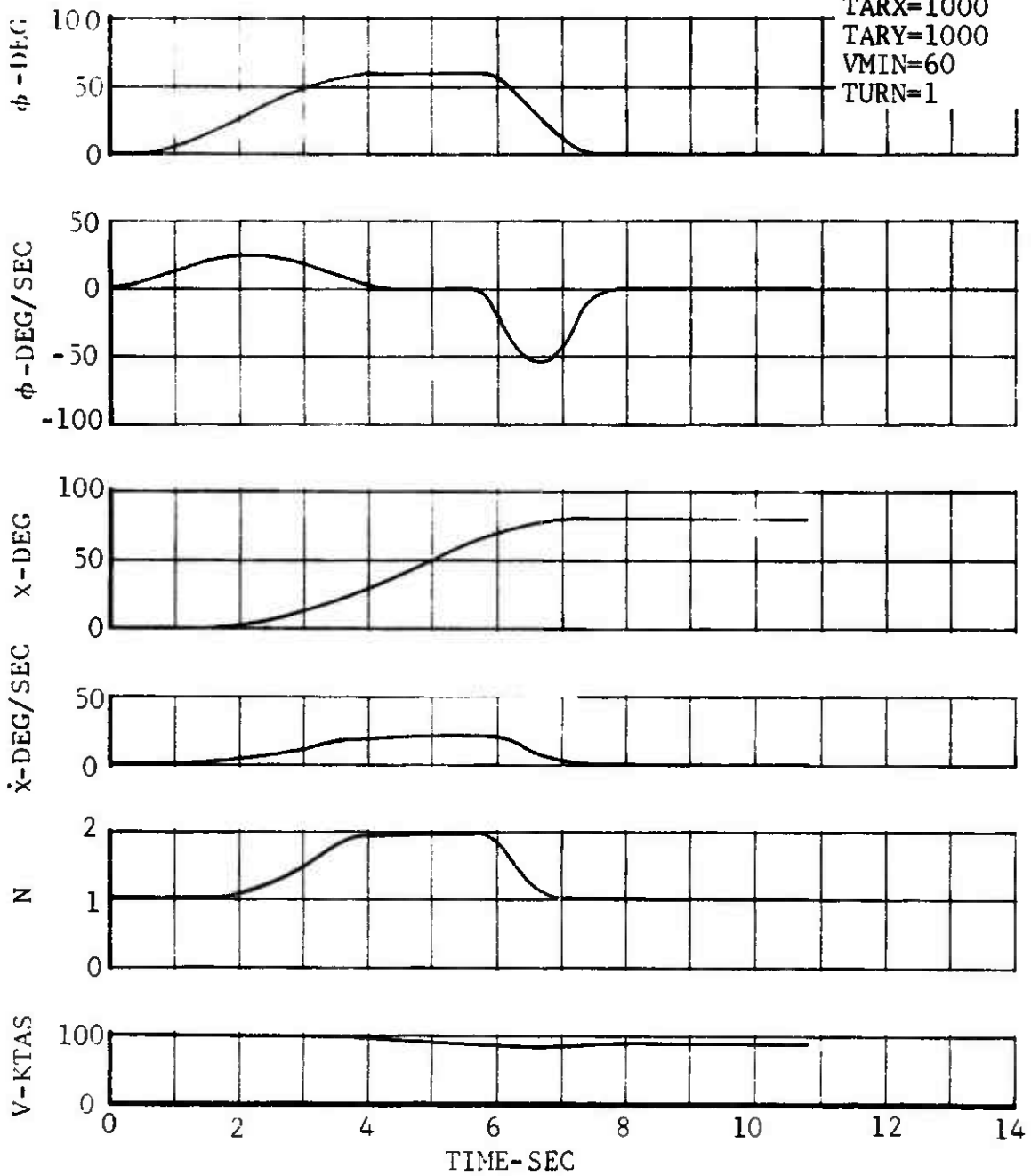


Figure 21. Time History of Return to Point at Constant Altitude for AH-1G Helicopter at 100 Knots and 9500 Pounds.

from the target. The recovery consists of a rolling pullout which returns the aircraft to level flight on the desired exit heading. This maneuver can be used to simulate the engagement of a target.

The first part of this flight controller selects the point at which the dive phase should be initiated. The controller identifies the point as illustrated in Figure 22. The altitude loss (DHE) and the distance translated toward the target (DXW) are estimated in obtaining γ_c while maintaining load factor above the minimum load factor. The horizontal distance of the aircraft from the target when the aircraft intersects the desired glide slope is calculated from

$$DXT = (Z - DHE - TARZ) / \tan \gamma_c \quad (104)$$

where $TARZ = Z_E$ position of the target

$\gamma_c =$ command dive angle

The distance from the current aircraft position and the point to initiate the dive is

$$FLDT = RANGE - DXT - DXW \quad (105)$$

where $RANGE = \sqrt{(TARX - X)^2 + (TARY - Y)^2}$

If $FLDT \geq 0$, then the aircraft cruises until the dive point is reached, as shown by the arrow on Figure 22. If $FLDT < 0$, the controller attempts to compute a dive angle based on the geometry of the aircraft position and target location. The value of this dive angle increases as the stage time for command generation is increased to prevent load factor from violating the minimum load factor. The stage time for command generation is increased until the estimated load factor is greater than the minimum allowed or until $V_{XYP} (t_1 + t_2) = RANGE$, at which time a message will indicate that the target cannot be reached based on the existing initial condition.

The flight controller executes the dive based on the information determined above. The amount of acceleration along the flight path is controlled by PSL. Lower values of PSL result in less acceleration for the same γ_c . The flight path of the aircraft should not violate the minimum slant range to the target during the recovery sequence. The estimated minimum slant range to the target is determined based on the current

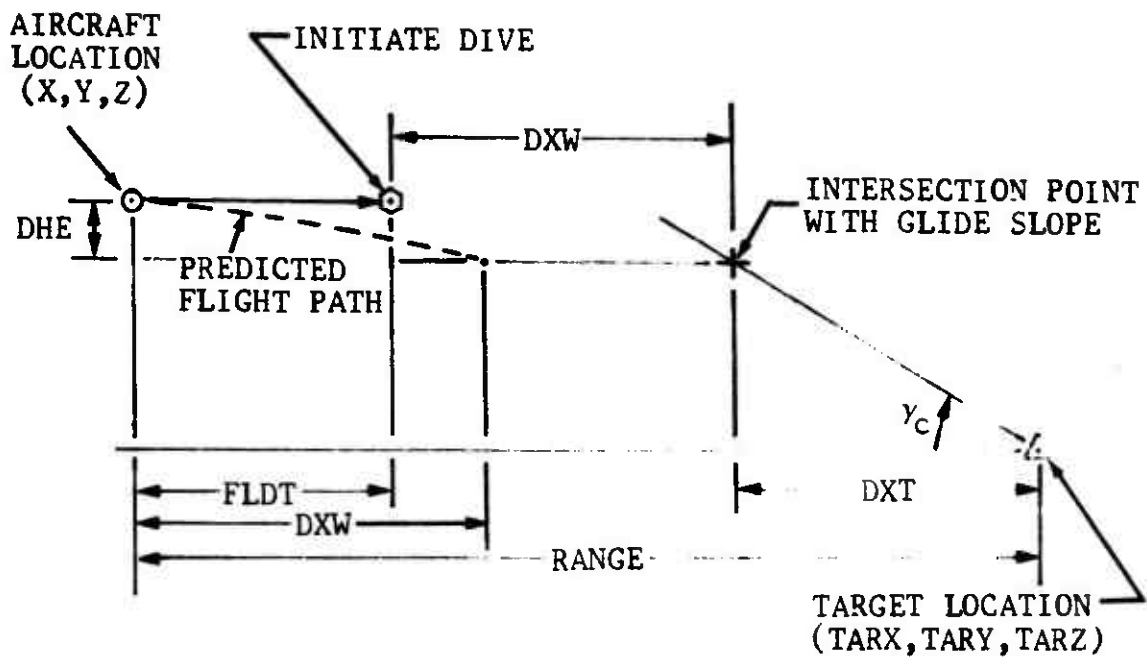


Figure 22. Prediction of Dive Point for Dive/Rolling Pullout Maneuver.

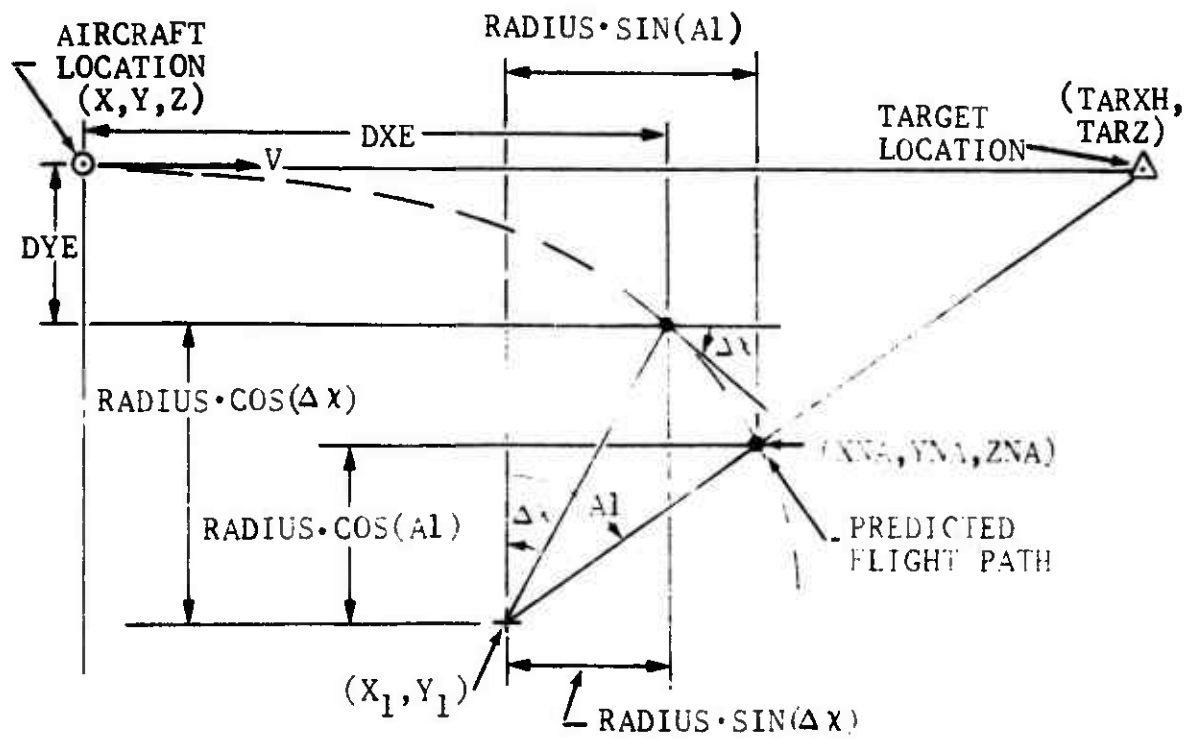


Figure 23. Prediction of Pullup Point for Dive/Rolling Pullout Maneuver.

initial conditions. The geometry of this procedure is shown in Figure 23.

The change in heading ($\Delta\chi$) is estimated from returning γ to zero while rolling into a turn. A procedure similar to the one used in the turn and climb controller is employed. The turn rate is determined from

$$\dot{\chi}_i = \left[\frac{g}{V} + \frac{\dot{\gamma}_i}{\cos \gamma_i} \right] \tan \phi_i \quad (106)$$

for each of the estimated values of ϕ_i , $\dot{\gamma}_i$, and γ_i . The turn rate is then integrated to provide $\Delta\chi$. The altitude loss (DHE) is computed from the integration of the estimated vertical velocities. The distances traveled in the horizontal plane in recovering from the dive and rolling into a turn are determined from integrating the estimated ground velocities which are based on the headings from Equation (106). Once the flight path is returned to the horizontal plane, a constant radius turn equivalent to the input value of nd is assumed. The center of rotation of this turn is calculated from

$$X_1 = DXE - \text{RADIUS} \sin(\Delta\chi) \quad (107)$$

$$Y_1 = DYE - \text{RADIUS} \cos(\Delta\chi) \quad (108)$$

The minimum distance from the target occurs when the flight path of the aircraft is tangent to the arc formed by cutting the sphere of minimum slant range with a plane at the altitude of the turn. This target point is estimated from the intersection of a straight line which joins the center of rotation of the turn and the target location with the predicted flight path of the aircraft. The range of the aircraft from the target in the horizontal plane is

$$\text{TARXH} = \sqrt{(\text{TARX}-X)^2 + (\text{TARY}-Y)^2} \quad (109)$$

The angle $A1$ is defined as

$$A1 = \tan^{-1} \left[\frac{(\text{TARXH} - X_1)}{Y_1} \right] \quad (110)$$

Now the points of closest approach become

$$XNA = X_1 + \text{RADIUS} \sin(A1) \quad (111)$$

$$YNA = Y_1 - \text{RADIUS} \cos(A1) \quad (112)$$

$$ZNA = Z - DHE$$

(113)

The estimated minimum slant range from the target is calculated from

$$SLANTE = \sqrt{(TARXH - XNA)^2 + (YNA)^2 + (TARZ - ZNA)^2} \quad (114)$$

Once the estimated minimum slant range becomes less than the minimum slant range, the recovery portion of the maneuver is initiated. The peak load factor is estimated and compared against the maximum value. If it violates the maximum load factor, then the stage time of the command generator is increased and the estimated slant range is corrected.

The final portion of this maneuver is the roll-out on the desired heading. This roll-out is accomplished the same as explained in the turn controller. Two values of MUF are used in this maneuver. One MUF is for the dive phase, while the other is for the rolling pullout and the roll-out on heading.

An example of this maneuver is presented in Figures 24 and 25. The input data required are desired load factor for the turn, desired dive angle, location of target (TARX, TARY, TARZ), minimum slant range to target, delta heading from present heading to leave target area, maximum load factor, minimum load factor, minimum velocity, maneuver urgency factor for dive, maneuver urgency factor for roll, and minimum power setting.

Climbing/Descending Turn at Constant Airspeed

The climbing/descending turn controller flies the aircraft to a specified altitude and heading at constant airspeed. This maneuver is performed by establishing a climb or dive angle while rolling into a turn. The turn is maintained until the desired altitude is established, after which roll-out is initiated at the proper time to establish the desired heading. The maneuver can be used in mission simulation to change altitudes while staying in a general area.

This maneuver is controlled through the proper choice of the flight path angle and the roll angle. Two options are available for determining these angles. If a desired load factor is specified, the remaining excess power is used to calculate a climb angle. For a descending turn, the descent angle is based on the minimum power setting. If a desired load factor is not specified, the climb angle is calculated using half of the excess power and the remaining excess power is used for the roll angle. For a descending turn, the descent angle is based on the minimum power setting while the roll angle is based on the excess power from level flight.

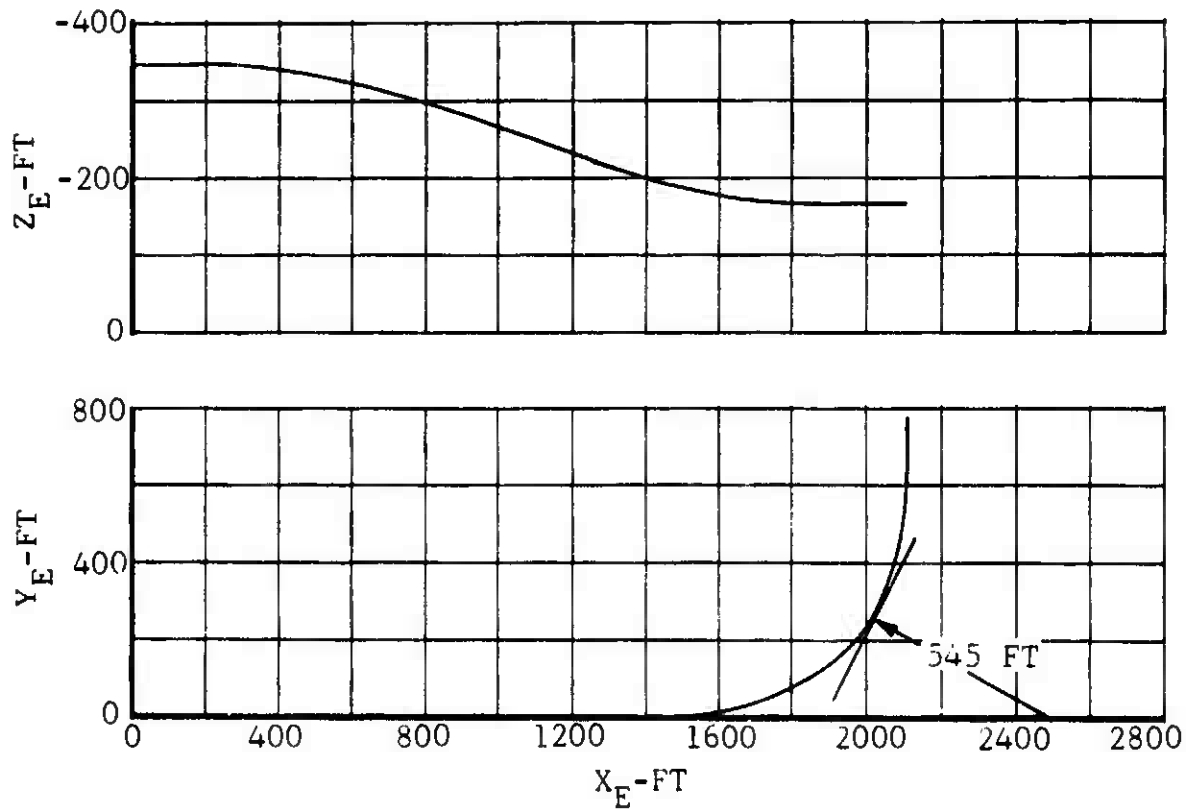


Figure 24. Ground Track of Dive/Rolling Pullout Maneuver.

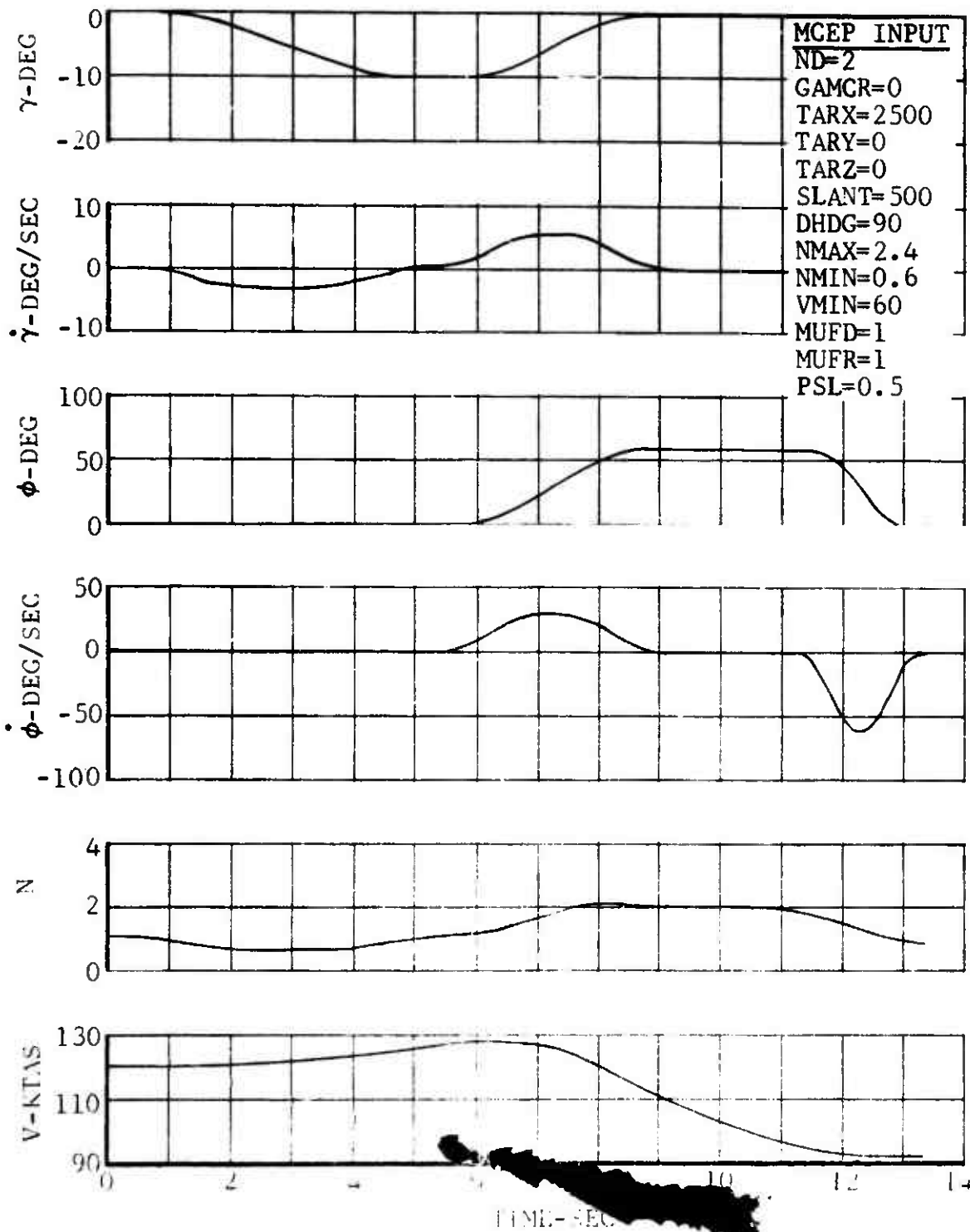


Figure 25. Time History of Dive/Rolling Pullout Maneuver for AH-1G Helicopter.

The stage times of the pitch and roll command generators are increased if the estimated peak load factor using Equation (53) is outside the appropriate load factor limit. The time to initiate recovery to arrive at the desired altitude is determined using the same procedure outlined in the climb/descent controller.

The time to initiate the roll-out to arrive at the desired heading is the same method used in the turn controller.

An example of this maneuver is shown in Figure 26. The input data required for the maneuver are the desired altitude, desired load factor, desired heading, maneuver urgency factor, minimum power setting, maximum load factor limit, and minimum load factor limit.

Sideward Acceleration/Deceleration

The sideward acceleration/deceleration controller accelerates the aircraft to the right or left from hover at constant altitudes while the nose of the aircraft is tracking a target. The aircraft is accelerated until the desired sideward velocity is reached and then the aircraft is decelerated to hover while still tracking the target. This maneuver can be used to evaluate low speed tactics.

This maneuver is controlled by the bank angle which the aircraft maintains in the acceleration phase of the maneuver. The limiting factor in this maneuver is the power available. The controller computes the power limited bank angle based on the maximum horsepower at the desired velocity. If the commanded bank angle is greater, then the commanded bank angle is reset to the power limited bank angle. A penalty can be imposed on flying to the right by subtracting some power from the maximum power available to account for the increased tail rotor power required. The controller uses the thrust vectoring method as developed in Reference 1 to compute the sideward acceleration resulting from a bank angle. The equivalent flat plate drag is based on the drag of the aircraft at a sideslip angle of 90° . The wind axes acceleration is computed from

$$a_{x_w} = g \left(\tan \phi - \frac{q^*_{l_1}}{GW} \right) \quad (115)$$

where $\frac{q^*_{l_1}}{GW} =$ tangent of the trim roll angle at the current velocity

MCEP INPUT

HC=550

ND=0

HDG=90

MUF=0.5

PSL=0.5

NMAX=2

NMIN=0.8

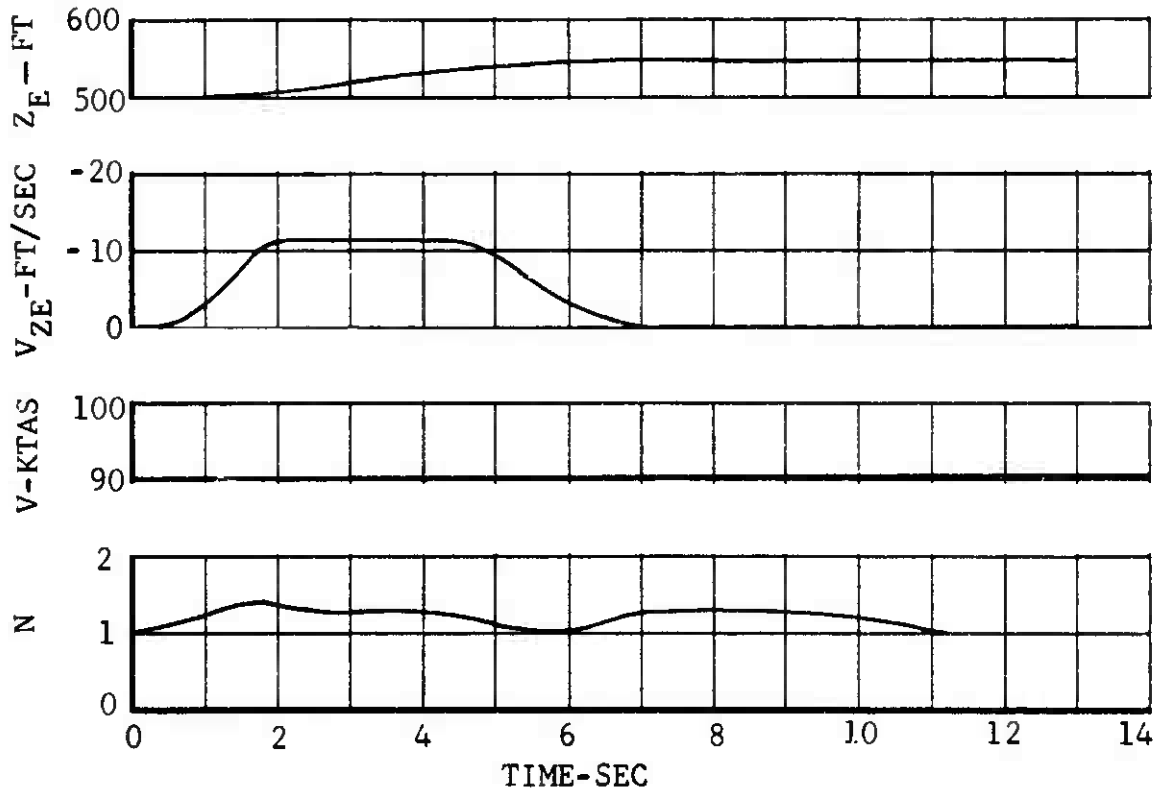


Figure 26. Time History of Climbing Turn at Constant Airspeed for AH-1G Helicopter at 90 Knots and 9500 Pounds.

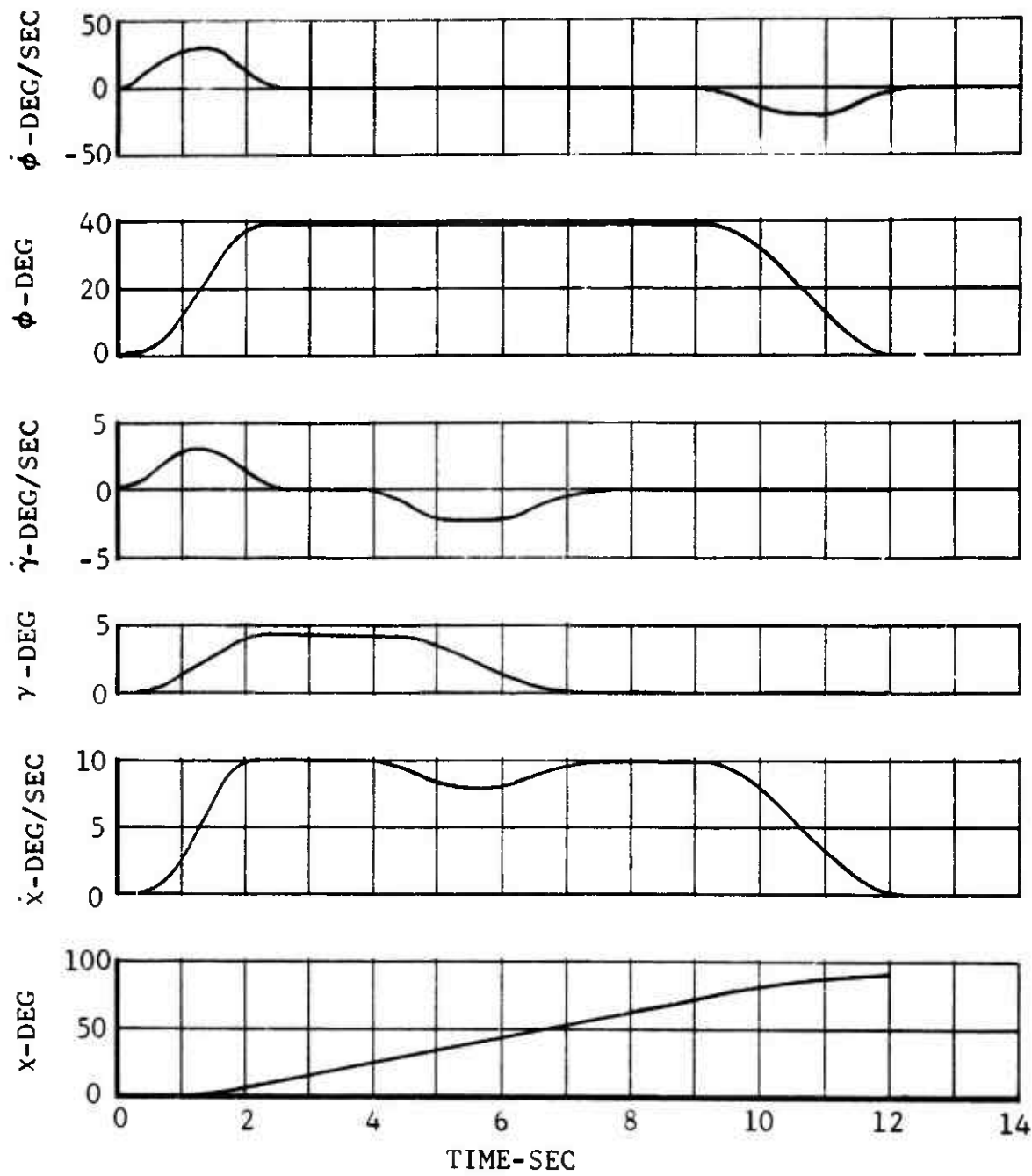


Figure 26. Contd.

f_1 = drag area ($C_D = 1$) of aircraft at 90° sideslip

q = dynamic pressure

The deceleration phase of this maneuver is initiated by rolling to a bank angle of equal magnitude but opposite sign as the commanded sideward velocity is approached. The deceleration phase is terminated by returning the bank angle to zero as hover is approached.

An example of this maneuver is given in Figure 27. The input data required for this maneuver are the command bank angle, command sideward velocity, final velocity, maneuver urgency factor, tail rotor power penalty, and location of target (TARX, TARY).

Sideward Acceleration/Pedal Turn Into Wind

The sideward acceleration/pedal turn into wind controller accelerates the aircraft to the right or left from hover at constant altitude while the nose of the aircraft is tracking a target. The aircraft is accelerated until the command sideward velocity is established. Then the aircraft stops tracking the target and swings its nose into the wind. This maneuver can be used to evaluate sideward acceleration in conjunction with other maneuvers.

The first portion of this maneuver is exactly the same as the sideward acceleration/deceleration maneuver. As the command sideward velocity is approached, the aircraft rolls to a roll angle at the command sideward velocity such that the thrust tilt balances drag; then the aircraft stops tracking the target and swings its nose into the wind. This portion of the maneuver is controlled in the same manner as the pedal turn maneuver except that the sideslip angle (β) is reduced to zero instead of making a heading change. The controller integrates $\dot{\beta}$ to compute β . The trim roll angle is reduced to zero in the same time as β is reduced to zero. After β is reduced to zero, the aircraft has the proper conditions to use the other maneuvers such as the climb/descent maneuver.

An example of this maneuver is presented in Figure 28. The input data required for this maneuver are command sideward velocity, maneuver urgency factor for rolling, command bank angle, time to reach desired $\dot{\beta}$, desired β , and target location.

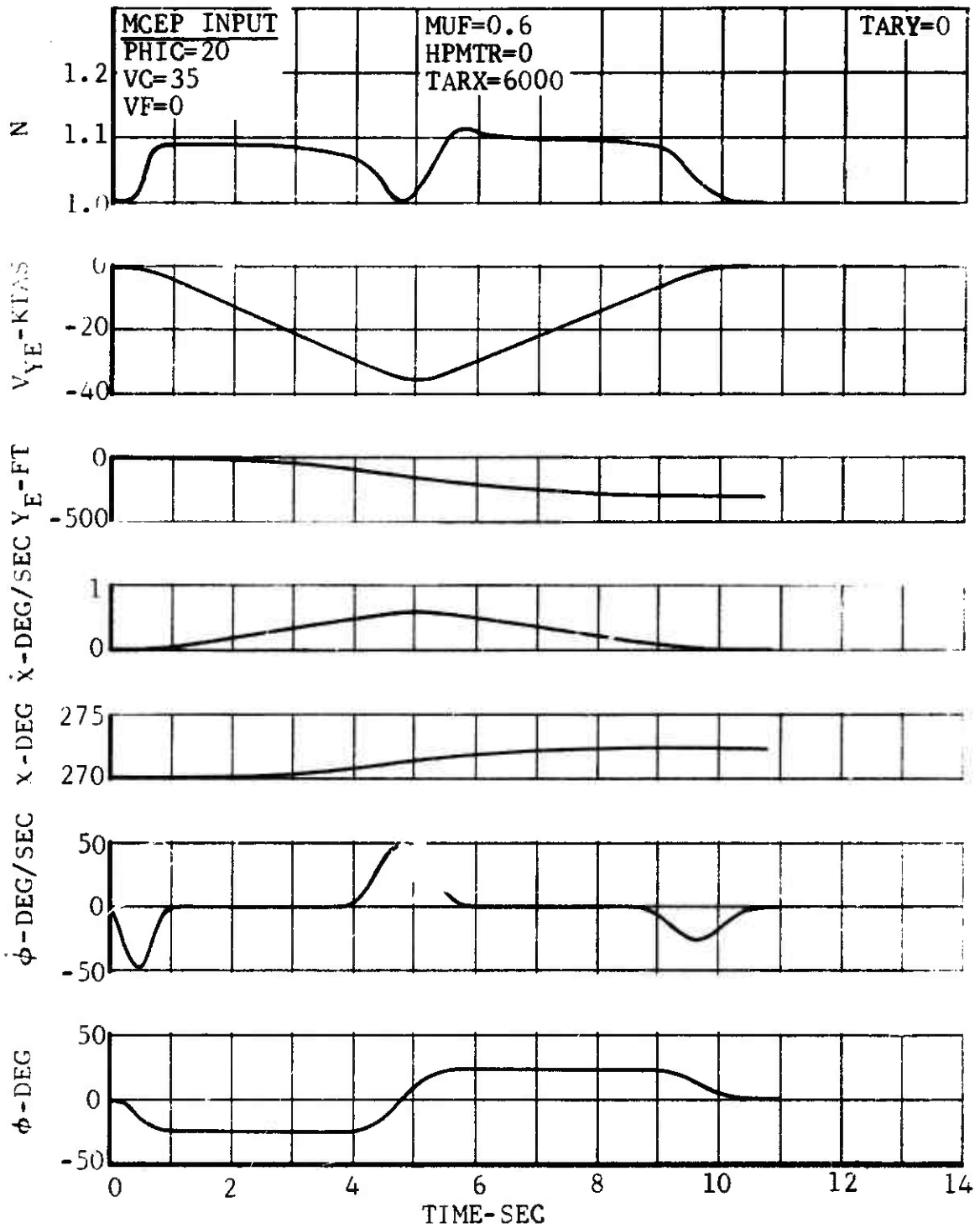


Figure 27. Time History of Sideward Acceleration From Hover and Deceleration to Hover for AH-1G Helicopter at 8500 Pounds.

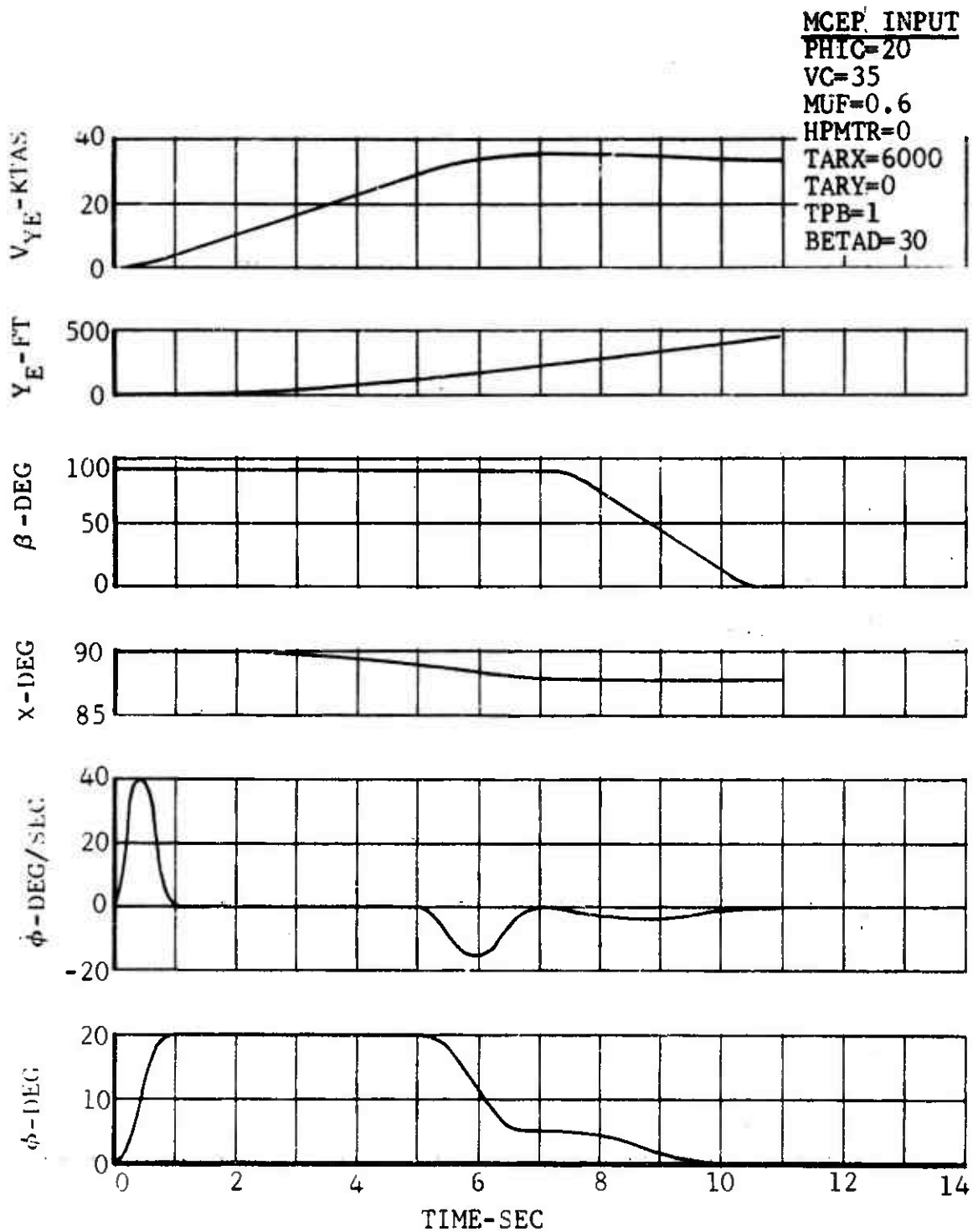


Figure 28. Time History of Sideward Acceleration From Hover and Turn Into the Wind for AH-1G Helicopter at 8500 Pounds.

Orbit at Constant Airspeed

The orbit controller rolls the aircraft into a turn of specified radius and maintains a steady turn for a specified amount of time. After the orbit time is satisfied, the controller flies the aircraft until it is time to roll out on the desired heading. This maneuver can be used to represent loiter.

The orbit controller performs the same commands as the turn controller with the exceptions of determining the command bank angle and of monitoring the time spent in the turn. The specified radius is converted to a command bank which is compared against the power limit bank angle. If the command bank angle is greater, the command bank angle is reset to the power limit bank angle. The controller does not start determination of the roll-out time until the time in the maneuver is greater than the specified orbit time. Then the roll-out point is determined using the roll-out prediction of the turn controller.

An example of the maneuver is shown in Figure 29. The input requirements for the maneuver are the desired radius, maneuver urgency factor, time of orbit, desired heading, and the direction of turn.

Pedal Turn at Hover

The pedal turn controller turns the aircraft over a spot through a desired heading change. This maneuver can be used in mission simulation to line the nose of the aircraft with a target or to execute a heading change. This maneuver is restricted to use in hover.

The pedal turn is controlled by the desired heading change. The pedal input is assumed to be of the form illustrated in Figure 30. The controller estimates the command χ_c to generate the desired rate in the specified time from the following equations. The initial angular acceleration ($\dot{\chi}_0$) and rate (χ_0) are zero for this maneuver. The application of these constraints to the gain equations (Equations (77), (78), (79), and (80)) results in the following expressions for the gains.

$$\begin{aligned}GK_1 &= -GK_2 \\GK_3 &= -GK_2 \\GK_4 &= -GK_3\end{aligned}\tag{116}$$

MCEP INPUT
RADIUS=900
HDG=90
MUF=1
TORBIT=20
PHIDR=1

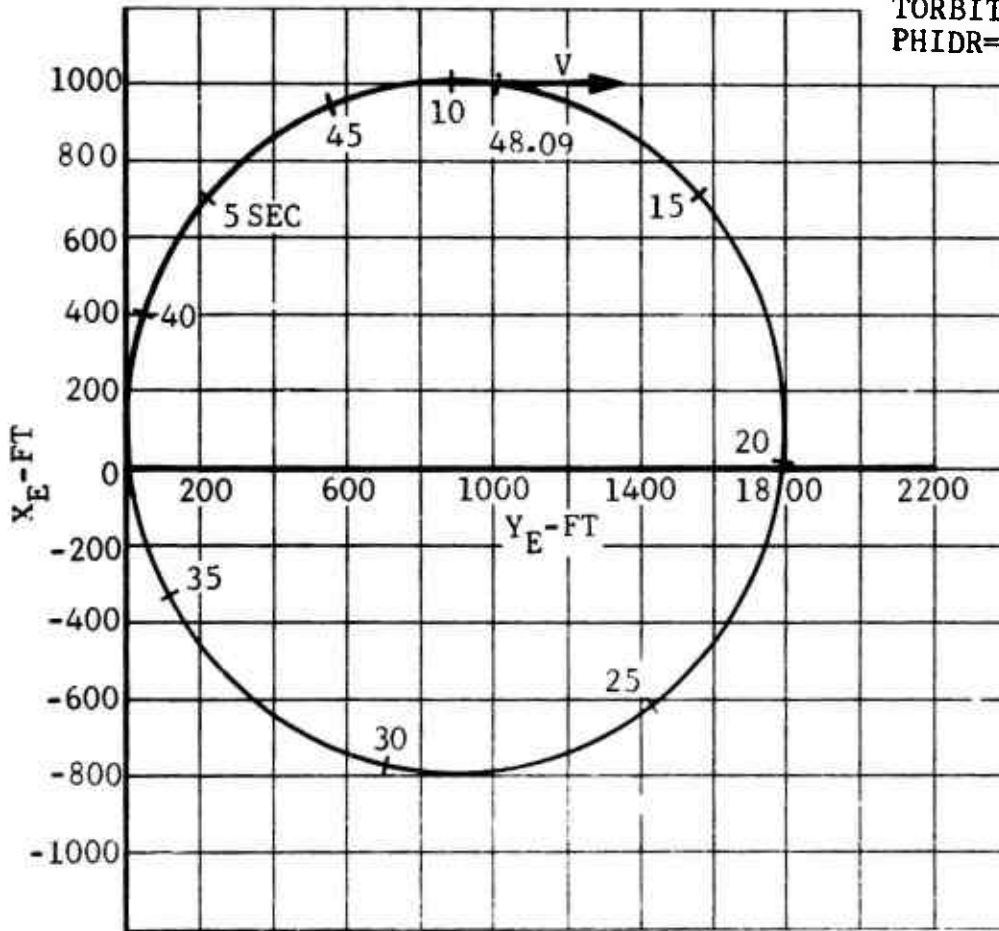
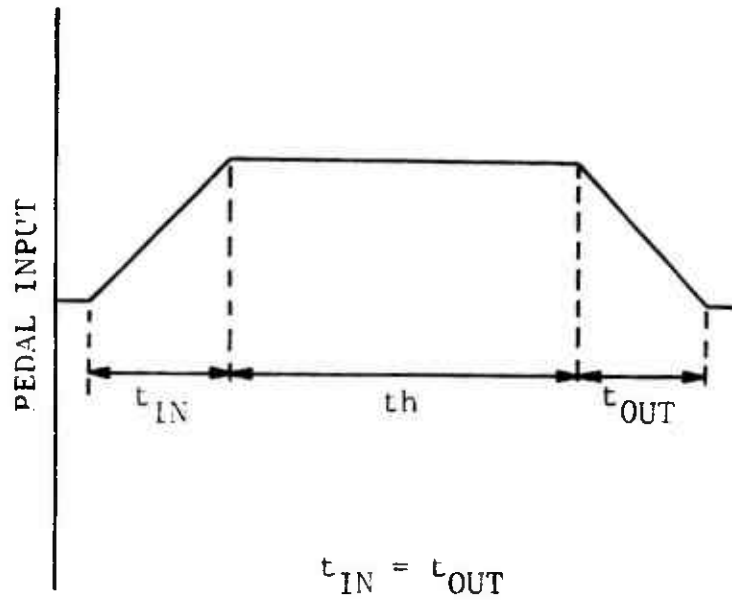


Figure 29. Ground Track of Orbit Maneuver.



$$t_{TOTAL} = 2 t_{IN} + t_h$$

Figure 30. Definition of Pedal Input for Pedal Turn Maneuver.

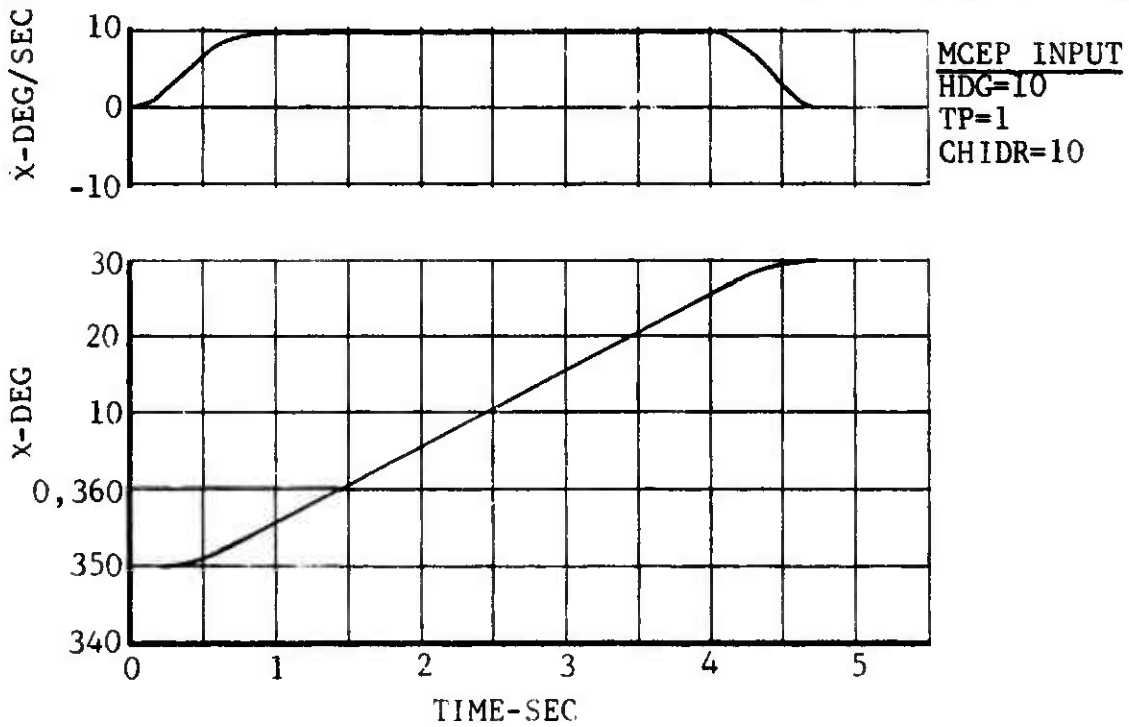


Figure 31. Time History of Pedal Turn Maneuver for AH-1G Helicopter at Hover.

The gains are based on achieving χ_c at the end of the fourth stage. The expression for χ_c can be determined from Equation (71) and the initial conditions.

Then, χ_c becomes

$$\chi_c = 0.5 GK_1 C_1 t_p^2 + \chi_o \quad (117)$$

The expression for peak rate ($\dot{\chi}_p$) can be determined from Equation (59) when $t=t_2$. This operation gives

$$\dot{\chi}_p = 0.5 GK_1 C_1 t_p \quad (118)$$

The value of GK_1 can be determined from Equation (118) and the input value of the desired rate ($\dot{\chi}_p = \dot{\chi}_D$). The expression for GK_1 becomes

$$GK_1 = 2\dot{\chi}_p / C_1 t_p \quad (119)$$

Now the value of χ_c can be estimated using Equations (119) and (117). Then, χ_c may be written as

$$\chi_c = \dot{\chi}_p t_p + \chi_o \quad (120)$$

Assuming that a steady rate would be required to achieve the desired heading, the total angular displacement can be expressed as

$$\chi_D = \chi_c + \dot{\chi}_p t_h \quad (121)$$

The time to maintain steady rate can be determined from Equation (121) to be

$$t_h = \frac{(\chi_D - \chi_o)}{\dot{\chi}_p} - t_p \quad (122)$$

If the time to maintain steady rate is less than one time increment, the controller commands $\chi_c = \chi_D$; and the angular displacement is achieved as presented in Command Generation.

An example of this maneuver is presented in Figure 31. The input requirements for this maneuver are the heading required, time to reach peak rate of change of heading, and the desired rate ($\dot{\chi}_D$).

Collective Pop-Up at Constant Attitude and Low Airspeed

The collective pop-up controller changes the altitude of the aircraft while maintaining constant attitude. The ground speed is constant during the maneuver. This maneuver can be used in evaluating low speed tactics.

The controller flies this maneuver at maximum power available, and determines the maximum load factor which can be achieved using maximum power available for the given flight condition. The load factor reaches N_{MAX} in time t_{pn} .

$$t_{pn} = (n-1)/(MUF \cdot VJERK) \quad (123)$$

where $VJERK$ = rate of change of load factor

Then the controller maintains load factor at the value which requires maximum power available. The aircraft initiates recovery to arrive at the desired altitude by decreasing linearly the load factor in time t_{pn} to the specified minimum value of load factor as illustrated in Figure 32. This minimum load factor is held for the required time which results in coming out at the desired altitude while linearly increasing the load factor to 1 in time t_{pn} . The time to hold the minimum load factor is calculated as

$$t_{out} = -t_{pn} - \frac{(V_{ZE} + 0.5 a_{zE} t_{pn})}{(1-N_{MIN})g} \quad (124)$$

where N_{MIN} = minimum load factor

If $t_{out} < 0$, the controller computes a value of N_{MIN} which will give the correct altitude change for a linear decrease in load factor to N_{MIN} in time t_{pn} followed by a linear increase in load factor to $n = 1$ in the same time as by the broken line in Figure 32. This value is determined from

$$N_{MIN} = 1 + \left(\frac{V_{ZE}}{t_{pn}} + 0.5 a_{zE} \right) / g \quad (125)$$

The altitude change is determined by the controller by integrating the appropriate acceleration to determine vertical velocity and position. When the sum of the estimated altitude change and the current altitude is greater than the desired altitude, the appropriate recovery technique is initiated.

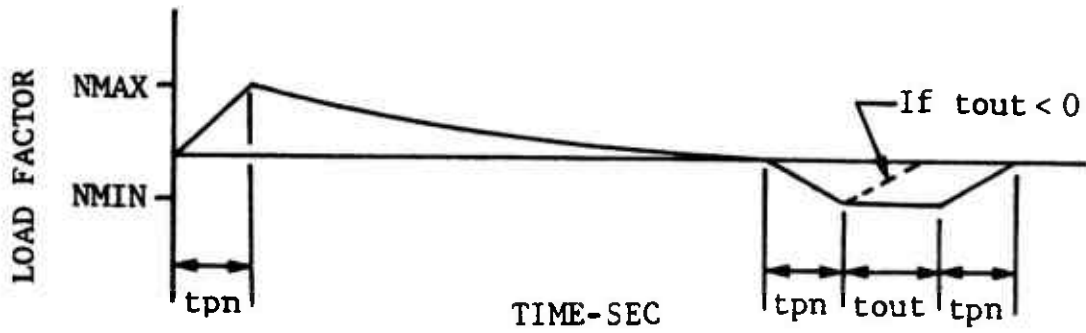


Figure 32. Definition of Recovery Load Factor for Collective Pop-Up Maneuver.

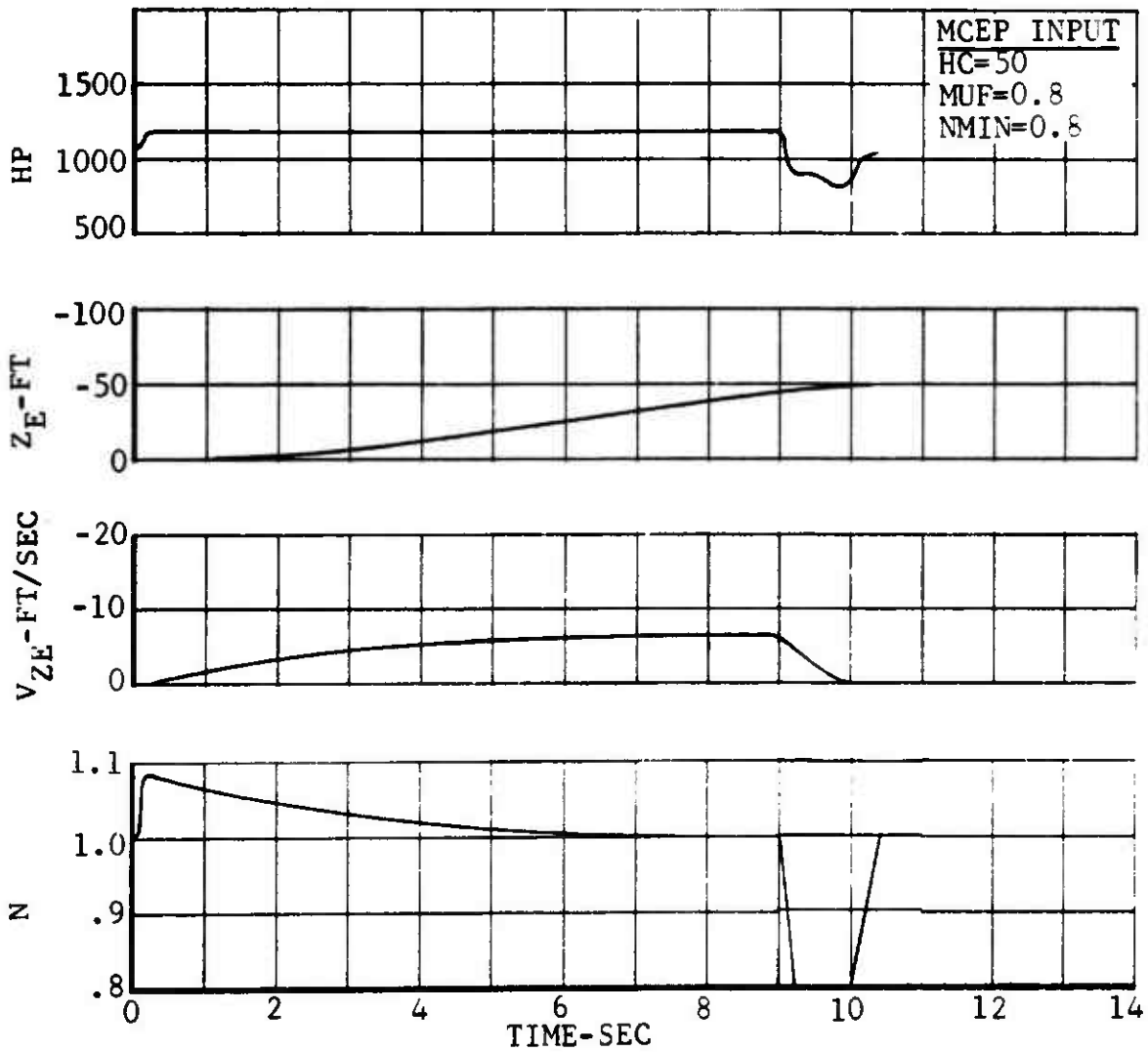


Figure 23. Time History of Collective Pop-Up Maneuver for AH-1G Helicopter at Hover and 9000 Pounds.

An example of this maneuver is presented in Figure 33. The input requirements for this maneuver are the desired altitude, maneuver urgency factor, and the minimum load factor.

Climbing Return to Target

The climbing return to target controller pulls the aircraft into a steep climb while rolling into a turn. As the aircraft approaches the desired minimum velocity, the controller initiates a dive to recover airspeed while maintaining the turn. The dive is terminated at the proper time to arrive at the desired altitude. The roll-out is initiated at the proper time to arrive on a heading which intersects the target. This maneuver can be used in the mission simulation to fly across a designated target.

This maneuver is controlled by the heading change required for the aircraft to achieve intersection with the target. The required heading change is calculated from the dot product of the velocity vector and the radius vector from the aircraft location to the target location, as given by Equation (103). The recovery from the dive portion of the maneuver is initiated when the sum of the estimated altitude loss and the current altitude is equal to the desired altitude. The altitude loss is estimated using the same procedure used in the climb/descent controller. The initiation of roll-out is predicted using the method used in the turn controller with the exception of the turn rate equation. Equation (106) is used for turn rate. The estimated peak load factors are computed using Equation (53) and are compared with the appropriate load factor limits. The stage times for command generation are increased to stay within these limits.

An example of this maneuver is given in Figure 34. The input requirements for this maneuver are the command altitude, location of the target in ground coordinates, maximum desired load factor, minimum desired load factor, command bank angle, command climb angle, minimum velocity, time to peak rate for roll-out, time to peak rate in gamma, time to peak rate in roll, minimum power setting, and time to apply full power.

EVALUATION OF MISSION PROFILE

The evaluation of a mission profile in quantitative terms is made easier by MCEP data in the form of histograms and statistical parameters. MCEP is designed to allow the sensitivity of the flight path to various parameters to be evaluated by means of the quantitative data from the mission profile. The choice of criteria for assigning merit and the selection of parameters to be evaluated depend on the user's particular mission requirements.

MCEP INPUT

HC=500	GAMC=15
TARX=0	VMIN=40
TARY=0	TPO=1
TARZ=0	TPP=2
NMAX=2	TPR=3
NMIN=0.8	PSL=0.5
PHIC=60	TACCEL=1

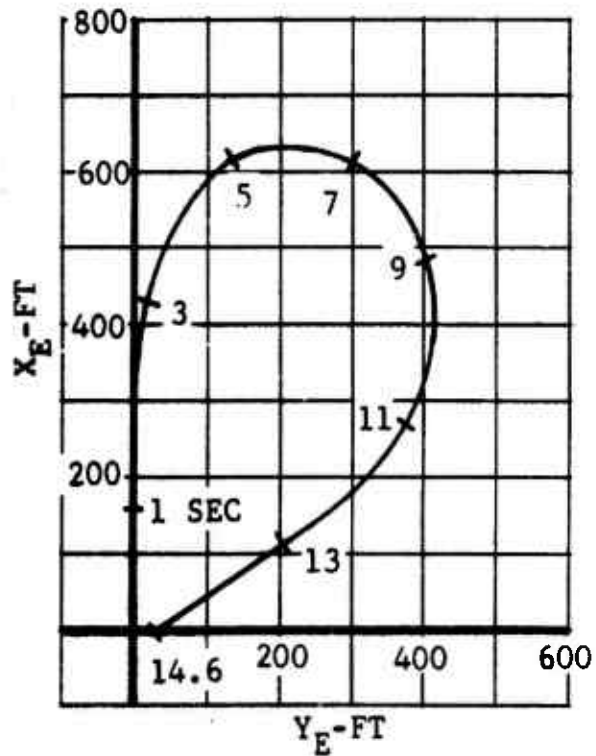


Figure 34. Ground Track of Climbing Return to Target for AH-1G Helicopter at 90 Knots Entry Airspeed.

MCEP provides a detailed output of the important flight path parameters for each maneuver. Time histories of the wind axes accelerations, flight path velocity, flight path position, vertical velocity, phi, gamma, chi, rates of change with respect to time of phi, gamma, and chi, load factor, power required, power supplied by the engine, and time are provided upon request. A summary page is available at the conclusion of each maneuver. This page provides a comparison of the actual values of certain parameters achieved during the maneuver with the desired values. This comparison gives insight into the performance of the aircraft in terms of flight path parameters. A comparison of actual value versus desired value is recorded for the flight path angle, slant range, minimum load factor, maximum load factor, minimum velocity, maximum velocity, exit heading, maximum bank angle, and aim points when applicable to the maneuver performed.

MCEP provides histograms of power, altitude, velocity and load factor at the conclusion of each summary page for each maneuver. These histograms provide information for the number of occurrences and the relative cumulative frequency of occurrence for specified intervals. This information provides data for determining the proportion of flight time spent in a given flight regime.

The flexibility of being able to easily change the limiting parameters such as maximum or minimum load factor allows the user to define the impact of that particular limit on the actual flight path. From this type of comparison, the user can determine a minimum value of a specified parameter which yields a satisfactory flight profile.

SIMULATION OF AH-1G HELICOPTER GUNSHIP MISSION USING MCEP

A typical AH-1G gunship mission is used to demonstrate MCEP. The mission profile is based on data from References 4 and 5 and is a typical escort mission.

DEFINITION OF MISSION PROFILE

The AH-1G dashes ahead of troop-carrying helicopters to clear the landing zone. After the landing zone is cleared, the AH-1G loiters above the landing zone to provide suppressive fire if required during the landing of the utility helicopter. After the landing, the AH-1G returns to base.

The mission is detailed as follows. The AH-1G takes off and accelerates to an airspeed of 70 knots. A climbing turn is executed to obtain a cruising altitude of 2500 feet at a heading of 0 degrees. Now the AH-1G accelerates to a cruise airspeed of 90 knots which is maintained until the aircraft is in the general landing zone area. Once in this area, the AH-1G descends to 800 feet and accelerates to 115 knots. This airspeed is maintained until the landing zone is recognized. Then the AH-1G climbs to 1600 feet and decelerates to 60 knots while looking for targets. A target is identified in the landing zone at a slant range of 1700 meters. The AH-1G dives on the target using a 20-degree dive angle. During the dive, appropriate ordnance is expended, and a rolling pullout is executed to maintain a minimum slant range of 700 meters from the target. During the rolling pullout, the AH-1G turns about 120 degrees to the right and covers with 7.62 mm minigun fire.

Then the AH-1G climbs to 1600 feet and turns back to the landing zone. An orbit is established around the landing zone, and the AH-1G is available for quick-reaction fire if this becomes necessary. After the landing is completed, it rolls out on a heading of 180 degrees and climbs to 2500 feet. It then accelerates to 90 knots and cruises back to home base. Here a descending turn is executed to an altitude of 25 feet, and the airspeed is reduced to hover.

The mission profile is separated into the individual maneuvers of Table I which best described the desired action. The mission profile using MCEP maneuvers is defined in Table II.

RESULTS AND INTERPRETATION OF SIMULATION OF MISSION PROFILE

The mission profile outlined in Table II was simulated using MCEP. The mission consisted of 22 individual maneuvers. The required input data for the AH-1G helicopter and the initial flight conditions are given in Table III. For convenience, the

TABLE II. DEFINITION OF MISSION PROFILE
USING MCEP MANEUVERS

Profile Step Number	Maneuver ID Number	Maneuver	Request
1.	M14	Collective Pop-Up	Climb to 10 feet
2.	M02	Acceleration	Accelerate to 70 knots
3.	M09	Climbing Turn	Climb to 2500 feet and arrive at a heading of 0 degree
4.	M02	Acceleration	Accelerate to 90 knots
5.	M07	Cruise	Fly to aim point of $X_E=20,000$ feet and $Y_E=0$ feet
6.	M04	Descent	Descend to 800 feet while maintaining heading
7.	M02	Acceleration	Accelerate to 115 knots
8.	M01	Cruise	Cruise to 25,000 feet range of landing zone at $X_E=65,000$ feet and $Y_E=0$
9.	M04	Climb	Climb to 1600 feet while maintaining heading
10.	M02	Deceleration	Decelerate to 60 knots
11.	M08	Dive/Rolling Pullout	Execute a 20-degree dive onto a target located in the landing zone at $X_E=65,000$ feet and $Y_E=0$ feet. Maintain a minimum slant range of 2300 feet from target and exit landing zone to the right after a heading change of 120 degrees.
12.	M04	Climb	Climb to 1600 feet
13.	M06	Auto Turn	Turn back to the landing zone

TABLE II - Continued

Profile Step Number	Maneuver ID Number	Maneuver	Request
14.	M02	Acceleration	Stabilize velocity at 70 knots
15.	M01	Cruise	Return to 1500 feet from landing zone located at $X_E=65,000$ feet and $Y_E=0$ feet
16.	M03	Turn	Change heading 60 degrees to the right to parallel landing zone
17.	M12	Orbit	Establish an orbit of radius 800 feet around the landing zone and exit on heading of 180 degrees to return to base
18.	M04	Climb	Climb to 2500 feet while maintaining heading
19.	M02	Acceleration	Accelerate to 90 knots
20.	M01	Cruise	Return to vicinity of base
21.	M04	Descent	Descend to 50 feet
22.	M02	Deceleration	Decelerate to hover

form of the output data was standardized. In some cases, this means labels such as "desired," "actual," and "error" are not meaningful but simply identify end points of the maneuver segment.

The summary page for profile step 1 is presented in Table IV. The entry altitude was 0 and the exit altitude was 10 feet. The maximum flight path angle was 90 degrees. The results of profile step 2 are given in Table V. The AH-1G accelerated to 68.9 knots, which is within the velocity error band of 2 knots. Profile step 3 was a climbing turn to 2500 feet and 0 degrees heading. These results are given in Table VI. The difference between the desired minimum load factor and the actual minimum load factor indicates that the pushover did not need to use the minimum g load factor limit. The maximum load factor limit was exceeded slightly. The aircraft climbed to 2500 feet and the exit heading was 0 degrees. The power, altitude, velocity, and load factor histograms for this maneuver are shown in Table VII. The relative frequency gives the fraction of total flight time spent in each interval, while the relative cumulative frequency gives the fraction of flight time spent in the current interval and all preceding intervals.

The results of the acceleration in profile step 4 are shown in Table VIII. The velocity is stabilized within 1.1 knots of the commanded velocity. The aim point evaluation does not apply for this maneuver. The cruise maneuver of profile step 5 results in an error of 38 feet in slant range as indicated in Table IX. The AH-1G helicopter descends to 800 feet altitude in profile step 6. The summary of this maneuver is presented in Table X. The load factors stayed within the minimum and maximum load factor limits. The aim point evaluation is only meaningful for the altitude. The roll-in time is the time required to establish the descent angle and stay within the minimum load factor limit. Histogram data for the descent maneuvers are shown in Table XI. Profile step 7 consists of accelerating to 113.4 knots as given in Table XII. The aircraft now cruises to the general area of the landing zone as requested in profile step 8. This maneuver is summarized in Table XIII. The AH-1G now climbs to 1600 feet of altitude in profile step 9 as shown in Table XIV. Profile step 10 results in the aircraft decelerating to 61.8 knots. This maneuver is summarized in Table XV.

The AH-1G helicopter has entered the landing zone area and is ready for the engagement of targets in profile step 11. A target is recognized at $X_E=65,000$ feet. The desired minimum slant range from the target was 2300 feet, and the actual was 2293. The aim point comparison is not used for this maneuver. The coordinates of the closest point of approach are printed

in the "actual" row under the aim point heading. Histograms of the maneuver are presented in Table XVII. The results of profile step 12 for a climb to 1600 feet are given in Table XVIII. Profile step 13 asked for an auto turn back to the landing zone. The results of this maneuver are presented in Table XIX. The time to achieve the bank angle was 1.4 seconds, and this bank angle was maintained for 14.55 seconds. The desired exit heading gives the value of the heading which should point the nose of the aircraft to the aim point. The aircraft decelerates to 178 knots in profile step 14 as shown in Table XX. In profile step 15, the AH-1G cruises along the line toward the landing zone as shown in Table XXI. A turn at constant airspeed is executed in profile step 16 to parallel the landing zone as presented in Table XXII. The aim point evaluation is applicable for this maneuver. Histograms of this maneuver are presented in Table XXIII. For profile step 17 an orbit is established in the vicinity of the landing zone. This orbit is maintained for about 5 minutes as given in Table XXIV. At the conclusion of the orbit, the aircraft rolls out on a heading toward home base. A summary of the ground track of the above maneuvers in the landing zone is presented in Figure 35.

The return to home base is accomplished by a climb to cruise altitude of 2500 feet as requested in profile step 18. A summary of this maneuver is given in Table XXV. Profile steps 19, 20, 21, and 22 return the AH-1G to home base. The results of these maneuvers are given in Tables XXVI through XXIX.

Variations of the input parameters to each maneuver can be made to evaluate their impact on the flight path for this mission profile. This simulation demonstrates the method of representing a mission profile in the context of MCEP maneuvers.

TABLE III. AH-1G HELICOPTER INPUT DATA

MANEUVER CRITERIA EVALUATION PROGRAM

AH-1G HELICOPTER
ESCORT MISSION FOR UTILITY HELICOPTERS
DEMONSTRATION OF MCEP

HELICOPTER INPUT DATA

VARIABLE	DIGITAL NAME	VALUE	UNITS
NUMBER OF BLADES	B	2.000	N.D.
ROTOR CHORD	C	2.200	FT
ROTOR RADIUS	R	22.000	FT
MAIN ROTOR INDUCED VELOCITY FACTOR	K _i	2.140	N.D.
TIP SPEED	WR	746.000	FT/SEC
BLADE SECTION LIFT CURVE SLOPE	A2D	6.280	/RAD
BLADE DRAG COEFFICIENT	DELO	0.008	N.D.
	DEL1	0.0	/RAD
	DEL2	1.000	/RAD* ² RAD
DRAG DIVERGENT MACH NUMBER	MCRD	0.750	N.D.
DIVERGENT THRUST COEFFICIENT CURVE	TC1	0.100	N.D.
	TC2	0.200	N.D.
MAXIMUM THRUST COEFFICIENT CURVE	TCM1	0.360	N.D.
	TCM2	0.0	N.D.
CLIMB/DESCENT EFFICIENCY FACTOR	HPEFF	0.800	N.D.
FUSELAGE ANGLE OF ATTACK COEFFICIENTS	KAF1	8.600	
	KAF2	2.400	1/G*G
	KAF3	10.400	1/G
	KAF4	1.000	
	KAF5	17.600	SEC/FT
	KAF6	0.800	N.D.
	KAF7	1.500	W/G
	KAF8	240.000	N.D.
WING AREA	SW	0.0	FT* ²
WING INCIDENCE	I _w	0.0	DEG
INDUCED VELOCITY FACTOR	K _i	0.0	N.D.
WING ASPECT RATIO	ASR	0.0	N.D.
WING COEFFICIENT OF DRAG AT ZERO LIFT	CD0	0.0	N.D.
WING LIFT CURVE SLOPE	A2D _w	0.0	/RAD
FLAT PLATE DRAG COEFFICIENT	CD _{FP}	0.0	N.D.
WING EFFICIENCY FACTOR	WEFF	0.0	N.D.
WING INCIDENCE CHANGE WITH LOAD FACTOR	DELWON	0.0	DEG/G
MAXIMUM POSITIVE LIFT COEFFICIENT	CLMAXP	0.0	N.D.
MAXIMUM NEGATIVE LIFT COEFFICIENT	CLMAXN	0.0	N.D.
LIMIT DIVE VELOCITY	VOL	100.000	KT
MAXIMUM VELOCITY TO THE RIGHT	VXRT	55.000	KT
MAXIMUM VELOCITY TO THE LEFT	VXLT	-55.000	KT

TABLE III - Continued

VARIABLE	DIGITAL NAME	VALUE	UNITS
TIME CONSTANT FOR GAMMA	TAUP	0.500	N.D.
TIME CONSTANT FOR ROLL	TAUR	0.300	N.D.
TIME CONSTANT FOR CHI	TAUJ	0.300	N.D.
MAXIMUM RATE FOR GAMMA	ARPMX	30.000	DEG/SEC
MAXIMUM RATE FOR ROLL	ARRMX	60.000	DEG/SEC
MAXIMUM RATE FOR CHI	ARYMX	60.000	DEG/SEC
MAXIMUM ANGLE FOR GAMMA	GAMMP	60.000	DEG
MINIMUM ANGLE FOR GAMMA	GAMMN	-60.000	DEG
VERTICAL JERK LIMIT	VJERK	0.500	G/SEC
ERROR IN ANGLE CALCULATION	EPA	0.080	DEG
ERROR IN ANGULAR RATE CALCULATION	EPAV	0.050	DEG/SEC
AIRCRAFT FLIGHT CONDITION			
VARIABLE	DIGITAL NAME	VALUE	UNITS
GROSS WEIGHT	GW	9500.000	LB
EQUIVALENT FLAT PLATE DRAG(BETA=0)	F0	19.500	FT**2
EQUIVALENT FLAT PLATE DRAG(BETA=90)	F1	195.000	FT**2
VELOCITY	V	0.0	KT
ALTITUDE	H	0.0	FT
HEADING	CHI	0.0	DEG
AIR DENSITY	RHO	0.002	SLUGS/FT**3
SPEED OF SOUND	VS	1117.000	FT/SEC

TABLE IV. SUMMARY OF PROFILE STEP 1

TYPE OF MANEUVER: COLLECTIVE POPUP

	EXECUTION TIME -SEC	TARGET LOCATION - FT		
		XE	YE	ZE
ROLL IN	0.0	0.	0.	0.
ACHIEVE G	0.0			
HOLD G	0.0			

	TIME SEC.	AIRCRAFT LOCATION - FEET			VELOCITY KNOTS	HEADING DEG
		XE	YE	ZE		
ENTRY	0.0	0.	0.	0.	0.0	0.0
EXIT	7.00	0.	0.	-10.	0.0	0.0

	FLT PATH ANGLE	SLANT RANGE	LOAD FACTOR-G		VELOCITY-KT		EXIT HEADING
			MIN	MAX	MIN	MAX	
DESIRED	0.0	0.	0.800	1.029	0.0	0.0	0.0
ACTUAL	90.0	0.	0.800	1.029	0.0	1.3	0.0
ERROR	-90.0	0.	0.0	0.000	-0.0	-1.3	0.0

	BANK ANGLE MAX	AIM POINT - FEET		
		XE	YE	ZE
DESIRED	0.0	0.	0.	-10.
ACTUAL	0.0	0.	0.	-10.
ERROR	0.0	0.	0.	0.

TABLE V. SUMMARY OF PROFILE STEP 2

TYPE OF MANEUVER: ACCELERATION OR DECELERATION							
	EXECUTION TIME -SEC	TARGET LOCATION - FT					
		XE	YE	ZE			
ROLL IN	0.0	0.	0.	0.			
ACHIEVE G	0.0						
HOLD G	0.0						
	TIME SEC.	AIRCRAFT LOCATION - FEET			VELOCITY KNOTS	HEADING DEG	
		XE	YE	ZE			
ENTRY	7.00	0.	0.	-10.	0.0	0.0	
EXIT	18.30	661.	0.	-10.	68.9	0.0	
	FLT PATH ANGLE	SLANT RANGE	LOAD FACTOR-G		VELOCITY-KT		EXIT HEADING
			MIN	MAX	MIN	MAX	
DESIRED	0.0	0.	1.000	1.000	0.0	70.0	0.0
ACTUAL	0.0	0.	1.000	1.000	0.0	68.9	0.0
ERROR	0.0	0.	0.0	0.0	0.0	1.1	0.0
	BANK ANGLE MAX	AIM POINT - FEET					
		XE	YE	ZE			
DESIRED	0.0	0.	0.	0.			
ACTUAL	0.0	661.	0.	-10.			
ERROR	0.0	-661.	0.	10.			

TABLE VI. SUMMARY OF PROFILE STEP 3

TYPE OF MANEUVER: CLIMBING OR DESCENDING TURN

	EXECUTION TIME -SEC	TARGET LOCATION - FT		
		XE	YE	ZE
ROLL IN	0.0	0.	0.	0.
ACHIEVE G	0.0			
HOLD G	0.0			

	TIME SEC.	AIRCRAFT LOCATION - FEET			VELOCITY KNOTS	HEADING DEG
		XE	YE	ZE		
ENTRY	18.30	661.	0.	-10.	68.9	0.0
EXIT	156.50	968.	-49.	-2500.	68.4	0.0

	FLT PATH ANGLE	SLANT RANGE	LOAD FACTOR-G		VELOCITY-KT		EXIT HEADING
			MIN	MAX	MIN	MAX	
DESIRED	9.5	0.	0.800	1.400	68.9	68.9	0.0
ACTUAL	9.5	0.	0.951	1.409	68.1	68.9	0.0
ERROR	-0.0	0.	-0.151	-0.009	0.7	0.0	0.0

	BANK ANGLE MAX	AIM POINT - FEET		
		XE	YE	ZE
DESIRED	33.6	0.	0.	-2500.
ACTUAL	33.6	968.	-49.	-2500.
ERROR	0.0	-968.	49.	0.

TABLE VII. HISTOGRAMS FOR CLIMBING TURN MANEUVER

HORSEPOWER HISTOGRAM				
HORSEPOWER INTERVAL-HP	NUMBER OF OCCURRENCES	RELATIVE FREQUENCY	RELATIVE CUMULATIVE FREQUENCY	
0.0 - 50.00	0	0.0	0.0	
50.00- 100.00	0	0.0	0.0	
100.00- 150.00	0	0.0	0.0	
150.00- 200.00	0	0.0	0.0	
200.00- 250.00	0	0.0	0.0	
250.00- 300.00	0	0.0	0.0	
300.00- 350.00	0	0.0	0.0	
350.00- 400.00	0	0.0	0.0	
400.00- 450.00	0	0.0	0.0	
450.00- 500.00	0	0.0	0.0	
500.00- 550.00	0	0.0	0.0	
550.00- 600.00	0	0.0	0.0	
600.00- 650.00	19	0.0069	0.0069	
650.00- 700.00	8	0.0029	0.0098	
700.00- 750.00	35	0.0127	0.0224	
750.00- 800.00	54	0.0195	0.0420	
800.00- 850.00	9	0.0033	0.0452	
850.00- 900.00	9	0.0033	0.0485	
900.00- 950.00	8	0.0029	0.0514	
950.00- 1000.00	7	0.0025	0.0539	
1000.00- 1050.00	8	0.0029	0.0568	
1050.00- 1100.00	9	0.0033	0.0600	
1100.00- 1150.00	11	0.0040	0.0640	
1150.00- 1200.00	2588	0.9360	1.0000	
1200.00- 1250.00	0	0.0	1.0000	

ALTITUDE HISTOGRAM				
ALTITUDE INTERVAL-FT	NUMBER OF OCCURRENCES	RELATIVE FREQUENCY	RELATIVE CUMULATIVE FREQUENCY	
0.0 - 200.00	237	0.0857	0.0857	
200.00- 400.00	211	0.0763	0.1620	
400.00- 600.00	212	0.0767	0.2387	
600.00- 800.00	211	0.0763	0.3150	
800.00- 1000.00	211	0.0763	0.3913	
1000.00- 1200.00	212	0.0767	0.4680	
1200.00- 1400.00	211	0.0763	0.5443	
1400.00- 1600.00	211	0.0763	0.6206	
1600.00- 1800.00	211	0.0763	0.6969	
1800.00- 2000.00	212	0.0767	0.7736	
2000.00- 2200.00	211	0.0763	0.8499	
2200.00- 2400.00	211	0.0763	0.9262	
2400.00- 2600.00	204	0.0738	1.0000	
2600.00- 2800.00	0	0.0	1.0000	
2800.00- 3000.00	0	0.0	1.0000	

TABLE VII - Continued

VELOCITY HISTOGRAM

VELOCITY INTERVAL-KT	NUMBER OF OCCURRENCES	RELATIVE FREQUENCY	RELATIVE CUMULATIVE FREQUENCY
0.0 - 10.00	0	0.0	0.0
10.00- 20.00	0	0.0	0.0
20.00- 30.00	0	0.0	0.0
30.00- 40.00	0	0.0	0.0
40.00- 50.00	0	0.0	0.0
50.00- 60.00	0	0.0	0.0
60.00- 70.00	2765	1.0000	1.0000
70.00- 80.00	0	0.0	1.0000
80.00- 90.00	0	0.0	1.0000
90.00- 100.00	0	0.0	1.0000
100.00- 110.00	0	0.0	1.0000
110.00- 120.00	0	0.0	1.0000
120.00- 130.00	0	0.0	1.0000
130.00- 140.00	0	0.0	1.0000
140.00- 150.00	0	0.0	1.0000
150.00- 160.00	0	0.0	1.0000
160.00- 170.00	0	0.0	1.0000
170.00- 180.00	0	0.0	1.0000
180.00- 190.00	0	0.0	1.0000

LOAD FACTOR HISTOGRAM

LOAD FACTOR INTERVAL - G	NUMBER OF OCCURRENCES	RELATIVE FREQUENCY	RELATIVE CUMULATIVE FREQUENCY
0.60- 0.80	0	0.0	0.0
0.80- 1.00	42	0.0152	0.0152
1.00- 1.20	2673	0.9667	0.9819
1.20- 1.40	43	0.0156	0.9975
1.40- 1.60	7	0.0025	1.0000
1.60- 1.80	0	0.0	1.0000
1.80- 2.00	0	0.0	1.0000
2.00- 2.20	0	0.0	1.0000
2.20- 2.40	0	0.0	1.0000

TABLE VIII. SUMMARY OF PROFILE STEP 4

TYPE OF MANEUVER: ACCELERATION OR DECELERATION							
	EXECUTION TIME -SEC	TARGET LOCATION - FT					
		XE	YE	ZE			
ROLL IN	0.0	0.	0.	0.			
ACHIEVE G	0.0						
HOLD G	0.0						
	TIME SEC.	AIRCRAFT XE	LOCATION - FEET		VELOCITY KNOTS	HEADING DEG	
			YE	ZE			
ENTRY	156.50	968.	-49.	-2500.	68.4	0.0	
EXIT	162.80	1819.	-48.	-2500.	88.9	0.0	
	FLT PATH ANGLE	SLANT RANGE	LOAD FACTOR-G		VELOCITY-KT		EXIT HEADING
			MIN	MAX	MIN	MAX	
DESIRED	0.0	0.	1.000	1.000	68.4	90.0	0.0
ACTUAL	0.0	0.	1.000	1.000	68.4	88.9	0.0
ERROR	0.0	0.	0.0	0.0	0.0	1.1	-0.0
	BANK ANGLE MAX	AIM POINT - FEET					
		XE	YE	ZE			
DESIRED	0.0	0.	0.	0.			
ACTUAL	0.0	1819.	-48.	-2500.			
ERROR	0.0	-1819.	48.	2500.			

TABLE IX. SUMMARY OF PROFILE STEP 5

TYPE OF MANEUVER: CRUISE

	EXECUTION TIME -SEC	TARGET LOCATION - FT		
		XE	YE	ZE
ROLL IN	0.0	0.	0.	0.
ACHIEVE G	0.0			
MOLO G	0.0			

	TIME SEC.	AIRCRAFT LOCATION - FEET			VELOCITY KNOTS	HEADING DEG
		XE	YE	ZE		
ENTRY	162.80	1819.	-48.	-2500.	88.9	0.0
EXIT	283.95	19999.	-37.	-2500.	88.9	0.0

	FLT PATH ANGLE	SLANT RANGE	LOAD FACTOR-G		VELOCITY-KT		EXIT HEADING
			MIN	MAX	MIN	MAX	
DESIRED	0.0	0.	1.000	1.000	88.9	88.9	0.0
ACTUAL	0.0	38.	1.600	1.000	88.9	88.9	0.0
ERROR	0.0	-38.	0.0	0.0	0.0	0.0	0.0

	BANK ANGLE MAX	AIM POINT - FEET		
		XE	YE	ZE
DESIRED	0.0	20000.	0.	-2500.
ACTUAL	0.0	19999.	-37.	-2500.
ERROR	0.0	1.	37.	0.

TABLE X. SUMMARY OF PROFILE STEP 6

TYPE OF MANEUVER: CLIMB OR DESCENT							
	EXECUTION TIME -SEC	TARGET LOCATION - FT					
		XE	YE	ZE			
ROLL IN	2.40	0.	0.	0.			
ACHIEVE G	0.0						
HOLD G	0.0						
	TIME SEC.	AIRCRAFT LOCATION - FEET			VELOCITY KNOTS	HEADING DEG	
		XE	YE	ZE			
ENTRY	283.95	19999.	-37.	-2500.	88.9	0.0	
EXIT	398.50	37147.	-27.	-800.	89.1	0.0	
	FLT PATH ANGLE	SLANT RANGE	LOAD FACTOR-G		VELOCITY-KT		EXIT HEADING
			MIN	MAX	MIN	MAX	
DESIRED	-5.8	0.	0.800	1.400	83.9	88.9	0.0
ACTUAL	-5.8	0.	0.815	1.396	89.9	89.2	0.0
ERROR	-0.0	0.	-0.015	0.004	0.0	-0.3	0.0
	BANK ANGLE MAX	AIM POINT - FEET					
		XE	YE	ZE			
DESIRED	0.0	0.	0.	-800.			
ACTUAL	0.0	37147.	-27.	-800.			
ERROR	0.0	-37147.	27.	-0.			

TABLE XI. HISTOGRAMS FOR CLIMB MANEUVER

HCRSEPOWER HISTOGRAM				
HCRSEPOWER INTERVAL-HP	NUMBER OF OCCURRENCES	RELATIVE FREQUENCY	RELATIVE CUMULATIVE FREQUENCY	
0.0 - 50.00	0	0.0	0.0	
50.00- 100.00	0	0.0	0.0	
100.00- 150.00	0	0.0	0.0	
150.00- 200.00	0	0.0	0.0	
200.00- 250.00	0	0.0	0.0	
250.00- 300.00	0	0.0	0.0	
300.00- 350.00	0	0.0	0.0	
350.00- 400.00	2199	0.9594	0.9594	
400.00- 450.00	10	0.0044	0.9638	
450.00- 500.00	9	0.0039	0.9677	
500.00- 550.00	8	0.0035	0.9712	
550.00- 600.00	8	0.0035	0.9747	
600.00- 650.00	9	0.0039	0.9786	
650.00- 700.00	20	0.0087	0.9873	
700.00- 750.00	8	0.0035	0.9908	
750.00- 800.00	5	0.0022	0.9930	
800.00- 850.00	6	0.0026	0.9956	
850.00- 900.00	10	0.0044	1.0000	
900.00- 950.00	0	0.0	1.0000	
950.00- 1000.00	0	0.0	1.0000	
1000.00- 1050.00	0	0.0	1.0000	
1050.00- 1100.00	0	0.0	1.0000	
1100.00- 1150.00	0	0.0	1.0000	
1150.00- 1200.00	0	0.0	1.0000	
1200.00- 1250.00	0	0.0	1.0000	

ALTITUDE HISTOGRAM				
ALTITUDE INTERVAL-FT	NUMBER OF OCCURRENCES	RELATIVE FREQUENCY	RELATIVE CUMULATIVE FREQUENCY	
0.0 - 200.00	0	0.0	0.0	
200.00- 400.00	0	0.0	0.0	
400.00- 600.00	0	0.0	0.0	
600.00- 800.00	11	0.0048	0.0048	
800.00- 1000.00	275	0.1200	0.1248	
1000.00- 1200.00	261	0.1139	0.2387	
1200.00- 1400.00	261	0.1139	0.3525	
1400.00- 1600.00	261	0.1139	0.4664	
1600.00- 1800.00	261	0.1139	0.5803	
1800.00- 2000.00	261	0.1139	0.6942	
2000.00- 2200.00	261	0.1139	0.8080	
2200.00- 2400.00	261	0.1139	0.9219	
2400.00- 2600.00	179	0.0781	1.0000	
2600.00- 2800.00	0	0.0	1.0000	
2800.00- 3000.00	0	0.0	1.0000	

TABLE XI - Continued

VELOCITY HISTOGRAM

VELOCITY INTERVAL-KT	NUMBER OF OCCURRENCES	RELATIVE FREQUENCY	RELATIVE CUMULATIVE FREQUENCY
0.0 - 10.00	0	0.0	0.0
10.00- 20.00	0	0.0	0.0
20.00- 30.00	0	0.0	0.0
30.00- 40.00	0	0.0	0.0
40.00- 50.00	0	0.0	0.0
50.00- 60.00	0	0.0	0.0
60.00- 70.00	0	0.0	0.0
70.00- 80.00	0	0.0	0.0
80.00- 90.00	2292	1.0000	1.0000
90.00- 100.00	0	0.0	1.0000
100.00- 110.00	0	0.0	1.0000
110.00- 120.00	0	0.0	1.0000
120.00- 130.00	0	0.0	1.0000
130.00- 140.00	0	0.0	1.0000
140.00- 150.00	0	0.0	1.0000
150.00- 160.00	0	0.0	1.0000
160.00- 170.00	0	0.0	1.0000
170.00- 180.00	0	0.0	1.0000
180.00- 190.00	0	0.0	1.0000

LOAD FACTOR HISTOGRAM

LOAD FACTOR INTERVAL - G	NUMBER OF OCCURRENCES	RELATIVE FREQUENCY	RELATIVE CUMULATIVE FREQUENCY
0.60- 0.80	0	0.0	0.0
0.80- 1.00	2244	0.9791	0.9791
1.00- 1.20	24	0.0105	0.9895
1.20- 1.40	24	0.0105	1.0000
1.40- 1.60	0	0.0	1.0000
1.60- 1.80	0	0.0	1.0000
1.80- 2.00	0	0.0	1.0000
2.00- 2.20	0	0.0	1.0000
2.20- 2.40	0	0.0	1.0000

TABLE XII. SUMMARY OF PROFILE STEP 7

TYPE OF MANEUVER: ACCELERATION OR DECELERATION							
	EXECUTION TIME -SEC	TARGET LOCATION - FT					
		XE	YE	ZE			
ROLL IN	0.0	0.	0.	0.			
ACHIEVE G	0.0						
HOLD G	0.0						
	TIME SEC.	AIRCRAFT LOCATION - FEET			VELOCITY KNOTS	HEADING OEG	
		XE	YE	ZE			
ENTRY	398.50	37147.	-27.	-800.	89.1	0.0	
EXIT	409.15	38991.	-26.	-800.	113.4	0.0	
	FLT PATH ANGLE	SLANT RANGE	LOAD FACTOR-G		VELOCITY-KT		EXIT HEADING
			MIN	MAX	MIN	MAX	
DESIREO	0.0	0.	1.000	1.000	89.1	115.0	0.0
ACTUAL	0.0	0.	1.000	1.000	89.1	113.4	0.0
ERROR	0.0	0.	0.0	0.0	0.0	1.6	0.0
	BANK ANGLE MAX	AIM POINT - FEET					
		XE	YE	ZE			
DESIREO	0.0	0.	0.	0.			
ACTUAL	0.0	38991.	-26.	-800.			
ERROR	0.0	-38991.	26.	800.			

TABLE XIII. SUMMARY OF PROFILE STEP 8

TYPE OF MANEUVER: CRUISE

	EXECUTION TIME -SEC	TARGET LOCATION - FT		
		XE	YE	ZE
ROLL IN	0.0	0.	0.	0.
ACHIEVE G	0.0			
HOLD G	0.0			

	TIME SEC.	AIRCRAFT LOCATION XE	LOCATION YE	FEET ZE	VELOCITY KNOTS	HEADING DEG
ENTRY	409.15	38991.	-26.	-800.	113.4	0.0
EXIT	414.45	40005.	-26.	-800.	113.4	0.0

	FLT PATH ANGLE	SLANT RANGE	LOAD FACTOR-G		VELOCITY-KT		EXIT HEADING
			MIN	MAX	MIN	MAX	
DESIREO	0.0	25000.	1.000	1.000	113.4	113.4	0.0
ACTUAL	0.0	24995.	1.000	1.000	113.4	113.4	0.0
ERROR	0.0	5.	0.0	0.0	0.0	0.0	0.0

	BANK ANGLE MAX	AIM POINT - FEET		
		XE	YE	ZE
DESIREO	0.0	65000.	0.	-800.
ACTUAL	0.0	40005.	-26.	-800.
ERROR	0.0	24995.	26.	0.

TABLE XIV. SUMMARY OF PROFILE STEP 9

TYPE OF MANEUVER: CLIMB OR DESCENT

	EXECUTION TIME -SEC	TARGET LOCATION - FT		
		XE	YE	ZE
ROLL IN	4.80	0.	0.	0.
ACHIEVE G	0.0			
HOLD G	0.0			

	TIME SEC.	AIRCRAFT LOCATION XE	LOCATION YE	- FEET. ZE	VELOCITY KNOTS	HEADING DEG
ENTRY	414.45	40005.	-26.	-800.	113.4	0.0
EXIT	475.15	51518.	-19.	-1600.	112.7	0.0

	FLT PATH ANGLE	SLANT RANGE	LOAD FACTOR-G		VELOCITY-KT		EXIT HEADING
			MIN	MAX	MIN	MAX	
DESIRED	4.2	0.	0.800	1.400	113.4	113.4	0.0
ACTUAL	4.2	0.	0.817	1.365	112.6	113.4	0.0
ERROR	-0.0	0.	-0.017	0.035	0.8	0.0	0.0

	BANK ANGLE MAX	AIM POINT - FEET		
		XE	YE	ZE
DESIRED	0.0	0.	0.	-1600.
ACTUAL	0.0	51518.	-19.	-1600.
ERROR	0.0	-51518.	19.	0.

TABLE XV. SUMMARY OF PROFILE STEP 10

TYPE OF MANEUVER: ACCELERATION OR DECELERATION

	EXECUTION TIME -SEC	TARGET LOCATION - FT		
		XE	YE	ZE
ROLL IN	0.0	0.	0.	0.
ACHIEVE G	0.0			
MOLO G	0.0			

	TIME SEC.	AIRCRAFT LOCATION - FEET			VELOCITY KNOTS	HEADING DEG
		XE	YE	ZE		
ENTRY	475.15	51518.	-19.	-1600.	112.7	0.0
EXIT	507.80	56215.	-16.	-1600.	61.8	0.0

	FLT PATH ANGLE	SLANT RANGE	LOAD FACTOR-G		VELOCITY-KT		EXIT HEADING
			MIN	MAX	MIN	MAX	
DESIRED	0.0	0.	1.000	1.000	60.0	112.7	0.0
ACTUAL	0.0	0.	1.000	1.000	61.8	112.7	0.0
ERROR	0.0	0.	0.0	0.0	-1.8	0.0	0.0

	BANK ANGLE MAX	AIM POINT - FEET		
		XE	YE	ZE
DESIRED	0.0	0.	0.	0.
ACTUAL	0.0	56215.	-16.	-1600.
ERROR	0.0	-56215.	16.	1600.

TABLE XVI. SUMMARY OF PROFILE STEP 11

TYPE OF MANEUVER: DIVE AND ROLLING PULLOUT

	EXECUTION TIME -SEC	TARGET LOCATION - FT		
		XE	YE	ZE
ROLL IN	0.0	65000.	0.	0.
ACHIEVE G	0.0			
HOLD G	0.0			

	TIME SEC.	AIRCRAFT LOCATION - FEET			VELOCITY KNOTS	HEADING DEG
		XE	YE	ZE		
ENTRY	507.80	56215.	-16.	-1600.	61.8	0.0
EXIT	568.90	62852.	846.	-958.	80.6	121.1

	FLT PATH ANGLE	SLANT RANGE	LOAD FACTOR-G		VELOCITY-KT		EXIT HEADING
			MIN	MAX	MIN	MAX	
DESIRED	-20.0	2300.	0.800	2.200	60.0	190.0	120.0
ACTUAL	-19.9	2293.	0.782	2.148	61.8	116.6	121.1
ERROR	-0.1	7.	0.018	0.052	-1.8	73.4	-1.1

	BANK ANGLE MAX	AIM POINT - FEET		
		XE	YE	ZE
DESIRED	60.0	65000.	0.	0.
ACTUAL	60.0	62966.	450.	-958.
ERROR	0.0	2034.	-450.	958.

TABLE XVII. HISTOGRAMS FOR DIVE/ROLLING PULLOUT

HORSEPOWER HISTOGRAM

HORSEPOWER INTERVAL-HP	NUMBER OF OCCURRENCES	RELATIVE FREQUENCY	RELATIVE CUMULATIVE FREQUENCY
0.0 - 50.00	0	0.0	0.0
50.00- 100.00	0	0.0	0.0
100.00- 150.00	0	0.0	0.0
150.00- 200.00	0	0.0	0.0
200.00- 250.00	0	0.0	0.0
250.00- 300.00	0	0.0	0.0
300.00- 350.00	0	0.0	0.0
350.00- 400.00	265	0.2167	0.2167
400.00- 450.00	10	0.0082	0.2249
450.00- 500.00	12	0.0098	0.2347
500.00- 550.00	15	0.0123	0.2469
550.00- 600.00	20	0.0164	0.2633
600.00- 650.00	745	0.6092	0.8724
650.00- 700.00	18	0.0147	0.8872
700.00- 750.00	5	0.0041	0.8913
750.00- 800.00	3	0.0025	0.8937
800.00- 850.00	3	0.0025	0.8962
850.00- 900.00	2	0.0016	0.8978
900.00- 950.00	2	0.0016	0.8994
950.00- 1000.00	3	0.0025	0.9019
1000.00- 1050.00	1	0.0008	0.9027
1050.00- 1100.00	2	0.0016	0.9043
1100.00- 1150.00	2	0.0016	0.9060
1150.00- 1200.00	115	0.0940	1.0000
1200.00- 1250.00	0	0.0	1.0000

ALTITUDE HISTOGRAM

ALTITUDE INTERVAL-FT	NUMBER OF OCCURRENCES	RELATIVE FREQUENCY	RELATIVE CUMULATIVE FREQUENCY
0.0 - 200.00	0	0.0	0.0
200.00- 400.00	0	0.0	0.0
400.00- 600.00	0	0.0	0.0
600.00- 800.00	0	0.0	0.0
800.00- 1000.00	141	0.1153	0.1153
1000.00- 1200.00	78	0.0638	0.1791
1200.00- 1400.00	70	0.0572	0.2363
1400.00- 1600.00	185	0.1513	0.3876
1600.00- 1800.00	749	0.6124	1.0000
1800.00- 2000.00	0	0.0	1.0000
2000.00- 2200.00	0	0.0	1.0000
2200.00- 2400.00	0	0.0	1.0000
2400.00- 2600.00	0	0.0	1.0000
2600.00- 2800.00	0	0.0	1.0000
2800.00- 3000.00	0	0.0	1.0000

TABLE XVII - Continued

VELOCITY HISTOGRAM

VELOCITY INTERVAL-KT	NUMBER OF OCCURRENCES	RELATIVE FREQUENCY	RELATIVE CUMULATIVE FREQUENCY
0.0 - 10.00	0	0.0	0.0
10.00- 20.00	0	0.0	0.0
20.00- 30.00	0	0.0	0.0
30.00- 40.00	0	0.0	0.0
40.00- 50.00	0	0.0	0.0
50.00- 60.00	0	0.0	0.0
60.00- 70.00	868	0.7097	0.7097
70.00- 80.00	37	0.0303	0.7400
80.00- 90.00	94	0.0769	0.8168
90.00- 100.00	59	0.0482	0.8651
100.00- 110.00	59	0.0482	0.9133
110.00- 120.00	106	0.0867	1.0000
120.00- 130.00	0	0.0	1.0000
130.00- 140.00	0	0.0	1.0000
140.00- 150.00	0	0.0	1.0000
150.00- 160.00	0	0.0	1.0000
160.00- 170.00	0	0.0	1.0000
170.00- 180.00	0	0.0	1.0000
180.00- 190.00	0	0.0	1.0000

LOAD FACTOR HISTOGRAM

LOAD FACTOR INTERVAL - G	NUMBER OF OCCURRENCES	RELATIVE FREQUENCY	RELATIVE CUMULATIVE FREQUENCY
0.60- 0.80	37	0.0303	0.0303
0.80- 1.00	239	0.1954	0.2257
1.00- 1.20	776	0.6345	0.8602
1.20- 1.40	26	0.0213	0.8814
1.40- 1.60	27	0.0221	0.9035
1.60- 1.80	19	0.0155	0.9191
1.80- 2.00	21	0.0172	0.9362
2.00- 2.20	78	0.0638	1.0000
2.20- 2.40	0	0.0	1.0000

TABLE XVIII. SUMMARY OF PROFILE STEP 12

TYPE OF MANEUVER: CLIMB OR DESCENT

	EXECUTION TIME -SEC	TARGET LOCATION - FT		
		XE	YE	ZE
ROLL IN	8.00	0.	0.	0.
ACHIEVE G	0.0			
HOLD G	0.0			

	TIME SEC.	AIRCRAFT LOCATION - FEET			VELOCITY KNOTS	HEADING DEG
		XE	YE	ZE		
ENTRY	568.90	62852.	846.	-958.	80.6	121.1
EXIT	601.20	60632.	4525.	-1601.	80.0	121.1

	FLT PATH ANGLE	SLANT RANGE	LOAD FACTOR-G		VELOCITY-KT		EXIT HEADING
			MIN	MAX	MIN	MAX	
DESIRED	10.6	0.	0.800	1.400	80.6	80.6	121.1
ACTUAL	10.6	0.	0.802	1.386	79.7	80.6	121.1
ERROR	-0.0	0.	-0.002	0.014	0.9	0.0	0.0

	BANK ANGLE MAX	AIM POINT - FEET		
		XE	YE	ZE
DESIRED	0.0	0.	0.	-1600.
ACTUAL	0.0	60632.	4525.	-1601.
ERROR	0.0	-60632.	-4525.	1.

TABLE XIX. SUMMARY OF PROFILE STEP 13

TYPE OF MANEUVER: AUTO TURN

	EXECUTION TIME -SEC	TARGET LOCATION - FT		
		XE	YE	ZE
ROLL IN	1.40	0.	0.	0.
ACHIEVE G	1.40			
HOLD G	14.55			

	TIME SEC.	AIRCRAFT XE	LOCATION - FEET YE ZE	VELOCITY KNOTS	HEADING DEG
ENTRY	601.20	60632.	4525. -1601.	80.0	121.1
EXIT	618.55	61790.	5241. -1601.	80.0	300.8

	FLT PATH ANGLE	SLANT RANGE	LOAD FACTOR-G		VELOCITY-KT		EXIT HEADING
			MIN	MAX	MIN	MAX	
DESIRED	0.0	0.	1.000	1.300	80.0	80.0	300.2
ACTUAL	-0.0	0.	1.000	1.300	79.9	80.0	300.8
ERROR	0.0	0.	0.0	0.000	0.1	-0.0	-0.6

	BANK ANGLE MAX	AIM POINT - FEET		
		XE	YE	ZE
DESIRED	-39.7	65000.	0.	-1601.
ACTUAL	-39.7	61790.	5241.	-1601.
ERROR	-0.0	3210.	-5241.	0.

TABLE XX. SUMMARY OF PROFILE STEP 14

TYPE OF MANEUVER: ACCELERATION OR DECELERATION

	EXECUTION TIME -SEC	TARGET LOCATION - FT		
		XE	YE	ZE
ROLL IN	0.0	0.	0.	0.
ACHIEVE G	0.0			
HOLD G	0.0			

	TIME SEC.	AIRCRAFT LOCATION - FEET			VELOCITY KNOTS	HEADING DEG
		XE	YE	ZE		
ENTRY	618.55	61790.	5241.	-1601.	80.0	300.8
EXIT	625.45	62244.	4481.	-1601.	71.8	300.8

	FLT PATH ANGLE	SLANT RANGE	LOAD FACTOR-G		VELOCITY-KT		EXIT HEADING
			MIN	MAX	MIN	MAX	DEG
DESIRED	0.0	0.	1.000	1.000	70.0	80.0	300.8
ACTUAL	0.0	0.	1.000	1.000	71.8	80.0	300.8
ERROR	0.0	0.	0.0	0.0	-1.8	0.0	0.0

	BANK ANGLE MAX	AIM POINT - FEET		
		XE	YE	ZE
DESIRED	0.0	0.	0.	0.
ACTUAL	0.0	62244.	4481.	-1601.
ERROR	0.0	-62244.	-4481.	1601.

TABLE XXI. SUMMARY OF PROFILE STEP 15

TYPE OF MANEUVER: CRUISE

	EXECUTION TIME -SEC	TARGET LOCATION - FT		
		XE	YE	ZE
ROLL IN	0.0	0.	0.	0.
ACHIEVE G	G.0			
HOLD G	0.0			

	TIME SEC.	AIRCRAFT XE	LOCATION YE	- FEET ZE	VELOCITY KNOTS	HEADING DEG
ENTRY	625.45	62244.	4481.	-160.	71.8	300.8
EXIT	656.5C	64172.	1250.	-1601.	71.8	300.8

	FLT PATH ANGLE	SLANT RANGE	LOAD FACTOR-G		VELOCITY-KT		EXIT HEADING
			MIN	MAX	MIN	MAX	
DESIRED	0.0	1500.	1.000	1.000	71.8	71.8	300.8
ACTUAL	0.0	1499.	1.000	1.000	71.8	71.8	300.8
ERROR	0.0	1.	0.0	0.0	0.0	0.0	0.0

	BANK ANGLE MAX	AIM POINT - FEET		
		XE	YE	ZE
DESIRED	0.0	65000.	0.	-1601.
ACTUAL	0.0	64172.	1250.	-1601.
ERROR	0.0	828.	-1250.	0.

TABLE XXII. SUMMARY OF PROFILE STEP 16

TYPE OF MANEUVER: LEVEL TURN

	EXECUTION TIME -SEC	TARGET LOCATION - FT		
		XE	YE	ZE
ROLL IN	1.60	0.	0.	0.
ACHIEVE G	1.60			
HOLD G	2.55			

	TIME SEC.	AIRCRAFT LOCATION - FEET			VELOCITY KNOTS	HEADING OEG
		XE	YE	ZE		
ENTRY	656.50	64172.	1250.	-1601.	71.8	300.8
EXIT	662.25	64735.	930.	-1601.	71.8	1.1

	FLT PATH ANGLE	SLANT RANGE	LOAD FACTOR-G		VELOCITY-KT		EXIT HEADING
			MIN	MAX	MIN	MAX	
DESIREO	0.0	0.	1.000	1.400	71.8	71.8	0.8
ACTUAL	0.0	0.	1.000	1.400	71.7	71.8	1.1
ERROR	0.0	0.	0.0	0.000	0.1	-0.0	-0.3

	BANK ANGLE MAX	AIM POINT - FEET		
		XE	YE	ZE
DESIREO	44.4	0.	0.	-1601.
ACTUAL	44.4	64735.	930.	-1601.
ERROR	0.0	-64735.	-930.	0.

TABLE XXIII. HISTOGRAMS FOR TURN AT CONSTANT AIRSPEED AND ALTITUDE MANEUVER

HORSEPOWER HISTOGRAM			
HORSEPOWER INTERVAL-HP	NUMBER OF OCCURRENCES	RELATIVE FREQUENCY	RELATIVE CUMULATIVE FREQUENCY
0.0 - 50.00	0	0.0	0.0
50.00- 100.00	0	0.0	0.0
100.00- 150.00	0	0.0	0.0
150.00- 200.00	0	0.0	0.0
200.00- 250.00	0	0.0	0.0
250.00- 300.00	0	0.0	0.0
300.00- 350.00	0	0.0	0.0
350.00- 400.00	0	0.0	0.0
400.00- 450.00	0	0.0	0.0
450.00- 500.00	0	0.0	0.0
500.00- 550.00	0	0.0	0.0
550.00- 600.00	0	0.0	0.0
600.00- 650.00	27	0.2328	0.2328
650.00- 700.00	7	0.0603	0.2931
700.00- 750.00	4	0.0345	0.3276
750.00- 800.00	4	0.0345	0.3621
800.00- 850.00	4	0.0345	0.3966
850.00- 900.00	2	0.0172	0.4138
900.00- 950.00	5	0.0431	0.4569
950.00- 1000.00	63	0.5431	1.0000
1000.00- 1050.00	0	0.0	1.0000
1050.00- 1100.00	0	0.0	1.0000
1100.00- 1150.00	0	0.0	1.0000
1150.00- 1200.00	0	0.0	1.0000
1200.00- 1250.00	0	0.0	1.0000

ALTITUDE HISTOGRAM			
ALTITUDE INTERVAL-FT	NUMBER OF OCCURRENCES	RELATIVE FREQUENCY	RELATIVE CUMULATIVE FREQUENCY
0.0 - 200.00	0	0.0	0.0
200.00- 400.00	0	0.0	0.0
400.00- 600.00	0	0.0	0.0
600.00- 800.00	0	0.0	0.0
800.00- 1000.00	0	0.0	0.0
1000.00- 1200.00	0	0.0	0.0
1200.00- 1400.00	0	0.0	0.0
1400.00- 1600.00	0	0.0	0.0
1600.00- 1800.00	116	1.0000	1.0000
1800.00- 2000.00	0	0.0	1.0000
2000.00- 2200.00	0	0.0	1.0000
2200.00- 2400.00	0	0.0	1.0000
2400.00- 2600.00	0	0.0	1.0000
2600.00- 2800.00	0	0.0	1.0000
2800.00- 3000.00	0	0.0	1.0000

TABLE XXIII - Continued

VELOCITY HISTOGRAM

VELOCITY INTERVAL - FT	NUMBER OF OCCURRENCES	RELATIVE FREQUENCY	RELATIVE CUMULATIVE FREQUENCY
0.0 - 10.00	0	0.0	0.0
10.00- 20.00	0	0.0	0.0
20.00- 30.00	0	0.0	0.0
30.00- 40.00	0	0.0	0.0
40.00- 50.00	0	0.0	0.0
50.00- 60.00	0	0.0	0.0
60.00- 70.00	0	0.0	0.0
70.00- 80.00	116	1.0000	1.0000
80.00- 90.00	0	0.0	1.0000
90.00- 100.00	0	0.0	1.0000
100.00- 110.00	0	0.0	1.0000
110.00- 120.00	0	0.0	1.0000
120.00- 130.00	0	0.0	1.0000
130.00- 140.00	0	0.0	1.0000
140.00- 150.00	0	0.0	1.0000
150.00- 160.00	0	0.0	1.0000
160.00- 170.00	0	0.0	1.0000
170.00- 180.00	0	0.0	1.0000
180.00- 190.00	0	0.0	1.0000

LOAD FACTOR HISTOGRAM

LOAD FACTOR INTERVAL - G	NUMBER OF OCCURRENCES	RELATIVE FREQUENCY	RELATIVE CUMULATIVE FREQUENCY
0.60- 0.80	0	0.0	0.0
0.80- 1.00	0	0.0	0.0
1.00- 1.20	42	0.3621	0.3621
1.20- 1.40	74	0.6379	1.0000
1.40- 1.60	0	0.0	1.0000
1.60- 1.80	0	0.0	1.0000
1.80- 2.00	0	0.0	1.0000
2.00- 2.20	0	0.0	1.0000
2.20- 2.40	0	0.0	1.0000

TABLE XXIV. SUMMARY OF PROFILE STEP 17

TYPE OF MANEUVER: ORBIT

	EXECUTION TIME -SEC	TARGET LOCATION - FT		
		XE	YE	ZE
RCLL IN	1.00	0.	0.	0.
ACHIEVE G	1.00			
HOLD G	309.95			

	TIME SEC.	AIRCRAFT LOCATION - FEET.			VELOCITY KNOTS	HEADING DEG
		XE	YE	ZE		
ENTRY	662.25	64735.	930.	-1601.	71.8	1.1
EXIT	974.20	64733.	-667.	-1599.	71.8	179.8

	FLT PATH ANGLE	SLANT RANGE	LOAD FACTOR-G		VELOCITY-KT		EXIT HEADING
			MIN	MAX	MIN	MAX	
DESIRED	0.0	0.	1.000	1.152	71.8	71.8	180.0
ACTUAL	-0.0	0.	1.000	1.152	71.8	71.8	179.8
ERRJR	0.0	0.	0.0	0.000	0.0	-0.0	0.2

	BANK ANGLE MAX	AIM POINT - FEET		
		XE	YE	ZE
DESIRED	-29.7	0.	0.	-1601.
ACTUAL	-29.7	64733.	-667.	-1599.
ERROR	-0.0	-64733.	667.	-2.

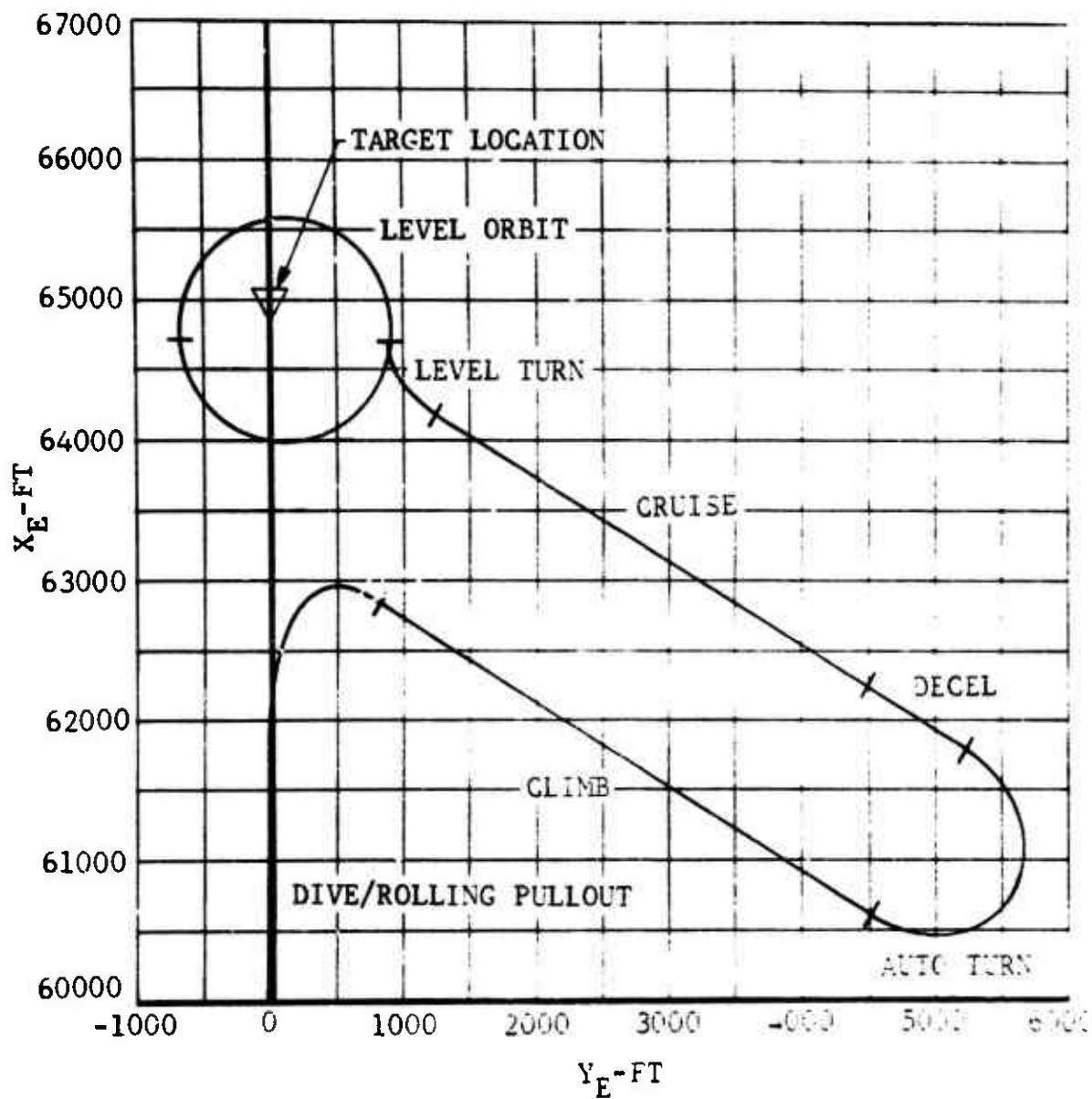


Figure 35. Summary of Ground Track for Demonstration Manuever in Landing Zone Area.

TABLE XXV. SUMMARY OF PROFILE STEP 18

TYPE OF MANEUVER: CLIMB OR DESCENT

	EXECUTION TIME -SEC	TARGET LOCATION - FT		
		XE	YE	ZE
ROLL IN	8.60	0.	0.	0.
ACHIEVE G	0.0			
HOLD G	0.0			

	TIME SEC.	AIRCRAFT LOCATION - FEET			VELOCITY KNOTS	HEADING DEG
		XE	YE	ZE		
ENTRY	974.20	64733.	-607.	-1599.	71.8	179.8
EXIT	1015.75	59847.	-653.	-2501.	71.2	179.8

	FLT PATH ANGLE	SLANT RANGE	LOAD FACTOR-G		VELOCITY-KT		EXIT HEADING
			MIN	MAX	MIN	MAX	
DESIRED	12.5	0.	0.800	1.400	71.8	71.8	179.8
ACTUAL	12.5	0.	0.804	1.385	70.9	71.8	179.8
ERROR	-0.0	0.	-0.004	0.015	0.9	0.0	0.0

	BANK ANGLE MAX	AIM POINT - FEET		
		XE	YE	ZE
DESIRED	0.0	0.	0.	-2500.
ACTUAL	0.0	59847.	-653.	-2501.
ERROR	0.0	-59847.	653.	1.

TABLE XXVI. SUMMARY OF PROFILE STEP 19

TYPE OF MANEUVER: ACCELERATION OR DECELERATION

	EXECUTION TIME -SEC	TARGET LOCATION - FT		
		XE	YE	ZE
ROLL IN	0.0	0.	0.	0.
ACHIEVE G	0.0			
HCLO G	0.0			

	TIME SEC.	AIRCRAFT LOCATION - FEET			VELOCITY KNOTS	HEADING DEG
		XE	YE	ZE		
ENTRY	1015.75	59847.	-653.	-2501.	71.2	179.8
EXIT	1020.70	59178.	-651.	-2501.	89.4	179.8

	FLT PATH ANGLE	SLANT RANGE	LOAD FACTOR-G		VELOCITY-KT		EXIT HEADING
			MIN	MAX	MIN	MAX	
DESIREO	0.0	0.	1.000	1.000	71.2	90.0	179.8
ACTUAL	0.0	0.	1.000	1.000	71.2	89.4	179.8
ERROR	0.0	0.	0.0	0.0	0.0	0.6	0.0

	BANK ANGLE MAX	AIM POINT - FEET		
		XE	YE	ZE
DESIREO	0.0	0.	0.	0.
ACTUAL	0.0	59178.	-651.	-2501.
ERROR	0.0	-59178.	651.	2501.

TABLE XXVII. SUMMARY OF PROFILE STEP 20

TYPE OF MANEUVER: CRUISE

	EXECUTION TIME -SEC	TARGET LOCATION - FT		
		XE	YE	ZE
ROLL IN	0.0	0.	0.	0.
ACHIEVE G	0.0			
HOLD G	0.0			

	TIME SEC.	AIRCRAFT LOCATION - FEET			VELOCITY KNOTS	HEADING DEG
		XE	YE	ZE		
ENTRY	1020.70	59178.	-651.	-2501.	89.4	179.8
EXIT	1229.50	27677.	-564.	-2501.	89.4	179.8

	FLT PATH ANGLE	SLANT RANGE	LOAD FACTOR-G		VELOCITY-KT		EXIT HEADING
			MIN	MAX	MIN	MAX	
DESIRED	0.0	0.	1.000	1.000	89.4	89.4	179.8
ACTUAL	0.0	565.	1.000	1.000	89.4	89.4	179.8
ERRCR	0.0	-565.	0.0	0.0	0.0	0.0	0.0

	BANK ANGLE MAX	AIM POINT - FEET		
		XE	YE	ZE
DESIRED	0.0	27700.	0.	-2501.
ACTUAL	0.0	27677.	-564.	-2501.
ERRDR	0.0	23.	564.	0.

TABLE XXVIII. SUMMARY OF PROFILE STEP 21

TYPE OF MANEUVER: CLIMB OR DESCENT

	EXECUTION TIME -SEC	TARGET LOCATION - FT		
		XE	YE	ZE
ROLL IN	2.40	0.	0.	0.
ACHIEVE G	0.0			
MOLO G	0.0			

	TIME SEC.	AIRCRAFT LOCATION XE	LOCATION - FEET		VELOCITY KNOTS	HEADING DEG
			YE	ZE		
ENTRY	1229.50	27677.	-564.	-2501.	89.4	179.8
EXIT	1391.75	3250.	-496.	-50.	89.6	179.8

	FLT PATH ANGLE	SLANT RANGE	LOAD FACTOR-G		VELOCITY-KT		EXIT HEADING
			MIN	MAX	MIN	MAX	
DESIREO	-5.9	0.	0.800	1.400	89.4	89.4	179.8
ACTUAL	-5.9	0.	0.814	1.399	89.4	89.6	179.8
ERROR	-0.0	0.	-0.014	0.001	0.0	-0.3	0.0

	BANK ANGLE MAX	AIM POINT - FEET		
		XE	YE	ZE
DESIREO	0.0	0.	0.	-50.
ACTUAL	0.0	3250.	-496.	-50.
ERROR	0.0	-3250.	496.	-0.

TABLE XXIX. SUMMARY OF PROFILE STEP 22

TYPE OF MANEUVER: ACCELERATION OR DECELERATION

	EXECUTION TIME -SEC	TARGET LOCATION - FT		
		XE	YE	ZE
ROLL IN	0.0	0.	0.	0.
ACHIEVE G	0.0			
HOLD G	0.0			

	TIME SEC.	AIRCRAFT LOCATION - FEET			VELOCITY KNOTS	HEADING DEG
		XE	YE	ZE		
ENTRY	1391.75	3250.	-496.	-50.	89.6	179.8
EXIT	1413.65	1066.	-490.	-50.	0.9	179.8

	FLT PATH ANGLE	SLANT RANGE	LOAD FACTOR-G		VELOCITY-KT		EXIT HEADING
			MIN	MAX	MIN	MAX	
DESIRED	0.0	0.	1.000	1.000	0.0	89.6	179.8
ACTUAL	0.0	0.	1.000	1.000	0.9	89.6	179.8
ERROR	0.0	0.	0.0	0.0	-0.9	-0.0	0.0

	BANK ANGLE MAX	AIM POINT - FEET		
		XE	YE	ZE
DESIRED	0.0	0.	0.	0.
ACTUAL	0.0	1066.	-490.	-50.
ERROR	0.0	-1066.	490.	50.

LITERATURE CITED

1. Wood, T. L., and Livingston, C. L., AN ENERGY METHOD FOR PREDICTION OF HELICOPTER MANEUVERABILITY, BHC Report 299-099-557, December 28, 1971.
2. Wells, C. D., and Wood, T. L., MANEUVERABILITY - THEORY AND APPLICATION, Journal of the American Helicopter Society, Volume 8, Number 1, January 1973.
3. Bird, B. J., Bennett, R. L., and McLarty, T. T., ROTOR-CRAFT FLIGHT SIMULATION WITH AEROELASTIC ROTOR REPRESENTATION, USAAMRDL Technical Report 71-68A to be published.
4. McDavitt, P. W., A SURVEY OF VIETNAM RETURNEES - ARMED HELICOPTER OPERATIONAL DATA AND CAPABILITY DESIRED FOR FUTURE SYSTEMS, Sikorsky Aircraft Division of United Aircraft, June 1967, AD814904(U).
5. Buffum, F. G., ATTACK HELICOPTER MISSION AND TARGETS, Weapons Planning Groups, N.W.C., June 1971, NWC TP 5131 (Confidential).

APPENDIX
USER'S GUIDE

The required input data for MCEP are listed below. The program requires a set of basic data which describe the helicopter to be evaluated. The helicopter data are followed by the necessary information for histograms of power, altitude, velocity, and load factor. If a wing is used, then the wing data cards are required. These cards are followed by any number of maneuver sets consisting of a maneuver identification card and maneuver data cards. The data are input fields of G10.0, with the exception of the logic variables which have a field of L1.

Identification

Card 01

Columns 1-70 Identifying Comments

Card 02

Columns 1-70 Identifying Comments

Card 03

Columns 1-70 Identifying Comments

Helicopter Group

Card 04

Columns 1-10	number of rotor blades, B	-
11-20	rotor chord, C	ft
21-30	rotor radius, R	ft
31-40	flat plate drag ($C_D=1$) area at $\beta=0^\circ$, F_0	ft ²
41-50	flat plate drag ($C_D=1$) area at $\beta=90^\circ$, F_1	ft ²
51-60	main rotor induced velocity factor, K3	-
61-70	tip speed, WR	ft/sec
71-80	blade section lift curve slope, A2D	/rad

The main rotor induced velocity factor, K3, represents the increased induced velocity at low airspeeds to improve correlation with measured data (Ref. 1, pp 16, 45, 47).

Card 05

Columns 1-10	constant part of blade C_D , DELO ($C_D = \delta_0 + \delta_1\alpha + \delta_2\alpha^2$)	-
11-20	α varying part of blade C_D , DEL1 ($C_D = \delta_0 + \delta_1\alpha + \delta_2\alpha^2$)	/rad
21-30	α^2 varying part of blade C_D , DEL2 ($C_D = \delta_0 + \delta_1\alpha + \delta_2\alpha^2$)	/rad ²
31-40	drag divergence Mach number, MCRO	-
41-50	efficiency factor for computing climb and descent power, HP _{EFF} ($HP_{V_Z} = -gw V_{ZE}/550 HP_{EFF}$)	-
51-60	error in angular displacement for gain calculation, EPA	deg
61-70	error in angular rate for gain calculation, EPAV	deg/sec

Card 06

Columns 1-10	time constant for gamma, TAUP (time to reach 63% of peak rate)	sec
11-20	time constant for roll, TAUR (time to reach 63% of peak rate)	sec
21-30	time constant for chi, TAUY (time to reach 63% of peak rate)	sec
31-40	maximum roll rate, ARRMX	deg/sec
41-50	maximum gamma rate, ARPMX	deg/sec
51-60	maximum chi rate, ARYMX	deg/sec
61-70	maximum negative gamma	deg
71-80	maximum positive gamma	deg

Card 07

Columns 1-10	constant in $[t_c]_{Div}$ expression, TC1	
11-20	velocity constant in $[t_c]_{Div}$ expression, TC2	
21-30	maximum time to apply power, TMAX	sec

31-40	minimum time to apply power, TMIN	sec
41-50	constant in $t_{c_{max}}$, TCM1	-
51-60	velocity constant in $t_{c_{max}}$, TCM2	-
61-70	maximum sideward velocity to left, VMLT	kt
71-80	maximum sideward velocity to right, VMRT	kt

Card 08

Columns 1-10	fuselage angle of attack coefficient, KAF1	$\frac{(\text{ft}/\text{sec})^{1.6}}{(\text{ft}^2-\text{lb})^{.5}}$
11-20	fuselage angle of attack coefficient, KAF2	$1/g^2$
21-30	fuselage angle of attack coefficient, KAF3	$1/g$
31-40	fuselage angle of attack coefficient, KAF4	$\frac{(\text{ft}^2-\text{lb})^{.5}}{(\text{ft}/\text{sec})^{1.6}}$
41-50	fuselage angle of attack coefficient, KAF5	sec/ft
51-60	fuselage angle of attack coefficient, KAF6	-
61-70	fuselage angle of attack coefficient, KAF7	deg
71-80	fuselage angle of attack coefficient, KAF8	-

Card 09

Columns 1-10	gross weight, GW	lb
11-20	limit dive velocity, VDL	kt
21-30	maximum power available, HPMAX	hp

31-40	air density, RHO	slug/ft ³
41-50	speed of sound, VS	ft/sec
51-60	time increment for integration, DDT	sec
61-70	rate of change of vertical load factor, VJERK	/sec
71	Wing = $\begin{cases} \text{F no wing} \\ \text{T wing} \end{cases}$	-

Card 10

Columns 1-10	velocity, V	kt
11-20	altitude, H	ft
21-30	X position in Earth reference, XE	ft
31-40	Y position in Earth reference, YE	ft
41-50	heading, CHI	deg
51-60	starting time, T	sec

Card 11

Columns 1-10	upper limit for power histogram, PMAX(1)	hp
11-20	lower limit for power histogram, PMIN(1)	hp
21-30	interval size for power histogram, DHIS(1)	hp

Card 12

Columns 1-10	upper limit for altitude histogram, PMAX(2)	ft
11-20	lower limit for altitude histogram, PMIN(2)	ft
21-30	interval size for altitude histogram, DHIS(2)	ft

Card 13

Columns 1-10	upper limit for velocity histogram, PMAX(3)	kt.
--------------	---	-----

11-20	lower limit for velocity histogram, PMIN(3)	kt
21-30	interval size for velocity histogram, DHIS(3)	kt

Card 14

Columns 1-10	upper limit for load factor histogram, PMAX(4)	-
11-20	lower limit for load factor histogram, PMIN(4)	-
21-30	interval size for load factor histogram, DHIS(4)	-

The maximum number of intervals is limited to 200. If any interval size is set to zero, then histograms are bypassed.

If WING=F then the next two wing cards are omitted.

Wing Card 01

Columns 1-10	wing incidence when $n=1$, IW	deg
11-20	wing induced velocity factor, KW	-
21-30	wing area, SW	ft ²
31-40	wing aspect ratio, ASR	-
41-50	wing drag coefficient at zero angle of attack, CDO	-
51-60	2-D wing lift curve slope, AL2D	/rad
61-70	drag coefficient for flat plate, CDFP	-
71-80	wing efficiency factor, WEFF	-

Wind Card 02

Columns 1-10	rate of change of wing incidence with load factor, DIWDN	deg
11-20	maximum positive lift coefficient, CLMAXP	

Columns 21-30	maximum negative lift coefficient, CLMAXN	-
31	WINGPRT =	{ F suppress wing output data { T print wing data

At this point, the program expects maneuver identification cards. The program reads one maneuver identification card at a time. The maneuver called by the main program then reads the maneuver data card following the maneuver identification card. At the conclusion of the maneuver, the main program then reads the next maneuver identification card. If there are no more maneuver identification cards, then the program stops. The formats for the maneuver identification and maneuver data cards are presented below.

Cruise

Maneuver Identification Card

Columns 1-3: M01

Maneuver Data Card

Columns 1-10	X aim point in Earth reference, XCP	ft
11-20	Y aim point in Earth reference, YCP	ft
21-30	cruise time increment, DTI	sec
31-40	slant range to aim point, CSLANT	ft
41	multiple of time increment for time history output, MPRINT	-

If the aircraft is flying away from the aim point on entry into the cruise maneuver, the maneuver is terminated with a message to that effect. MPRINT controls the frequency of the time history output. Data are printed every MPRINT times the time increment. MPRINT may have values between 0 and 9. An MPRINT value of 0 or 1 prints every time point.

Acceleration/Deceleration

Maneuver Identification Card

Columns 1-3: M02

Maneuver Data Card

Columns 1-10	command velocity, VC	kt
11-20	velocity error band, VERR	kt
21-30	maneuver urgency factor, MUF	-
31-40	minimum power setting, PSL	-
41	multiple of time increment for time history output, MPRINT	-

Turn at Constant Airspeed and Altitude

Maneuver Identification Card

Columns 1-3: M03

Maneuver Data Card

Columns 1-10	desired load factor, ND	-
11-20	heading, HDG	deg
21-30	maneuver urgency factor, MUF	-
31-40	delta heading, HDCG	deg
41-50	direction of turn, ITURN	-
51	multiple of time increment for time history output, MPRINT	-

The turn maneuver can be used to turn to an absolute heading or a delta heading from the aircraft's present heading. If HDG=0 and HDCG=0, the aircraft will turn to 0 degree heading. If HDG=0 and HDCG \neq 0, then aircraft will turn to present heading plus HDCG. If ITURN>0, a right is executed. If ITURN<0, a left turn is executed. If ITURN=0, a minimum heading change turn is executed.

Climb/Descent at Constant Airspeed

Maneuver Identification Card

Columns 1-3: M04

Maneuver Data Card

Columns 1-10	command altitude, HC	ft
11-20	maneuver urgency factor, MUF	-
21-30	minimum power setting, PSL	-
31-40	command flight path angle, GAMC	deg
41-50	maximum load factor, NMAX	-
51-60	minimum load factor, NMIN	-
61	multiple of time increment for time history output, MPRINT	-

If GAMC=0, the controller computes the appropriate flight path angle based on either MUF or PSL. If GAMC \neq 0, the controller checks to see if it is possible to maintain airspeed at this flight path angle. If not, the controller resets the flight path angle to the maximum allowed to maintain airspeed.

Pullup/Pushover at Desired Load Factor

Maneuver Identification Card

Columns 1-3: M05

Maneuver Data Card

Columns 1-10	desired load factor, ND	-
11-20	maximum load factor, NMAX	-
21-30	minimum load factor, NMIN	-
31-40	minimum power setting, PSL	-
41-50	time to achieve desired load factor, TP	sec
51-60	time to hold desired load factor, TH	sec
61-70	minimum velocity, VMIN	kt
71	multiple of time increment for time history output, MPRINT	-

Auto Turn at Constant Airspeed

Maneuver Identification Card

Columns 1-3: M06

Maneuver Data Card

Columns 1-10	desired load factor, ND	-
11-20	maneuver urgency factor, MUF	-
21-30	X aim point in Earth reference, XAP	ft
31-40	Y aim point in Earth reference, YAP	ft
41	multiple of time increment for time history output, MPRINT	-

Return to Target at Constant Altitude

Maneuver Identification Card

Columns 1-3: M07

Maneuver Data Card

Columns 1-10	desired load factor, ND	-
11-20	time to peak roll rate for roll in, TP	sec
21-30	maneuver urgency factor, MUF	-
31-40	X location of target in Earth reference, TARX	ft
41-50	Y location of target in Earth reference, TARY	ft
51-60	minimum velocity, VMIN	kt
61-70	direction of turn, TURN	-
71	multiple of time increment for time history output, MPRINT	-

If TURN>0, a right roll occurs. If TURN<0, a left roll occurs.
If TURN=0, a minimum heading change occurs.

Dive/Rolling Pullout

Maneuver Identification Card

Columns 1-3: M08

Maneuver Data Card

Columns 1-10	desired load factor, ND	-
11-20	desired dive angle, GAMCR	deg
21-30	X location of target in Earth reference, TARX	ft
31-40	Y location of target in Earth reference, TARY	ft
41-50	Z location of target in Earth reference, TARZ	ft
51-60	minimum slant range to target, SLANT	ft
61-70	delta heading, DHDG	deg
71-80	maximum load factor, NMAX	g

Maneuver Data Card

Columns 1-10	minimum load factor, NMIN	-
11-20	minimum velocity, VMIN	kt
21-30	maneuver urgency factor for dive, MUFD	-
31-40	maneuver urgency factor for roll, MUFR	-
41-50	minimum power setting, PSL	-
51	multiple of time increment for time history output. MPRINT	-

The sign of DHDG determines the sign of the bank angle. If GAMCR=0, the controller computes the required dive angle to intersect the target.

Climbing/Descending Turn at Constant Airspeed

Maneuver Identification Card

Columns 1-3: M09

Maneuver Data Card

Columns 1-10	command altitude, HC	ft
11-20	desired load factor, ND	-
21-30	desired heading, HDG	deg
31-40	maneuver urgency factor, MUF	-
41-50	minimum power setting, PSL	-
51-60	maximum load factor, NMAX	-
61-70	minimum load factor, NMIN	-
71	multiple of time increment for time history output, MPRINT	-

If ND=0, the controller selects the flight path angle and bank angle. If ND≠0, the controller uses the remaining power available to compute the flight path angle.

Sideward Acceleration/Deceleration

Maneuver Identification Card

Columns 1-3: M10

Maneuver Data Card

Columns 1-10	command bank angle, PHIC	deg
11-20	command velocity, VC	kt
21-30	final velocity, VF	kt
31-40	maneuver urgency factor, MUF	-
41-50	power required for tail rotor, HPMTR	hp
51-60	X location of target in Earth reference, TARX	ft
61-70	Y location of target in Earth reference, TARY	ft
71	multiple of time increment for time history output, MPRINT	-

This maneuver requires that the final velocity, VF, be zero.

Sideward Acceleration/Pedal Turn Into Wind

Maneuver Identification Card

Columns 1-3: M11

Maneuver Data Card

Columns 1-10	command bank angle, PHIC	deg
11-20	command velocity, VC	kt
21-30	maneuver urgency factor, MUF	-
31-40	power required to tail rotor, HPMTR	hp
41-50	X location of target in Earth reference, TARX	ft
51-60	Y location of target in Earth reference, TARY	ft
61-70	time to peak $\dot{\beta}$, TPB	sec
71-80	desired $\dot{\beta}$, BETAD	deg/sec

Maneuver Data Card

Column 1	multiple of time increment for time history output, MPRINT	-
----------	--	---

Orbit at Constant Airspeed

Maneuver Identification Card

Column 1-3: M12

Maneuver Data Card

Columns 1-10	turn radius, RADIUS	ft
11-20	exit heading, HDG	deg
21-30	maneuver urgency factor MUF	-
31-40	time of orbit, TORBIT	sec
41-50	direction of turn, PHIDR	-
51	multiple of time increment for time history output, MPRINT	-

Pedal Turn at Hover

Maneuver Identification Card

Columns 1-3: M13

Maneuver Data Card

Columns 1-10	desired heading, HDG	deg
11-20	time to peak rate of change of heading, TP	sec
21-30	desired rate of change of heading, CHDR	deg/sec
31	multiple of time increment for time history output, MPRINT	-

Collective Pop-Up at Constant Attitude and Low Airspeed

Maneuver Identification Card

Columns 1-3: M14

Maneuver Data Card

Columns 1-10	command altitude, HC	ft
11-20	maneuver urgency factor, MUF	-
21-30	minimum load factor, NMIN	-
31	multiple of time increment for time history output, MPRINT	-

Climbing Return to Target

Maneuver Identification Card

Columns 1-3: M15

Maneuver Data Card

Columns 1-10	command altitude, HC	ft
11-20	X location of target in Earth reference, TARX	ft
21-30	Y location of target in Earth reference, TARY	ft
31-40	Z location of target in Earth reference, TARZ	ft

Columns 41-50	maximum load factor, NMAX	-
51-60	minimum load factor, NMIN	-
61-70	command bank angle, PHIC	deg
71-80	command climb angle, GAMC	deg

Maneuver Data Card

Columns 1-10	minimum velocity, VMIN	kt
11-20	time to peak rate for rollout, TPO	sec
21-30	time to peak $\dot{\gamma}$, TPP	sec
31-40	time to peak $\dot{\phi}$, TPR	sec
41-50	minimum power setting, PSL	-
51-60	time to apply full power, TACCEL	sec
61	multiple of time increment for time history output, MPRINT	-

LIST OF SYMBOLS

<u>Symbol</u>		<u>Units</u>
a	lift curve slope	/rad
a_i	acceleration at the i th time point	ft/sec ²
a_{i-1}	acceleration at the $(i-1)$ th time point	ft/sec ²
a_{2D}	two-dimensional section lift curve slope	/rad
a_{x_E}	component of linear acceleration in X_E direction	ft/sec ²
a_{x_W}	component of linear acceleration in X_W direction	ft/sec ²
a_{y_E}	component of linear acceleration in Y_E direction	ft/sec ²
a_{y_W}	component of linear acceleration in Y_W direction	ft/sec ²
a_{z_E}	component of linear acceleration in Z_E direction	ft/sec ²
a_{z_W}	component of linear acceleration in Z_W direction	ft/sec ²
A	rotor disc area (πR^2)	ft ²
Al	angle between radius vector from center of rotation to target and perpendicular to radius vector from aircraft to target	rad
AR	aspect ratio, (b^2/S_w)	-
b	number of blades or wing span	- or ft
c	rotor chord	ft
\vec{c}	resultant vector of cross product of velocity vector and radius vector	
CSLANT	minimum slant range to aim point	ft
C_1, C_2, C_3	constants used in evaluating angular acceleration, rate, and displacement	-

LIST OF SYMBOLS - Continued

<u>Symbol</u>		<u>Units</u>
C_{DFP}	drag coefficient of flat plate	-
C_{D_w}	drag coefficient of wing	-
C_{D_0}	drag coefficient at $\alpha = 0$	-
$C_{L_{MAXN}}$	maximum negative lift coefficient	-
$C_{L_{MAXP}}$	maximum positive lift coefficient	-
C_{L_w}	wing lift coefficient	-
C_{L_α}	wing three-dimensional lift curve slope	/rad
dt	time increment	sec
DHE	predicted altitude change in returning gamma to zero	ft
DXE	predicted distance traveled in $X_E Y_E$ plane in recovering from dive and rolling into turn	ft
DXT	distance from target to projection of intersection point with glide slope into the $X_E Y_E$ plane	ft
DXW	predicted distance traveled in $X_E Y_E$ plane in obtaining dive angle	ft
DYE	predicted distance traveled in $X_E Y_E$ plane perpendicular to initial line of sight from aircraft to target in recovering from dive and rolling into a turn	ft
D_w	wing drag	lb
e	wing efficiency factor	-
\bar{e}	flat plate drag area ($C_D = 1$)	ft ²

LIST OF SYMBOLS - Continued

<u>Symbol</u>		<u>Units</u>
f_1	flat plate drag area ($C_D = 1$) at $\beta = 90^\circ$	ft ²
FLDT	predicted distance to initiation of dive	ft
\bar{F}_a	aerodynamic force vector	lb
F_{ax}, F_{ay}, F_{az}	scalar components of aerodynamic force vector	lb
\bar{F}_W	total force vector	lb
$F_{x_W}, F_{y_W}, F_{z_W}$	scalar components of total force vector	lb
g	unit of acceleration ($=32.2$ ft/sec ²)	ft/sec ²
GK_1	gain for angular acceleration in the first stage	rad/sec ²
GK_2	gain for angular acceleration in the second stage	rad/sec ²
GK_3	gain for angular acceleration in the third stage	rad/sec ²
GK_4	gain for angular acceleration in the fourth stage	rad/sec ²
GW	gross weight	lb
HP	total power required to maintain air-speed, altitude, and load factor	hp
HPA	power supplied from the engine	hp
HP_{MAX}	maximum allowable value of HPA	hp
HP_{MIN}	minimum desired value of HPA	hp
$i, i-1$	points in time	-
$\bar{i}_E, \bar{j}_E, \bar{k}_E$	earth axes unit vectors (X, Y, and Z axes, respectively)	-

LIST OF SYMBOLS - Continued

<u>Symbol</u>		<u>Units</u>
i_w	wing incidence	deg
i_{w_0}	wing incidence when $n = 1$	deg
$\bar{i}_w, \bar{j}_w, \bar{k}_w$	wind axes unit vectors (X, Y, and Z axes, respectively)	-
KAF1	coefficient in fuselage angle of attack expression	$\frac{(\text{ft}/\text{sec})^{1.6}}{(\text{ft}^2\text{-lb})^{.5}}$
KAF2	coefficient in fuselage angle of attack expression	$1/g^2$
KAF3	coefficient in fuselage angle of attack expression	$1/g$
KAF4	coefficient in fuselage angle of attack expression	$\frac{(\text{ft}^2\text{-lb})^{.5}}{(\text{ft}/\text{sec})^{1.6}}$
KAF5	coefficient in fuselage angle of attack expression	sec/ft
KAF6	coefficient in fuselage angle of attack expression	-
KAF7	coefficient in fuselage angle of attack expression	deg
KAF8	coefficient in fuselage angle of attack expression	-
K_w	wing induced velocity factor	-
L_w	wing lift	lb
m	mass, $\frac{GW}{g}$	slugs
ΔM	Mach number increment	-
MUF	maneuver urgency factor	-
n	load factor	-
nd	desired load factor	-

LIST OF SYMBOLS - Continued

<u>Symbol</u>		<u>Units</u>
NMAX	maximum desired load factor	-
NMIN	minimum desired load factor	-
P_W	roll rate, wind axes	deg/sec
PSL	minimum power setting, HPA/HPMAX	-
q	free stream dynamic pressure	lb/ft ²
q_w	dynamic pressure at the wing	lb/ft ²
q_W	pitch rate, wind axes	deg/sec
r_W	yaw rate, wind axes	deg/sec
R	rotor radius	ft
\bar{R}	radius vector from aircraft location to aim points	ft
RADIUS	turn radius	ft
SLANT	distance from estimated center of rotation and aim point	ft
SLANTE	estimated minimum slant range from target	ft
S_w	wing area	ft ²
t	time	sec
\tilde{t}	time increment between updates of linear acceleration	sec
t_c	blade loading coefficient	-
$[t_c]_{Div}$	blade loading coefficient where power increases from stall	-
$t_{c_{max}}$	maximum blade loading coefficient ($t_{c_{max}} = TCM1 + TCM2 \mu$)	-
t_{IN}	time to achieve desired turn rate in pedal turn maneuver	sec

LIST OF SYMBOLS - Continued

<u>Symbol</u>		<u>Units</u>
t_{OUT}	time to arrest desired turn rate in pedal turn maneuver	sec
t_f	total time for command generator response	sec
t_h	time to hold steady rate in pedal turn	sec
t_i, t_{i-1}	time at the i th point and $(i-1)$ th point	sec
t_{out}	time to maintain minimum load factor in recovery phase of pop-up	sec
T_{MAX}	maximum time for application of power in acceleration maneuver	sec
T_{MIN}	minimum time for application of power in acceleration maneuver	sec
t_p	time to reach peak rate in pedal turn	sec
t_p	time to reach peak rate	sec
t_{pn}	time to reach maximum load factor in collective pop-up	sec
t_{pr}	time to peak roll rate	sec
t_s	length of each stage of command generator	sec
$t_1, t_2,$ t_3, t_4	stage time for command generator	sec
T	rotor thrust	lb
$[T]$	transformation matrix	-
$TARX$	X_E location of target	ft
$TARXH$	location of target in $X_E Y_E$ plane	ft
$TARY$	Y_E location of target	ft
$TARZ$	Z_E location of target	ft
TCl	constant coefficient of $[t_c]_{Div}$	-

LIST OF SYMBOLS - Continued

<u>Symbol</u>		<u>Units</u>
TC2	velocity coefficient of $[t_c]_{Div}$	-
TCM1	constant coefficient of $t_{c_{max}}$	-
TCM2	velocity coefficient of $t_{c_{max}}$	-
v_i	rotor-induced velocity	ft/sec
V	airspeed along flight path	ft/sec
\dot{V}	flight path acceleration	ft/sec ²
\bar{V}	flight path velocity vector	ft/sec
VJERK	rate of change of load factor for collective pop-up	/sec
V_{ERR}	error band on velocity for acceleration maneuver	kt
V_i, V_{i-1}	velocity at ith time and (i-1)th time	ft/sec
V_{XE}	component of velocity vector in X_E direction	ft/sec
V_{XYP}	magnitude of velocity vector in the $X_E Y_E$ plane	ft/sec
V_{YE}	component of velocity vector in Y_E direction	ft/sec
V_{ZE}	component of velocity vector in Z_E direction	ft/sec
V_{Z_i}	estimated values of vertical velocity for recovery	ft/sec
W	magnitude of weight vector	lb
\bar{W}	weight vector	lb
WF	velocity weighting factor for controlling velocity in acceleration maneuver	-

LIST OF SYMBOLS - Continued

<u>Symbol</u>		<u>Units</u>
X, Y, Z	aircraft location in $X_E Y_E Z_E$ reference system	ft
XAP	X aim point in earth reference	ft
XC, YC	predicted center of rotation for auto turn in earth reference	ft
XNA	predicted X_E coordinate of aircraft's closest approach to target	ft
X_1	predicted X_E location for center of rotation for rolling pullout	ft
X_E, Y_E, Z_E	earth axes	-
X_i, X_{i-1}	position at ith time and (i-1)th time	ft
X_W, Y_W, Z_W	wind axes	-
YAP	Y aim point in earth reference	ft
YNA	predicted Y_E coordinate of aircraft's closest approach to target	ft
Y_1	predicted Y_E location for center of rotation for rolling pullout	ft
ZNA	predicted Z_E coordinate of aircraft's closest approach to target	ft
a	angle of attack	deg
a_F	angle of attack of fuselage	deg
a_{STALL}	angle of attack for stall (positive)	rad
a'_{STALL}	angle of attack for stall (negative)	rad
a_w	angle of attack of wing	rad
β	sideslip angle	deg
$\dot{\beta}$	time rate of change of β	deg/sec

LIST OF SYMBOLS - Continued

<u>Symbol</u>		<u>Units</u>
γ	flight path angle	deg
$\dot{\gamma}$	time rate of change of γ	deg/sec
γ_C	commanded flight path angle	deg
δ_0	profile drag coefficient at $\alpha = 0$	
δ_1	profile drag coefficient change with α	/deg
δ_2	profile drag coefficient change with α^2	/deg ²
ϵ	angle between \bar{V} and \bar{K}	deg
η	efficiency factor for computing a_{x_W}	-
μ	rotor advance ratio	-
ρ	air density	slugs/ft ³
σ'	density ratio	-
τ	first order system time constant (time to reach 63% of peak rate)	sec
ϕ	roll angle	deg
ϕ_C	command roll angle	deg
$\dot{\phi}$	time rate of change of roll angle	deg/sec
$\dot{\phi}_{MAX}$	maximum allowable roll rate	deg/sec
$\ddot{\phi}$	roll angular acceleration	deg/sec ²
χ	heading angle	deg
$\dot{\chi}$	time rate of change of heading angle	deg/sec
χ_C	commanded heading angle	deg
χ_D	desired heading angle	deg
$\dot{\chi}_D$	time rate of change of desired heading angle	deg/sec
$\dot{\chi}_P$	peak time rate of change of heading angle	deg/sec

LIST OF SYMBOLS - Continued

<u>Symbol</u>		<u>Units</u>
χ_0	initial heading angle	deg
$\dot{\chi}_0$	time rate of change of χ_0	deg/sec
$\ddot{\chi}_0$	angular acceleration of initial heading	deg/sec ²
$\overline{\omega}_W$	angular velocity of the wind axes reference frame with respect to the earth axes	rad/sec
ΩR	rotor tip speed	ft/sec